TÉCNICO LISBOA

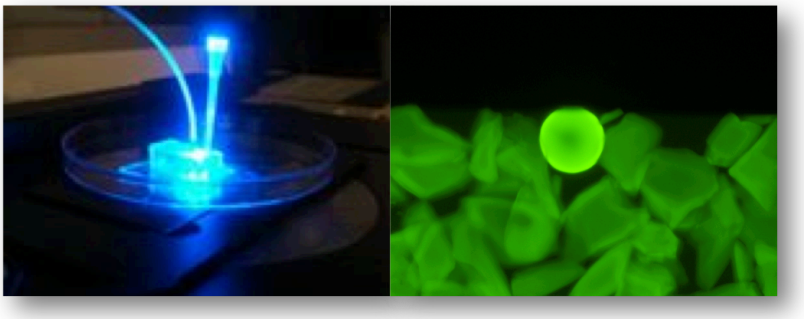

Bead-Based Microfluidic System for DNA/RNA detection

Catarina Raquel Fernandes Caneira

Thesis to obtain the Master of Science Degree in

Biomedical Engineering

Supervisor(s): Doctor João Pedro Estrela Rodrigues Conde

Doctor Francisco Javier Enguita

Examination Committee

Chairperson: Doctor Cláudia Alexandra Martins Lobato da Silva

Supervisor: Doctor João Pedro Estrela Rodrigues Conde

Member off the Committee: Doctor Ana Margarida Nunes da Mata Pires de Azevedo

November 2015

Agradecimentos

Gostaria de começar por agradecer ao Prof. Dr. João Pedro Conde por me ter concedido a oportunidade de trabalhar no INESC-MN, numa área que me deu imenso prazer e me desafiou durante este percurso. Agradeço ainda todo o encorajamento, ajuda, conselhos e motivação que o Prof. Dr. João Pedro me deu e que foram cruciais para me ajudarem a completar esta tese. Agradeço também à Dr^{a}. Virginia Chu pelos mesmo motivos e por ter mostrado um interesse constante no meu trabalho.

Agradeço ainda ao Dr. Francisco Enguita pelas discussões sobre o tema de miRNAs, pelo interesse e sobretudo pelo positivismo em ralação a este trabalho. Um especial agradecimento pela boa vontade em fornecer algumas das amostras biológicas usadas neste trabalho.

Agradeço à Dr^{a}. Ana Azevedo por ter aceite fazer parte do júri de avaliação desta tese e à Professora Dr^{a}. Cláudia Lobato por ter me acompanhado desde o início desta minha viagem, como tutora nos primeiros anos do meu curso, e terminando agora este ciclo aceitando ser presidente do júri.

Não poderia deixar de agradecer ao meus colegas do INESC-MN pela companhia, opiniões construtivas e preciosa ajuda durante este trabalho. Em particular, gostaria de agradecer à Hanna por ter me introduzido ao trabalho de laboratório e pela boa disposição e motivação que apresentava todos os dias. Agradeço também à Inês que para além de ter sido uma constante companhia no laboratório, teve a amabilidade de fornecer as Beads em que este trabalho se baseou. Agradeço ainda ao Rúben e ao Narayanan por toda a paciência, ajuda, opiniões e boa disposição que sempre demonstram para comigo.

Finalmente, agradeço profundamente o apoio da minha família, em particular à minha mãe e ao meu pai por terem sido o meu suporte durante estes anos e terem sempre acredito nas minhas capacidades.

Abstract

Circulating MicroRNAS (miRNAS) have been studied as a new generation of biomarkers for cardiovascular diseases that can be used for diagnosis and prognosis of a wide range of cardiovascular disorders. The development of a porous bead based microfluidic system that is able to detect miRNA promises great potential for the development of a low-cost, fast, sensitive and portable diagnostic system. In this work, a microfluidic system that uses as immobilization platform agarose beads to detect DNA/RNA was studied, with possible application for miRNAs.

PDMS microchannel were sealed against a PDMS membrane. Several immobilization platforms were tested. A DNA probe was immobilized onto the agarose beads surface and fluorescence intensity was measured. Using the beads fluorescence intensity signal was enhanced 200-fold when compared with an immobilization performed in a bare channel. Protocol optimizations for the flow rate, channel dimension and blocking method were performed. Chemiluminescence and colorimetric detection methods were also tested with a limit of detection 10pM and 100pM, respectively. Biological matrixes were also used during experiments (human serum and fetal calf serum) and it was verified that it was possible to detect signal.

Key words: microfluidic system, agarose beads, nucleic acid hybridization, cardiovascular diseases.

Resumo

MicroRNAs (miRNAs) em circulação têm sido estudados como uma nova geração de biomarcardores para doenças cardiovasculares e que podem, potencialmente, ser usados para diagnóstico e prognóstico de doenças cardíacas. O desenvolvimento de um sistema microfluídico baseado em esferas porosas, que possa detectar miRNAS, apresenta um grande potencial para desenvolver um sistema de baixo-custo, rápido, sensível e portátil. Nesta tese, foi estudado um sistema microfluídico que usa como plataforma de imobilização esferas de agarose para a detecção de DNA/RNA e com possível aplicação aos miRNAs.

Os canais foram fabricados em PDMS e selados contra uma membrana de PDMS. Várias plataformas de imobilização foram testadas. Sondas de DNA foram imobilizadas na superfície das esferas de agarose e a intensidade de fluorescência foi medida para as diferentes plataformas. Provou-se que, com o uso das esferas, o sinal de imobilização aumenta 200 vezes em relação à imobilização feita num canal simples. O protocolo foi optimizado, tendo-se alterado fluxos de imobilização, dimensões do canal a usar e escolhido o melhor método de bloqueio. Utilizou-se ainda como método de deteção quimioluminescência e colorimetria sendo que o limite de deteção encontrado foi de 10pM e 100pM, respectivamente. Testou-se ainda a aplicabilidade do sistema ao uso de matrizes biológicas (soro humano e soro fetal de vitela) verificando-se que foi possível a detecção de sinal.

Palavras-chave: Sistema microfluídico, esferas de agarose, hibridação de ácidos nucleicos, doenças cardiovasculares.

Index

List of Tables

List of Figures

List of Abbreviations

ACS - Acute Coronary Syndrome

Ago -Argonaut

Ago2 –Argonaute2

AMI -Acute Myocardial Infarction

ANP - Atrial Natriuretic Peptide

APTES – (3-Aminopropyl) triethoxysilane

BNP/NT – proBNP - Brain Natriuretic Peptide and N-Terminal Brain Natriuretic Peptide

BSA – Bovine Serum Albumin

CAD – Cardiac Acute Disease

CB- Cardiac Biomarkers

CCT – Cardiac Computed Tomography

CCT- Cardiac Computed Tomography

CD40 – Cluster of Differentiation 40

cDNA – complementary DNA

CHD – Coronary Artery Disease

CK-MB - Myocardial Muscle Creatine Kinase

CMR - Cardiovascular Magnetic Resonance

CMR – Cardiovascular Magnetic Resonance Imaging

CPG – Controlled Pore Beads

CRP – C Reactive Protein

cTn - Cardiac Troponins

CVD – Cardiovascular Diseases

DEAE – Diethylaminoethyl

DIG – Digoxigenin

DM – Diabetes *Mellitus*

DNA- Deoxyribonucleic Acid

dsDNA – Double stranded DNA

dT - Oligo

DWL – Direct Wite Lithography

ECG – Electrocardiography

EU - European Union

FCS – Fetal Calf Serum

FITC - Flourescein Isothiocyanate

H-FABP - Heart-type Fatty Acid Binding Protein

HDL – High-density Lipoprotein

HF – Heart Failure

HPCL – High Performance Liquid Chromatography

IHD – Ischemic Heart Disease

IPA – 2 -Isopropanol

ISH – *In situ* Hybridization

LNA- Locked Nucleic Acid

LoB – Limit of Blank

LoD – Limit of Detection

MEMS – Microelectrical Mechanical System

miRNAs - micro RNAs

MMO - Microcystic Macular Edema

MPO – Myeloperoxidase

mRNAs - messenger RNA

NB - Northern Blotting

ncDNA- non-complementary DNA

NGS – Next Generation Sequencing

NPMI – Nucleophosmin

NSTEMI – Non-ST Elevation after Myocardial Infarction

PAA – Sodium Polyacrilate

PBS – Phosphate Buffer Saline

PDMS – Polydimethylsyloxane

PEG – Polyethylene Glycol

PGMEA – Propylene Glycol Monomethyl Esther Acetate

PoC - Point of Care Device

RISC - RNA Induced Silencing Complex

RNA - Ribonucleic Acid

ROC – Receiver Operate Characteristics

SD – Standard Variation

siRNA- Small Interfering RNA

SPR – Surface Plasmon Resonance

ssDNA – Single Stranded DNA

STEMI - ST Elevation after Myocardial Infarction

$\mathbf{T_m}$ - Melting Temperatures

TMB – 3,3'5,5'-Tetramethylbenzidine

TNFα – Tumor Necrosis Factor alfa

UA - Unstable Angina

UTR - Untranslated Region

1. Introduction

This first chapter starts with the motivation for this work. Then the theoretical information needed to contextualize the work developed will be revised. In the second chapter the methods used to achieve the objectives described before will be explained. In the third chapter the results of this work will be presented and discussed. The fourth chapter will conclude about the present work and future outlooks will be mentioned.

1.1 Motivation

Molecular or nucleic acid-based diagnosis of human disorders are based on the detection of pathogenic mutations or a host response which indicate a disease (proteins or expression of genes) in deoxyribonucleic acid (DNA) or ribonucleic acid (RNA) samples. This method is used in order to facilitate detection, diagnosis, subclassification, prognosis, and monitoring treatment therapies [1].

Nowadays 95% of all deaths in the developing countries are due to a lack of proper diagnostic and the consequent treatments [2]. This includes both infectious and chronic diseases. In the developed countries, the strategy to deal with major disease burdens is shifting from a therapeutic to a diagnostic mode, as the cost of treating the disease lowers dramatically if it is found in early stages. Cardiovascular diseases (CVD) are the most common cause of death globally [3]. According to World Health Organization, in 2012, 31% of all global deaths were due to CVDs [4]. This number is expected to increase by 2030 making chronic diseases, that are now common in the developed countries, become also a priority to the developing countries [2] [3]. Overall CVD is estimated to cost the EU economy almost €196 billion a year, according to the most recent data from 2012 European Cardiovascular statistics [5].

The early detection of CVDs through effective diagnostics is crucial, not only to patient survival, but also to decrease the cost of these diseases. It is mandatory the development of a rapid, low-cost diagnostic tool that can be spread throughout a community for easy access and that would provide substantial benefit by allowing faster diagnosis and monitoring of disease [3] [6].

The emerging fields of microfluidics and nanotechnology promise exciting and integrated solutions to sample processing assay performance and analytic detection. The lab-on-a-chip has been recognized as an opportunity to bring accurate and sensitive diagnostic tests to the point-of-care (PoC), in high-income countries and in low-resource

settings, as well as in the developing countries [3] [7]. Combining PoC testing, one of the most promising areas for biosensor applications, and cardiac biomarkers research presents itself as a promising solution to achieve detection with high sensitivity and resolution [8]. It is extremely important to select the most clinical relevant cardiac biomarkers. A major challenge for the biomedical engineering community is to develop diagnostic tests to meet the needs of these people, the majority of whom are in the developing countries. Working in the microfluidic area it is important to remember that this should be a device with high sensitivity and reproducibility, portable, the most autonomous possible and inexpensive. However, there is much room for innovation, adaptation, and cost reduction before these technologies can impact health care in the developing countries [3].

1.2 Cardiovascular Diseases

CVD is a group of heart and vessels disorders. CVD is also related with atherosclerosis conditions and could lead to a heart attack or stroke. It includes coronary heart disease (CHD), stroke, hypertension, congestive heart failure, hardening of the arteries and other circulatory diseases [6][9]. CHD is the most usual type of CVD. The term acute coronary syndrome (ACS) refers to any group of clinical symptoms compatible with acute myocardial ischemia and covers the spectrum of clinical conditions ranging from unstable angina (UA) to non-ST segment elevation myocardial infarction (NSTEMI) to ST-segment elevation myocardial infarction (STEMI) [10]. STEMI is a type of heart attack and is the more severe type and it is usually recognize by changes on the electrocardiography (ECG). One change is the characteristic elevation in what is called the “ST segment” on the ECG which indicates that a relatively large amount of heart muscle damage is occurring because the coronary artery is totally blocked. NSTEMI is the less severe type and in this case it does not produce a characteristic elevation in the “ST segment” of the ECG meaning that the artery is only partially blocked.

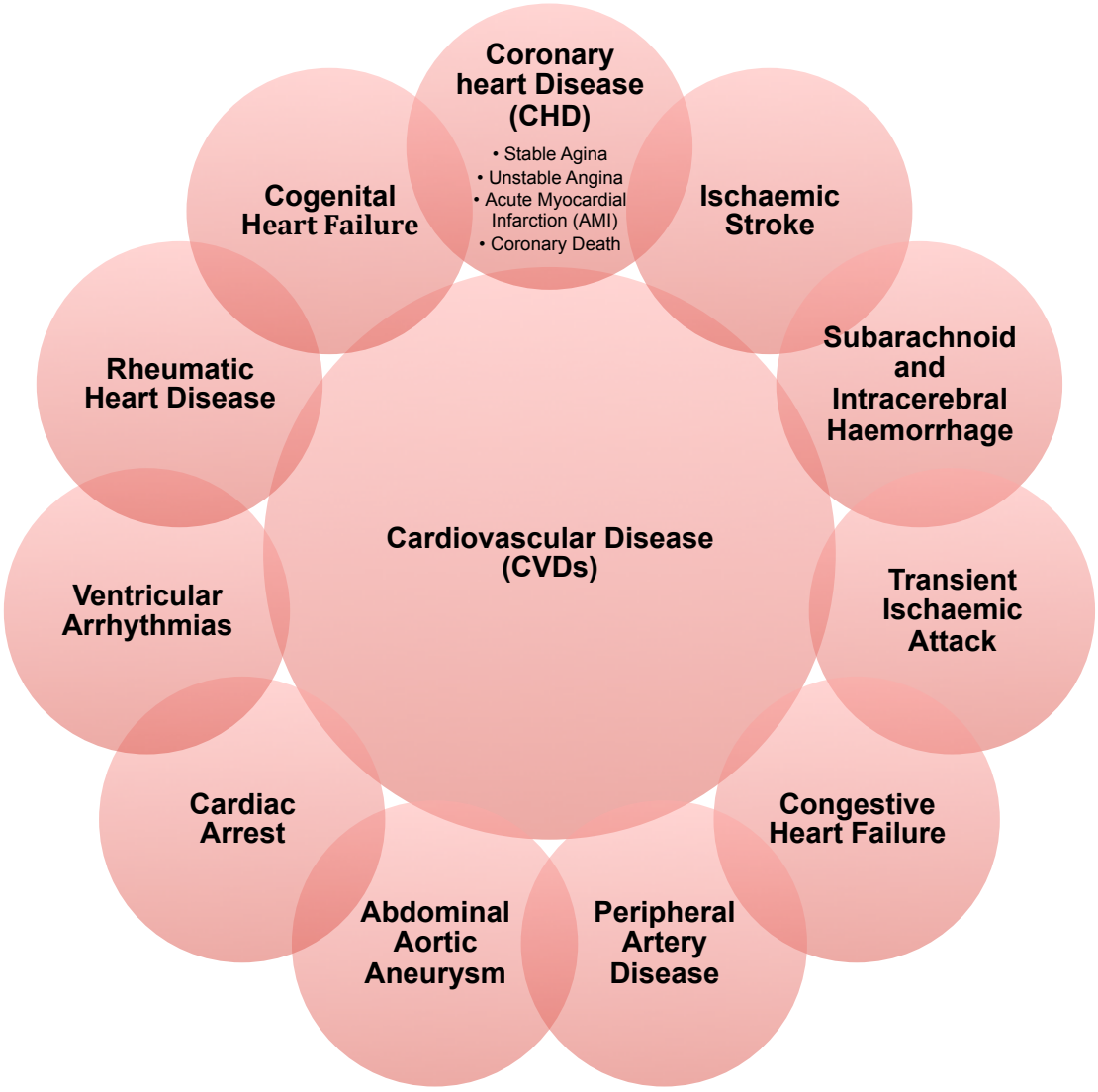

Figure 1 - Types of cardiovascular diseases [6][9][10].

Some common diagnostic tests that are performed when evaluating CVDs include diagnostic imaging such as conventional radiographs, echocardiography, cardiovascular magnetic resonance imaging (CMR), cardiac computed tomography (CCT), nuclear scintigraphy, ECG and angiography. Blood tests can also be used for CVD diagnosis [11]. These tests are used to evaluate disease severity and the response to treatments but they lack on specificity and/or sensitivity, or require invasive procedures such as angiography or intravascular ultrasound.

1.3 Cardiac Biomarkers

In 1954 the use of a biochemical marker for the study of myocardial infarction was

described for the first time. It was verified that glutamate oxaloactic transaminase activity, presented in serum, increased after an AMI [12]. The biomarker term was introduced for the first time in 1989 as "measurable and quantifiable biological parameters (e.g., specific enzyme concentration, specific hormone concentration, specific gene phenotype distribution in a population, presence of biological substances) which serve as indices for health and physiology related assessments, such as disease risk, psychiatric disorders, environmental exposure and its effects, disease diagnosis, metabolic processes, substance abuse, pregnancy, cell line development, epidemiologic studies, etc." [13]. In 2001 the term was defined as "a characteristic that is objectively measured and evaluated as an indicator of normal biological processes, pathogenic processes, or pharmacologic responses to a therapeutic intervention" [13]. Biomarkers can be obtained in a biosample, in a clinical test record from the person (like Holter) or in an imaging test and it gives information about disease trait, state and/or rate. They can be classified as antecedent biomarkers evaluating the risk of developing an illness, screening biomarkers, diagnostic biomarkers, staging biomarkers, or prognostic biomarkers to predict future disease course (recurrence and response to therapy) and monitoring efficacy of therapy [13].

A cardiac biomarker (CB) can be described as a biological analyte that is present in blood/plasma circulation at high levels if one suffers of CVD [12]. An ideal CB should have high clinical sensitivity and specificity, quick release in the blood to allow an early diagnosis, should remain during a long period of time and with high concentration values in the blood and it should be assayed quantitatively [6][12]. Nowadays, several CBs are available with potential as cardiac risk predictors and prognosis indicators. They can be grouped in inflammatory, acute muscle injury and cardiac stress [14]. Some CBs of each group used nowadays are summarized in Figure 2.

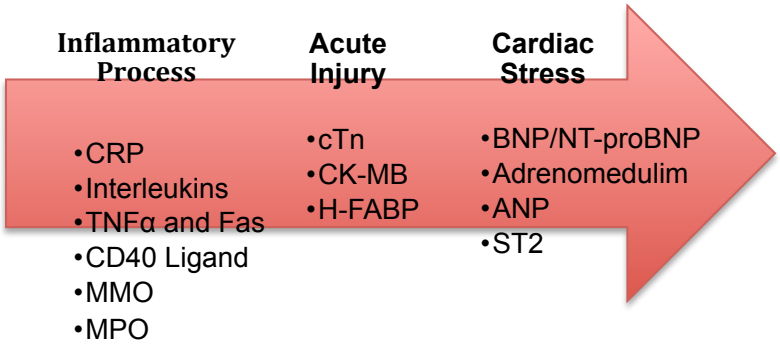

Figure 2 - Summary of cardiac CBs used to detect inflammatory process, acute injury and cardiac stress. Inflammatory Process: C Reactive Protein (CRP), Interleukins, Tumor Necrosis Factor alfa (TNFα) and Fas, Cluster of Differentiation 40 (CD40) ligand, Microcystic Macular Edema (MMO) and Myeloperoxidase (MPO); Acute injury: Cardiac Troponins (cTn), Myocardial Muscle Creatine Kinase (CK-MB) and Heart-type Fatty Acid Binding Protein (H-FABP); Cardiac Stress: Brain Natriuretic Peptide and N-Terminal Brain Natriuretic Peptide (BNP/NT-proBNP), Adrenomedulim, Atrial Natriuretic Peptide (ANP) and ST2 [14].

Inflammatory biomarkers are not specific for CVD if other organs are damaged. The cardiac troponins (cTn) are widely used as specific biomarker for myocardial tissue injury. Both cTnI and cTnT present cardio specific isoforms that are not related to skeletal muscle thus making them very specific for myocardial injury. In recent years it was verified that it is possible to have high levels of cTn in the blood stream without a cardiac pathology, for instance if one presents a chronic renal failure. Nevertheless, cTn is the golden standard as CB but the use of multiple biomarkers is a possible solution to improve diagnosis sensitivity and specificity [14]. Some biosensors have already been reported as a mean of detection of CVD using CBs present in Figure 2 [6].

1.4 Biosensors for Cardiac Biomarkers

It has been reported the use of fluorescence based biosensors. Hill *et al*. used an antibody sandwich assay based in fluorescence microsphere immunoarray platform for detection of cytokines like TNFα and interleukine [15]. Jung *et al.* used a competition based tagged internal standard assay to measure CRP in serum at subnanogram levels [16]. Song *et al*. used an antibody tagged fluoro-microbead guiding chip with four immunoreactions regions for multiple simultaneously assays to detect cTnI in human plasma [17]. Wu *et al.* used colorimetry instead and a PDMS-gold nanoparticle composite film based to detect cTnI [18]. Cristodoulides *et al.* used a cardiac chip that entrapped single polymeric spheres in micro-machined pits, flowing on each bead reagents/washes through the microfluidic structures. Optical signal obtained from single beads were used to detect simultaneously C-reactive protein and interleukin-6 present in human serum [19]. There are also a lot of studies using ELISA based methods, for instance, Darain *et al.* used a simple sandwich ELISA where antibodies were immobilized on in-channel polystyrene and a plastic based microfluidic chip was used for detection [20]. Cho *et al.* also presented a chemiluminometric biosensor for PoC testing using an immune-chromatography assay and an enzyme tracer that upon a chemical reaction produces light. Biotin-streptavidin capture technology was used to increase sensitivity. This system could detect cTnI at 0.027 $ngmL^{-1}$ levels [21]. Several surface plasmon resonance (SPR) based biosensors were also tested for CBs detection [22][23]. There were also reports on acoustic biosensors, electrochemical biosensors and magnetic biosensors. Magnetic biosensors are also a good option since the advance in the nanomaterials field and can hold a big promise for the future of biosensors. Furthermore, the use of magnetic particles surface functionalized allows for immobilization and separation of target analytes [6]. Woolley and Hayes reported sandwich immunoassay method with magnetic microbeads to capture the target analytes (myoglobin, heart-type fatty acid binding protein and cTnI) with levels of detection of 360aM, 67fM and 42 fM,

respectively [24].

It has also been reported the use of microRNAs (miRNAs) as novels biomarkers holding the promise of being very specific and accurate CBs [14].

1.5 Circulating MicroRNAs as novel Biomarkers for CVDs

Recent studies show that genomic biomarkers are effective in patient stratification and may predict cardiovascular events more accurately than current techniques. Therefore, nucleic acid-based biomarkers offer great potential to serve as novel, non-invasive, rapid, sensitive, and accurate tools in clinical management of important cardiovascular diseases.

MiRNAs are small (19-25 nucleotides length) non-coding RNA molecules that function as post-transcriptional regulators of gene expression by binding to the sites in the 3'-untranslated region of targeted messenger RNAs (mRNAs) [14] [25]. Before 1990, it was believed that miRNAs were only important in nonmamalian species [26]. In 1993 Ambros *et al*. discovered the lin-4, a gene that controls development on *Caenorhabditis elegans* model organism, it does not encode for a protein product but giving instead origin to a pair of small RNAs, one a 61 nucleotide length precursor of a 22 nucleotide length transcript [27][28]. These lin-4 RNAs were also shown to display antisense complementarity to multiple sites of the 3' untranslated region (UTR) of the lin-14 gene [28][29]. A change of mind started to happen. Along with these discoveries, Ruvkun *et al.* also found that LIN-4 protein synthesis is regulated post-transcriptionally and that LIN-14 protein levels are inversely proportional to the lin-4 RNA [29]. All this suggested that lin-4 RNAs regulated LIN-14 protein, through base paring, causing translational repression revealing the first miRNA and mRNA target interactions [26][28][29]. After 7 years, a second *C. elegans* miRNA was discovered (let-7), that repressed lin-41, lin-14, lin-28, lin 42 and daf-12 expression, confirming the miRNA existence and function [26]. The discovery of lin-7 homologs in many vertebrate species including humans opened a new field of studies in search of more miRNAs [26]. Nowadays there are thousands of unique mature human miRNAs documented online in the miRBase database and each miRNA can target multiple mRNAs and regulate almost 60% of mammalian protein encoding genes [30].

1.5.1 Biogenesis and Secretion

First, in the nucleus budding miRNA transcripts (pri-miRNA) are processed into a 60 nucleotides RNA hairpin (pre-miRNA) that was generated in the nucleus. Pri-miRNAs are processed into pre-miRNA by a RNase III enzyme endonuclease, Drosha, and DCGR8, a regulatory subunit of Drosha. They are dsRNA-specific endonucleases. Drosha gives rise to

2-nucleotide-long overhang at the 3' end at the cleavage site. The cleavage site is also left with 5´phosphate and a 3'-OH. DCGR8 presents two double stranded RNA-binding domains that are thought to help substrate recognition. The efficiency of DROSHA processing depends on the terminal loop size, stem structure and the flanking sequence of the Drosha cleavage site. Pre-miRNAs are then exported to cytoplasm by Exportion5 (Exp 5), a Ran-guanosine trisphophate cofactor (Ran-GTP) dependent nucleo/cytoplasmic cargo transporter. Exp 5 /Ran-GTP complex binds the minihelix-containing RNAs, such as pre-miRNA, with 3'overhang. It is hypothesized that Exp 5 also protects the pre-miRNAs since they are formed in the nucleus until they reach the cytoplasm. In the cytoplasm, once the complex is there, guanosine trisphophate is hydrolyzed to guanine diphosphate leading to a release of the pre-miRNA. The second event is the cleavage of the pre-miRNA present in the cytoplasm into 21-25-nucleotide mature miRNAs (containing both mature miRNA stand and its complementary strand [miRNA*]). This is done by another RNase III enzyme endonuclease, Dicer [30][31]. Some proteins like TRBP and PACT in humans that have a double-stranded RNA-binding domains, bind to Dicer and contribute to enhance the affinity of Dicer to the pre-miRNAs. Dicer proteins bind preferentially to the single-stranded 3'ends of double stranded RNAs and cleaves approximately 22 nucleotides away from the terminus [32]. The result is an intermediate miRNA duplex containing approximately 2 nucleotides in the 3' overhangs in both ends but only one of this strand can be detected in cells. One theory is that the RNA strand with less stable hydrogen bonding at the 5' end is selectively stabilized to become the mature miRNA and the complementary strand is degraded, justifying the presence of the uracil residue in the 5'end of so many miRNAs [27][30][31].

Dicer interacts with Argonaute (Ago) proteins, which could contribute for miRNA biogenesis by selecting or binding to and stabilizing the mature miRNAs. Ago proteins are the main constitution of the RNA-induced silencing complex (RISC). RISC works as an identifier of target messages (3'UTR) through complementarity with the miRNA and the mRNA. RISC can downregulate gene expression by two different mechanisms. The choice of the posttranscriptional mechanisms is not determined by if the small silencing RNA originated as a small interfering RNA (siRNA) or a miRNA, but by the target identification an degree of complementarity. One mechanism is the cleavage of the identified complementary target mRNA by RISC endonucleases. The other mechanism will negatively regulate gene expression by translational repression. In this last case ribosomes are slowed down during the translation or the translation continues at the same rate, but the synthesized polypeptide is specifically degraded [27][30][33]. In Figure 3 maturation process is represented.

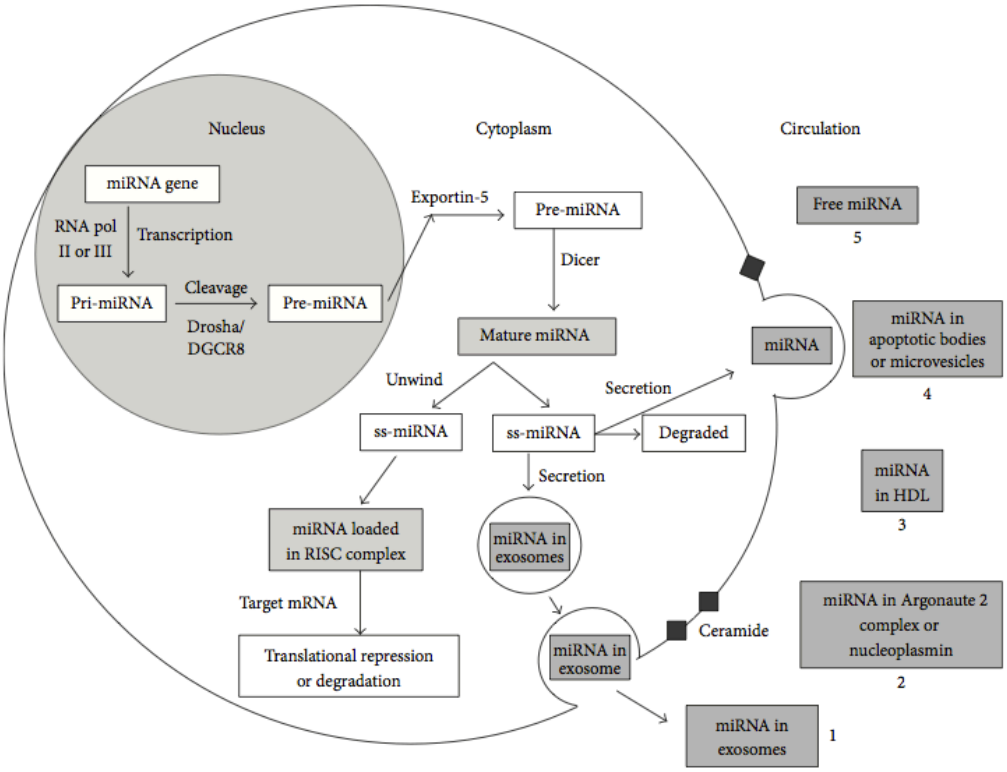

Figure 3 - Representation of the steps involved in intracellular biogenesis of miRNA and their secretion. MiRNA can be secreted outside the cell via exosomes (1), miRNA –protein complexes (2), HDL-miRNA complexes (3), apoptotic bodies or microvesicles through interaction with membrane proteins (4), and free miRNAs by natural spill or as products of dead cells (5). Adapted from Kondkar, and Abu-Amero (2014) [30].

1.5.2 Circulating miRNAs

It was found in 2008 that miRNAs can also be found in blood, and detected in plasma, serum, platelets, erythrocytes, and nucleated blood cells [30][34]. This is a major feature when searching biomarkers in easily accessible samples. It was also noticed that plasma miRNAs are remarkably stable under adverse conditions, for instance low and high pH, several freeze-thaw cycles or long storage period at room temperature [35]. Recently it was found that miRNAS can be packed into microvesicles (exosomes, microvesicles, and apoptotic bodies) or associated with RNA-binding proteins, such as Argonaute2 (Ago2), or lipoprotein complexes (high density lipoprotein [HDL]). This vesicular packaging or protein association prevents the miRNAs degradation [30] [34]. El-Hefnawy *et al.* were one of the firsts to demonstrate in 2004 that plasma RNA is protected from degradation due to packaging in protein or lipid vesicles [36].

Exosomes are small vesicles (50-100nm) from the endosome and are released when multivesicular bodies fuse with the plasma membrane. Microviscles are larger than exosomes (0.1-1μm) and are released by blebbing of the plasma membrane. Apoptotic

bodies are the largest (0.5-2 μm) with heterogeneous shape and are shed from cells during apoptosis [37]. Some miRNAs can be either more or less expressed in donor cells or in the secreted exosomes, suggesting the existence of cellular mechanisms that actively concentrate specific miRNA species in exosomes [38]. Nevertheless, it is thought that he majority of miRNAs are not found inside vesicle but rather are bound to RNA-binding proteins [34]. In a study done by Arroyo *et al.* it was found that vesicle-associated plasma miRNAs represent the minority, whereas potentially up to 90% of miRNAs in the circulation are present in a non–membrane-bound form [39]. A large portion of circulating miRNA is bound to Ago2 that presents high stability and nuclaophosmin (NPM1) [34][38]. HDL can also transport endonucleous miRNAs. HDL particles have an average size of 8-12nm, being substantially smaller than exosomes. Furthermore, they contain lipids, such as phosphatidylcholine, that are known to form stable ternary complexes with nucleic acids. How HDL is loaded with miRNAs is not known exactly. However, biophysical studies suggest that HDL simply binds to extracellular plasma miRNA through divalent cation bridging [34]. The stability of miRNAs in the circulation raises the intriguing possibility that they are taken up by distant cells to regulate their gene expression. Currently, the potential function of extracellular miRNAs is being studied intensively, and the first studies have confirmed that miRNAs may indeed have a role in cell-to-cell communication [34].

1.5.3 MiRNAs as Biomarkers in CVD

MiRNAs were found to be stable in plasma for 24 hours at room temperature and through 8 freeze-thaw cycles, giving them an appealing stability to be used as biomarkers [40]. They can be easily detected by quantitative analysis, using real-time PCR, deep sequencing or microarrays for instance. All this served as a motivation to use miRNAs as nouvels biomarkers and the development of PoC platforms to detect and measure miRNAs [30][34].

MiRNAs were first associated with cancer detection. MiRNA deregulation in cancer was first reported in 2002 by Dr. Carlos Croce [41]. In 2008, Lawrie *et al.* were the first to present evidence that miRNAs could be reliably detected in serum and demonstrated that elevated levels of miR-21 and miR-155 could efficiently discriminate patients with B-cell lymphoma from healthy control groups. In the five years since this landmark study, hundreds of studies have been published reporting the detection of miRNAs in blood as a potential diagnostic tool [41]. Since 2009 several groups have also reported the use of miRNAs as circulating biomarkers for diagnosis or prognosis of cardiovascular diseases such as myocardial infarction, HF, atherosclerosis, hypertension and type 2 diabetes mellitus (DM) [34]. Over 200 miRNAs have been detected in a healthy adult heart that are over expressed

in non-diseased cardiac tissue such as miR-1, miR-16, miR-27b, miR-30d, miR-126, miR-133, miR-143, miR-208 and let-7 family [25]. MiR-1 is the most abundant miRNA specific for cardiac and skeletal muscle and functions as differentiation and proliferation regulator during cardiogenesis and as a regulator of cardiomyocyte growth in the adult heart. It is also considerer pro-apoptotic in myocardial ischemia [25].

1.5.3.1 Acute Myocardial Infarction

AMI is the ideal scenario to establish the potential role of circulating miRNAs as biomarkers since it leads to a release of cardiac proteins such as cTn into bloodstream and release of cardiac-specific miRNAs into circulation [30]. AMI is characterized by cardiac cell death as a result of exposure to prolonged ischemia [42]. Plasma levels of miR-208b and miR-499 both have been highly associated with AMI. Also, it was demonstrated that measuring miR-1 in plasma is a good approach for blood-based detection of human AMI [38]. Studies show that miR-208 is an exclusive cardiac miRNA that is not detectable at a baseline, but rapidly increases in circulation after MI. Particularly, in plasma of AMI patients, miR-208b was the most upregulated miRNA (~3000 times more) comparing with healthy subjects showing correlation with the presence of cTnT, indicating myocardial injury. It was also found that mortality at 6 months after MI was correlated with elevated circulating levels of miR-208b, subjects with undetectable miR-208b had the best prognosis [43]. Wang *et al*. in a studied were 66 patients were evaluated using a biochemical marker cTnI (threshold >0.1 ng/ml) and other biomarkers and compared with 30 control subject that were separated between confirmed AMI patients and non-AMI patients with chest pain. Quantitative Real Time-PCR (RT-PCR) results revealed that miR-1, miR-133a, and miR-499 were detected at significantly higher levels in AMI patients' plasma. One interesting note is that miR-208a could not be detected in plasma samples from healthy control subjects or in non-AMI patients with chest pain and was readily detectible in 91% of the AMI patients. MiR-208a showed a superior receiver operating characteristic (ROC) curve, with an area under the curve of 0.965 (95% confidence interval 0.920-1.000) being very similar to the cTnI (0.987). In early stages of an AMI, miR-208a may even have advantages over cTnI since it can be detected in plasma of all patients within 4 hours of the onset of symptoms and cTnI was only detected 85% of the times in early stages [44]. Corsten *et al*. also studied miR-208b and in this case, when comparing patients with AMI with ones with atypical chest pain without cardiac cause, a 1600-fold increased of miR-208b was found in plasma of AMI patients with a ROC curve reveling an area under the curve of 0.944 (95% confidence interval 0.863-1.000) [45]. Other studies were also conducted, using rodents, to evaluate the exact time of miRNA release after AMI concluding that in the first hour miR-208a increased to significantly detectable

values and peaked after 3 hours. After that it started to decrease, and returning to undetectable levels 24 hours after AMI. Levels of miR-1, miR-133a, and miR-499 also increased significantly after AMI although they peaked after 6 hours of AMI still having elevated levels after 24 hours. Another important aspect verified was that tissue injury during surgical procedure of coronary artery ligation also effectively releases muscle borne miRNA into the blood. From the several miRNAs studied, it appears that miR-208a is the superior miRNA for diagnosis of AMI since it is only heart-specific and therefore minimally affected by non-cardiac tissue injury. MiR-1 and miR-333 may also be used to diagnose AMI but because they are highly expressed in skeletal muscle too, the plasma levels may be affected by other disorders of other organs. The combination of several miRNAs like miR-208a and miR-499 may provide an attractive signature for AMI diagnose [34].

1.5.3.2 Acute Coronary Syndrome

Widera *et al.* studied patients with STEMI, NSTEMI and unstable angina. Mir-208B was only detectable in patients with STEMI and NSTEMI. It also provided prognostic information for ACS given the fact that increasing levels of miR-208b were predictive of 6-month mortality and individual with undetectable levels of miR-208b had the best prognosis. Plasma levels of miR-133a were also higher in patients with NSTEMI and STEMI as compared to unstable angina and significantly associated with mortality risks [45]. Other studies showed that both miR-208b and miR-499 were highly elevated (>10^5 - fold) in both STEMI and NSTEMI and nearly undetectable in control subjects [30].

1.5.3.3 Heart Failure

Studies show no increase in miR-1, miR-208a, miR-208b and miR-499 in plasma of HF patients and seven microRNAs were validated in the plasma of HF patients (miR-423-5p, miR-18b*, miR-129-5p, miR- 1254, miR-675, HS_202.1 and miR-622) among which mature miR-423-5p was the most strongly related to the clinical diagnosis of HF with a ROC curve with an area under the curve of 0.91 (95% confidence interval 0.84-0.98). It was also noticed that the abundance of some miRNA were related to disease severity [34]. Fukushima *et al.* also found that endothelial-specific miR-126 was negatively correlated with age, brain natriuretic peptide and New York Heart Association class which indicates that it can be used as a biomarker for HF.

1.5.3.4 Coronary Artery Disease

Using Microarray analysis of miRNA expression in whole blood showed that in CAD patient there are present miR-140 and miR-182. Also, expression of miR-92 increased after

cardiac rehabilitation and is reduced in plasma of CAD patients. It was also found that miR-208 and miR-133 did not increase in CAD patients [34]. Hoekstra *et al.* found that in CAD patients circulating miR-135a was increased 5–fold and miR-147 was decreased 4-fold when compared with control subjects. It was also possible to distinguish between patients with unstable and stable angina since miR-134, miR-98 and miR-370 are present in high levels in plasma of unstable angina patients [46]. In patients with stable CAD it was also showed that cardiac muscle enriched miR-133a and miR-208a are elevated as well. Since endothelial activation is critical to atherosclerosis the detection of endothelial miRNAs (such as miR-92a) might identify patients at risk for CAD [30].

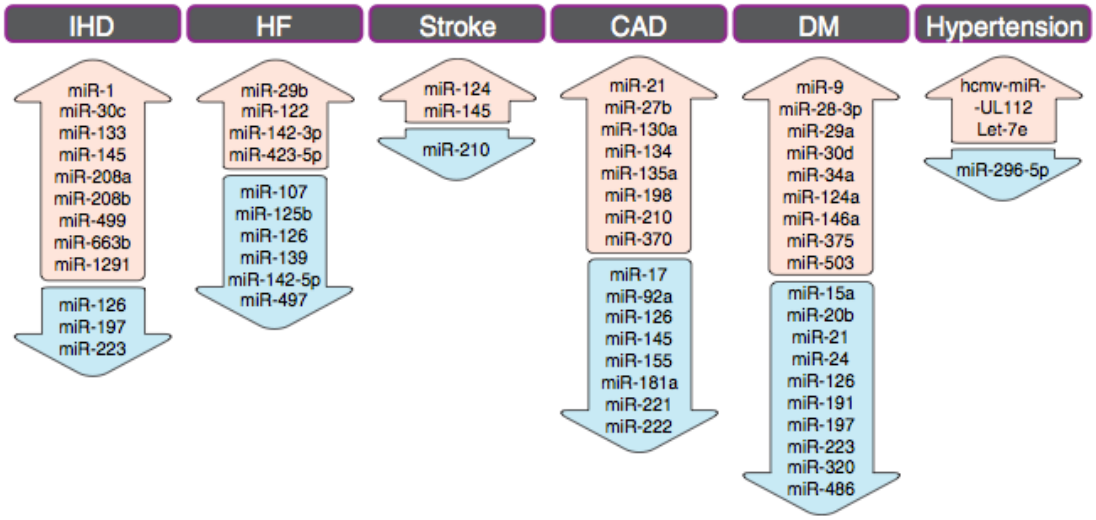

Figure 4 - Summary of circulating miRNAs that are upregulated and downregulated in several cardiovascular diseases. Adapted from Empel *et al.* (2012) [43].

1.6 State of the Art MicroRNAs detection methods

Nowadays several detection methods are available to determine the abundance of miRNAs. The expression profiles of many different miRNAs in parallel can be measured by microarray analysis or deep sequencing. Northern Blotting (NB), quantitative RT-PCR, and *in situ* hybridization (ISH) can be used to determine the level of individual miRNAs [26]. None of these methods is perfect since all have their limitations and the choice of the most suitable methods for miRNA detection mainly depends on the specific experimental setting. An ideal miRNA profiling methods should be sensitive enough to provide quantitative analysis of miRNA levels, even with small amounts of starting material. It should also be specific enough for reproducible detection of dingle nucleotide mismatch between miRNAs and it should be capable of processing multiple samples in parallel. Finally, it should be easy to perform

without the need of expensive reagents or equipment [47].

1.6.1 Northern Blotting Methods

Northern Blotting (NB) is the most standardized and widely used method of detecting miRNAs and it was used to identify the very first miRNA [29][47]. Although it is fairly time consuming and requires large amounts of RNA, it is the only approach that can visualize the expression product of a miRNA. After isolation of total RNA from cells or tissue, the small RNAs are fractionated by electrophoresis on a high percentage gel. After transferring these small RNAs from the gel onto a nitrocellulose membrane, to allow detection by hybridization with fluorescent or radio-labeled probes that are complementary to the target miRNA, the RNA is fixed onto the membrane by UV cross-linking and/or baking the membrane. Because of the small size and the low abundance of miRNA molecules, the use of an oligonucleotide probe with high sensitivity is essential for the detection of a given miRNA. NB technique allows the validation of predicted miRNAs by the examination of their expression levels and the determination of their sizes. However, there are several technical limitations that prevent the routine use of NB as miRNA expression profiling tool in clinics. Mature miRNA molecules are very short and their abundance in total RNA is also very low, leading to a poor sensitivity in Northern blot analysis. Moreover, this method is very time-consuming and not practical in clinical studies in which the detection of a large number of miRNAs might be required. The use in diagnostic is also limited by the relatively large amount of RNA sample required and the multiple handling steps. Therefore it has been replaced by techniques that are more sensitive and high-throughput techniques such as real-time reverse transcription-PCR (qRT-PCR) and the microarrays, but it is still used to validate results from the newer techniques [47]. Traditional NB protocols have gone through a number of improvements in recent years, including the incorporation of locked nucleic acid (LNA) and digoxigenin (DIG)-labeled oligonucleotide hybridization probes, decreasing the detection limit to 0.05 fM and reducing the exposure time by almost 1000-fold [48][49].

1.6.2 Microarray Technology

Microarray technology is also a solid phase assay type (like NB) and is one the most common technique used for miRNA profiling [47]. Multiple hybridization assays can be done by immobilizing spots of probe oligonucleotide on a solid surface and incubating with labeled complementary strands of the target sequence. A widely used strategy for microarray analysis is fluorescent labeling of miRNA followed by hybridization to capture probes on the array. However, the short length of miRNAs with inherently different melting temperatures (Tm) and the highly similar sequences between miRNA family members make probe design

more difficult than for mRNA arrays. MiRNA probes on a microarray must undergo the same hybridization conditions since they are all on the same microchip. These homogenized hybridization conditions can lead to sequence-dependent differential hybridization affinities that may result in either false positives due to non-specific hybridization or false negatives due to hybridization signals that do not exceed the background threshold. Although the development of chemically modified probe designs, such as LNA and 2'-O-(2-methoxyethyl)-(MOE) can elevate Tm and stabilize hybridization, synthesis and chemical modification of RNA probes can be costly. Like northern blotting, by incorporating LNA capture probes to target miRNAs, the specificity of a microarray increases significantly. More importantly, through selective integration of LNAs, the melting temperature normalizes across all of the captured probe-target duplexes [50][51][52]. The initial step in miRNA microarray profiling is the purification of RNA or miRNA from cells or tissue. Although it is possible the use of total RNA for microarray analysis, because miRNAs only make up for approximately 0.01% of all RNAs miRNA enrichment increases also the sensitivity. After extracting RNA, the mature miRNA can be labeled, usually by using t4 RNA ligase to attach 1 or 2 fluorophore-labeled nucleotides to the 3' end of the miRNA. Appropriate probe design is critical [26]. MiRNA microarrays have been effectively used to study the biogenesis of miRNAs, differential miRNA expression profiles, disease characterization and stem cell development to name a few applications. Tijsen *et al.* used microRNAs in plasma from either healthy controls and or patients suffering from heart failure indicating the feasibility of using microarray platform to detect changes in plasma miRNAs as a marker for heart diseases [53]. Despite having the benefit of usually being less expensive and allowing a large number of parallel measurements, microarray lacks specificity, sensitivity and the ability to perform absolute quantification of miRNA abundance. Consequently, it is rather used as a miRNA screening method and not as a quantitative assay platform [29]. Other disadvantages are the lack of reproducibility since it is dependent upon an evenly distributed surface functionalization and controlled two-dimensional surface reactions and the lack of standardization, since data from different microarrays platforms cannot be accurately compared.

1.6.3 Real –Time PCR

qRT-PCR is considered as the gold standard for gene expression analysis and is used to validate and accurately quantify miRNAS. There are several different approaches for this reaction. The most commonly used qRT-PCR-based miRNA profiling involves reverse transcription of miRNA to complementary DNA (cDNA), followed by real time PCR of the product [29]. The limited length of the mature miRNA, the lack of a common sequence feature like a poly (A) tail, and the fact that the mature miRNA sequence is also present in

the pri and pre-miRNA transcript, pose several challenges for appropriate reverse transcription. Reverse transcription of miRNA to cDNA can be achieved either by using miRNA-specific reverse transcription primers, or by polyadenylation of all miRNAs by *Escherichia coli* poly (A) polymerase, followed by reverse transcription using universal primers consisting of an oligo (dT) sequence on its 5' end [29][54]. In the first method miRNAs are reverse transcribed by using stem-loop specific reverse transcriptase primers. Stem-loop primers are designed to have a short single-stranded region that is complementary to the known sequence on the 3'end of the miRNA, a double stranded part (the stem), and the loop that contains the universal primer-binding sequence. The resulting cDNA is then used as a template for qRT-PCR with 1 miRNA-specific primer and a second universal primer. Stem-loop primers are more difficult to design, but their structure reduces annealing of the primer pre- and pri-miRNA, thereby increasing the specificity of the assay. The second method tails all the sequences with a common sequence and then reverse transcribes the miRNA by using a universal primer. This approach is very useful if several different miRNAs need to be analyzed from a small amount of initial material [29]. In conventional PCR the amplified product is detected after a few amplifications cycle but in qRT-PCR the accumulation of amplification product is measured during the process, in real time, given a quantification of product in the end of each cycle. This detection is done using a fluorescent reporter. Some of the fluorescent technologies that are most used to detect miRNA are SYBR Green I and TaqMan probes [55]. The specificity and sensitivity of any real-time assay is dependent on the design of the miRNA-specific primer. The miRNA-specific primer is in turn dependent on sequence, the GC content of a miRNA that influences de T_m against the complementary sequence of the miRNA-specific primer. Once more the use of LNAs in the oligonucleotide primer increases the thermostability of nucleic acid duplex. Nevertheless the major advantages of qRT-PCR over microarrays are the high sensitivity, specificity and the low amount of starting material that is necessary (nanograms of total RNA). Some disadvantages are the quantity of reagents needed, time consuming and labor intensive to scale method [55]. qRT-PCR is frequently used for miRNA expression profiling and validation of results found using other methods such as NB or microarray [29].

1.6.4 Next- Generation Sequencing

Since the development of massively parallel/next-generation sequencing (NGS), there has been an increase of miRNA identification and discovery. NGS allows not only the confirmation of known miRNAs at high speed and with high throughout, but also the discovery of new miRNAS [29][56]. NGS involves preparation of a cDNA library from the RNA sample, followed by the sequencing of millions of individual molecules. Obtained

sequence reads undergo a bioinformatical analysis to identify and quantify (relative abundance) both known and novel miRNAs using application tools such as miRDeep [56]. Although NGS is a high-throughput assay for miRNA expression profiling, disadvantages of this technique includes the high cost, the high amount of RNA used, and the sequence-specific biases due to enzymatic steps in cDNA library preparation. Nonetheless, *Rao et al.* reported the use of NGS to sequence small RNAs from the male and female adult murine hearts. The authors showed that 40% of the cardiac reads were miR-1 with other abundant miRNAs (miR-29a, miR-26a, and the let-7 family) [29]. There have also been reports of NGS used for differential expression analysis of miRNAs in different diseases, including ovarian cancer, suggesting the usefulness of this technique for diagnostics and early detection [57].

1.6.5 *In Situ* Hybridization

Detection of miRNA by ISH is technically challenging because of the small size of target sequences [29]. This method is based on the complementary binding of a nucleotide probe to a specific target sequence of DNA or RNA. These probes can be labeled with radio, fluorescent-, or antigen-labeled bases. Depending on the probe used, autoradiography, fluorescence microscopy, or immunohistochemistry, respectively, are used for visualization [58]. ISH allows the identification of the cellular origin of expression giving information about disease pathogenesis. The drawbacks are limited sensitivity and specificity, and it is a complicated and time-consuming technique [58].

1.7 Current limitations of MicroRNAs and future perspectives

MicroRNAs offer advantages over the traditional biomarkers since miRNAs are released early in MI and are stable in circulation. They can also be detected with specificity and sensitivity. Circulating miRNAs can offer a less invasive alternative to perform population wide screening. Although they present several advantages there are some issues to be resolved before they can be used in clinical practice. An important observation is that quantification of circulating miRNAs can be greatly affected by its origin (microvesicles, exosomes…) being a source of inconsistent findings. Plasma or serum can also be contaminated with miRNAs from other blood cells and should require a careful interpretation. The day-to-day variation of results and cost involved are also some important consideration. The isolation methods of miRNAs are laborious as well the detection methods used. Compared with the ELISA-based detection of cTn, the gold standard for detection of ACS, the PCR-based methods for detection of circulating miRNAs are highly time consuming. Efforts are underway to make these methods suitable for high-throughput analysis and less

time consuming. There is still a need of future research to understand better the role of circulating miRNAs as diagnostic and prognostic biomarker in CVD [30].

1.8 Microfluidics for Molecular Diagnostics

As stated in the section before the miRNA detection techniques present some drawbacks to allow the use of miRNA as biomarkers in clinical environment. There is a need of having an accurate, fast and inexpensive profiling method. Microfluidics platforms are an opportunity to have faster detection, as well as high throughput, lower reagents consumption and portability for the analytical system [59][60]. By coupling microfluidics technology with DNA hybridization assay it is possible to achieve high sensitivity, enhance hybridization kinetics and decrease the non-specific target-probe binding. It holds great potential to develop low-cost, rapid, automatic PoC diagnosis devices. Nevertheless there are some challenges in this field, such as having clinical relevant low-limit-of detection (LoD), signal enhancement since miRNAs are present in very little concentration in biological fluids and a capacity to do multiplexing [61]. In the next sections it is reviewed microfluidic DNA/RNA hybridization assays and introduced the concept of bead-based microfluidics assays for enhancement of the signal, the approach that was used in this thesis work.

1.8.1 Integrated Microfluidic Systems

Over the past 30 years, microfluidic devices suffered a big evolution but most of the progress in diagnostics applications has been made in the past 15 years [2]. Microfluidics started with microelectronics industry where researcher attempted to improve silicon-based micromachining process using photolithography, etching and bonding techniques. Microelectro-mechanical systems (MEMS) were introduced for the first time in 1979 by Terry *et al.* The term microfluidics refer to any technology that moves microscopic and nanoscale volumes of fluids through micro-sized channel on MEMS. A variety of materials, such as, silicon, glass, soft or hard polymers and biomaterial have been used for microfabrication [62]. One of the most used materials nowadays is the soft polymer polydimethylsiloxane (PDMS). When compared with silicon and glass, PDMS presents some advantages. PDMS is optically transparent to wavelengths between 300 and 2200nm, it is an electrical and thermal insulator (thermal conductivity ≈ 0.2 $W.m^{-1}.K^{-1}$), permeable to gas and nearly impermeable to water, inert and also nontoxic. Moreover, the elastomeric properties of this material allow a good water tightness of connections and also the fabrication of valves and pumps using membranes [2][63]. Also PDMS microfluidic chips can be disposable and hence prevent any cross-contamination [61]. Nevertheless, not many commercial products use devices

fabricated with PDMS due to a gap between academic and industry. Another limitation is the PDMS hydrophobic surface and tendency to swell in organic solvents [2].

Soft lithography is the technique of replicating structures from a master mold onto an elastomeric (such as PDMS) substrate and is a valuable tool for an integrated microfluidic system. Mold masters are typically fabricated by photolithography in order to define a stamp pattern. Stamps are made by curing a prepolymer of PDMS onto a mold master. Apart from "replica molding", a well-known technique for generating a polymer channel replicated from an original silicon master, soft lithography provides simple but robust routes toward the fabrication of micro/nano- structures onto a surface or within a channel [64]. The precision of the structures in the PDMS after molding is extremely high, reaching submicrometric values. But taking in account the elastomeric character of the material and also unpredictable aging phenomena, the optimal microchannel dimensions lie between 5 and 500 μm [63][64]. In the end, the structure must be sealed to glass, plastic or PDMS after a step of surface activation such as oxygen plasma exposure, corona discharge, or UV-ozone treatment. Duffy *et al* introduced surface oxidation to increase the bond strength by activating layers of cross-linked PDMS in oxygen plasma. Surface oxidation is believed to expose silanol groups (OH) at the surface of the PDMS layers that when brought together form covalent siloxane bonds (Si–O–Si). This approach makes the channels more hydrophilic, allowing for easier fluid filling for a period of time after the oxygen plasma treatment. However, the surfaces can quickly revert to their hydrophobic tendency if exposed to atmosphere. Oxygen plasma treatments are also advantageous because they enable the bonding of PDMS to other materials such as glass and prove to withstand higher pressures than the other sealing techniques [65].

1.8.2 Microfluidic DNA/RNA Hybridizations Assays

DNA hybridization in biological and biochemical analysis as been described since 1980s and is nowadays widely used in diagnostics applications. DNA hybridization assays are based on the ability of probe nucleic acids to bind specifically and selectively with their complementary strand target nucleic acid. Probe nucleic acids can be single-stranded nuclei acid (DNA, RNA or miRNA) or oligonucleotides with known sequence. Most current nucleic acid detection methods use labels couples to specific probes, such as fluorescent or chemiluminescent labels. It has also been reported the use of magnetic beads and gold nanoparticles as labels [61]. The advantages of applying microfluidics platforms in DNA hybridization have been demonstrated in several works [66][67][68].

Lange *et al.* demonstrated also that the ability to do DNA analysis with micrometer

resolution facilitates the realization of a functional hybridization assay in addition to low sample consumption, fast reaction rates and an enhancement of the hybridization efficiency [64][69]. Kim *et al.* showed that DNA hybridization reaction time in a microfluidic channel can generate higher signal intensity than a passive hybridization, that could take several hours, specially when working with sample with low concentrations [70]. Chung *et al.* not only confirmed the last results but also was able to decrease the non-specific target-probe binding [71]. In 2008, a technique that incorporated microarrays for the detection of miRNA was first described. The microfluidic biochip consisted of 8 microchannels and the oligomers synthesis was done inside the microchannel. For immobilization, each synthetic miRNA presented an additional tail region at the 3'end for attachment to the surface of the chip. The mature/test miRNA hybridized to the complementary sequence and a biotin labeled nucleotide is added enzymatically in the 5'region. The detection of biotin labeled miRNA was done using streptavidin-phycoerythrin. This allowed the detection to be as low as 20ng/µl. Microfluidics has also been integrated with qRT-PCR to create a high-throughput method for miRNA detection and other groups used microfluidic combined with microarrays technology. In 2012 Zhou *et al.* used a microfluidic microarray that could measure picolitre quantities of sample. In the table a list of miRNA detection methods using microfluidics is summarized [72].

Table 1 - Summary of miRNAs detected using nanotechnology based techniques, its origin and assay sensitivity. Adapted from Lingam *et al.* (2014) [72].

	Detection Method	miRNA Detected	Sample type	Sensitivity
MICROFLUIDICS BASED DETECTION TECHNIQUES	Microfluidic primer extension assay (MPEA)	Let-7 family	Human tissue	20ng/µl
	Fluidigm microfluidics	-	Human tissue, cell lines	10ng/µl
	Fluidigm microfluidics	miR-19a, -20b, -24, -26b, -30c, -93, -106a, -223, -451, -874, -1207-5p and miR-1274a	Prostate cancer patient sera	-
	Microfluidics combined with qRT-PCR	miR-16	Human cell lines	804 copies/ single cell
	Microfluidics combined with qRT-PCR	Global miRNA profiling	Mouse haema-topoietic stem cells	-
	Microfluidics combined with microarray	Global miRNA profiling	Human blood	N/A
	Microfluidics combined with nanotechnology and microarray	Let-7 family	Human cell lines	1fM- 300 copies/µl
	Laminar flow assisted dendritic amplification	miR-21	Synthetic	0.25 amol
	Microfluidics in combination with flow cytometry and fluorescence microscopy	miR-155	Human cell lines	-
	Microfluidics based synthesis of barcoded microparticles	miR-141	Human serum	300aM

Although the basic principle of microfluidics-based DNA/RNA hybridization assays is the same, the formats in which hybridization can be operated are various. In general the formats can be based on direct liquid flow, surface-based DNA/RNA hybridization and probe-functionalized microbeads or other material. In this work the format used was probe-functionalized microbeads. In the next section an overview of physical properties of this systems is presented and a review on the state of the art.

1.8.3 Bead-Based Microfluidic Assays

The integration of bead-based immunoaffinity assays into microfluidic chips is currently an area of growing interest, since the use of bead-based technologies addresses some of the drawback in surface-based DNA/RNA hybridization assays. Microbeads offer several advantages over traditional, planar technologies as a platform to immobilized biomecules, including large surface areas to support reactions (increasing sensitivity), the availability of pre-functionalized bead types, the ability to be assembled into arrays that test for multiple analytes simultaneously and reduced assay times compared to their macroscopic counterparts [73]. Also, analytes attached to the beads can be easily transported in a fluidic system using pressure-driven flow or electric fields, making bead-based microfluidic devices especially vital in providing rapid and accurate detection of disease biomarkers in PoC applications.

In 2002 Kohara *et al.* developed a DNA analysis platform called Bead-array using beads that were conjugated with DNA probes. The hybridization took 1 minute and a 1 amol of fluorescent-labeled oligo DNA was detected [74]. Kim *et al*. studied the hybridization efficiency when using probe-conjugated microbeads in a microfluidic DNA hybridization device. Target concentration, probe surface concentration and flow rate were studied. It was found that the microfluidic system could achieve a detection limit of ~10^{-10} M of DNA, a selectivity factor of ~$8x10^{3}$ and a typical hybridization time in the order of minutes [70]. Li *et al.* used magnetic beads with chemiluminescence detection to perform DNA hybridization with a LoD of 0.1pM [75]. In 2009 by coupling streptavidin-coated paramagnetic microbead, Berti *et al.* proposed an electrochemical geno-sensor for hybridization on a commercial microfluidic platform. The system could obtain a detection limit of 0.2nM [76]. Senapati *et al.* developed a bead-based microfluidic platform that functions by passing fluorescent-labeled DNA through a chamber packed with functionalized beads in a microfluidic channel with detection sensitivity in the range of 100pM [77].

Microbeads can be magnetic beads, metal nanoparticles (gold nanoparticles), liposomes or polymer beads. Agarose beads are a common support for protein detection,

DNA hybridization and affinity chromatography [78]. The system used in this work was inspired in miniaturized affinity chromatography systems that used a column separation packed with beads, presenting higher surface area per unit volume and reduced diffusion distances through the narrow fluid paths between neighbouring particles [79].

In the present work porous-agarose beads were used. The choice of agarose beads is based in part on the potential for scalability since it is derived from inexpensive source (i.e., seaweed). In addition it is possible to tune porosities and exhibit ultra-low nonspecific binding characteristics. The optical characteristics (clear polymer) make them ideal to perform optical detection allowing fluorescence, chemiluminescence and colorimetry [80]. The uniform spherical shape of the particles gives good flow properties and the lower the size of a microbead, the higher is the hybridization rate between DNA capture probes and target molecule. Also, beads with small agarose content correspond to larger pore size, and an easy transport of analytes allowing faster binding rates. Moreover, reactions in microbeads surfaces are more similar to reactions in solution than reactions on planar surfaces [80][81].

Due to the small-scale dimension of microfluidic channels, transport usually exists in the laminar flow regime. This is accessed by the Reynolds number (Equation 1, with ρ being the fluid density, U the average fluid velocity, H the hydraulic diameter of the channel and μ the fluid dynamic viscosity) and it is frequently on the laminar regime when is lower than 0.1. The small dimensions of the channel, which make H, defined by four times de cross sectional area of the channel over the wetted perimeter, a very small number. In this laminar flow regime, diffusion is the most important phenomena for mass transport [63].

$$Re = \frac{\rho U H}{\mu} \tag{1}$$

Accordingly with the results of Thompson *et al.* using a model system of agarose beads functionalized with streptavidin is similar to models for ligands immobilized in flat surfaces but, in this case, taking in account three-dimensional surface and the inclusion of surface exclusion (steric hindrance) effects. Also they do not take in account the kinetics occurring inside the bead but only the kinetics at the beads surface. It was showed that due to non-slip boundaries condition at the beads surface, the fluid velocity slows down considerably in this vicinity. Due to the small Reynolds number, there was no separation bubble downstream the bead. The structure of the flow field impacts the mass transfer analyte to the bead's surface. In the absence of surface exclusion effects and considering a well mixed case of uniform analyte concentration as the analyte diffusion coefficient increases (Equation 2, where κ is Boltzmann's constant, T is the absolute temperature of the

fluid and d_A is the effective diameter of an analyte molecule), the Damkohler number decreases (Equation 3, where k_a association reaction rate constant and R_T is the concentration of the immobilized receptor sites on the bead), and the kinetics at the bead surface becomes progressively more reaction rate limited. (See equation 2 and 3)

$$D = \frac{kT}{3\pi\mu d_A} \tag{2}$$

$$D_a = \frac{k_a R_T H}{D} \tag{3}$$

The binding rate can be accelerated not only by increasing the analyte diffusion rate, but also by increasing the flow rate. At higher flow speeds, in which it is more likely for reaction limitation to exist, just a small fraction of flowing molecules is actually exploited. However, the cost of losing molecules has the benefit of allowing a faster achievement of maximum binding density. This speed is also positively influenced by the molecule concentration in solution in a quasi-linear behavior. They estimated the k_a to be 1.6 x10^5 $M^{-1}S^{-1}$ and the k_d (dissociation reaction rate constant) to be 3x$10^{-5}$$s^{-1}$ and it is referent to a biotin-streptavidin system. The minimum analyte concentration that the beads array could detected within 10 minute of incubation time was of ~9pM. They also showed that fluorescent intensity of the beads is independent of the focal plane position along the beads height [73]. Nevertheless, is important to notice that in this case a single compressed bead was modeled instead of a pack of beads. Due to this some interactions factors between the beads were not taken in account, which could influence the results when applied to the system used in this work.

Chou *et al.* studied the kinetics inside the beads and concluded, with computer simulations, that at high densities of capture probe, mass transfer of free analytes to the internal core of the porous bead matrix is limited. This gives high signal localized at the rim of the bead. However, if the initial capture probes at the rim of the bead become bound, a moving boundary of bound analytes develops and penetrates radially towards the center of the bead matrix. This moving boundary continues as free analytes bind to internal capture probe site, until the bead is completely saturated with bound analytes. However, lower capture probe densities result in lower saturation intensities, but allow for faster analyte binding into the bead matrix. These results were later confirmed experimentally [80].

Currently, microbeads are captured in microfluidic devices by physical entrapment or magnetic fields. These methods create a mass of trapped beads that cannot be easily analyzed individually [78]. The easiest integrated method is the mechanical barrier, especially if the beads are agarose beads without magnetic properties. The mechanical

barriers used can be a dam or pillar structure. Dam structures are easy to fabricate but in other hand results in a nonuniform flow profiles. Although pillar type structures allow uniform liquid flow the fabrication process is more complex when compared with dam structures. A dam type of structure was used in this work to trap beads inside the channel [79].

In this work it is used the affinity of streptavidin to biotin to create a complex streptavidin-biotinylated DNA probe and thus perform immobilization onto the beads. It was used a ratio of 4:1 DNA-biotin to streptavidin with a prior incubation step before the immobilization is performed (since it was showed in previous work to be the optimal ratio for the immobilization of probe DNA in a bare channel) [82]. The immobilization of the previous mix to beads surface is due to electrostatically interactions, since the probe DNA backbone is negatively charged and the beads are positively charged. Nevertheless having this complex works as an amplification step since streptavidin allows in the limit the binding of 4 biotinylated DNA. This could also help to have the DNA probes in such a position that enable an easier target hybridization, instead of having probe DNAs completed binding to the beads in all the strand length. Also this allowed maintaining the protocol for immobilization in a bare channel and thus having less variability if comparison between the bead assay and the bare channel assay was needed. According to Neish *et al*. at a molar ratio of 1:1 DNA-biotin to streptavidin, the most common structure observed was streptavidins occupied by a single DNA-biotin molecule (60%), but having also almost 12% of streptavidins occupied by two DNA-biotin molecules. When the molar ratio of DNA-biotin to streptavidin was increased to 10:1 the occupancy by one or two DNA-biotin molecule was almost the same (~38% in both cases) [83].

Due to the small amount of volume per sample in microfluidics applications the detection method is always a challenge. Several techniques are currently used and every single one tries to be highly sensitivity and specific to the target analyte. Some of the detection technologies being used are electrochemical, mechanical and optical. Electrochemical detection biosensors present a low shelf life and a mechanical detection technique involves expensive micro/nanofabrication process. The optical detection is the most widely used and presents some advantages in comparison to the last ones like minimal sample preparation, real time detection and the use of equipment present in every laboratory [84]. In this work optical detection methods were used.

1.9 Limit of Detection

The LoD is usually used to define the sensitivity of the systems. For all the analysis the results are qualitative rather than quantitative. To calculate the limit of blank (LoB) and the LoD the following equation were used as presented by Ambruster and Pry [85].

The limit of blank gives the value of highest DNA concentration that can be found in replicates of a blank sample. The blank sample contains only buffer and 0% of DNA. The LoB is defined as

$$LoB = mean_{Blank} + 1.645(SD_{Blank}) \quad (4)$$

The limit of detection is the lowest analyte concentration that can be distinguished with certainty from the LoB and as so, detectable. It depends on the LoB and in replicas of a sample that contain the lowest known concentration

$$LoD = LoB + 1.645(SD_{Low\ Concentration\ samole}) \quad (5)$$

The LoD can also be calculated using several replicas (e.g, n=20) of a black sample as determining the mean value and SD and then calculate the LoD as

$$LoD = mean_{Blank} + 3*(SD_{Blank}) \quad (6)$$

In this work equations 4 and 5 where used to obtained the LoD. One problem with this method is that there is no certain that a low concentration of analyte will be distinguishable from the blank sample signal. Besides that, the LoD in equation 6 can be used if the SD of the blank sample is similar to the SD with analyte, if not the analyte should account for the LoD and the equation 5 should be used.

1.10 Aim of Studies

The objective of this work was to develop a bead based hybridization assay to allow the detection of target analytes such as miRNAs. The system was optimized using first probe and target DNAs to achieve clinical relevant LoD. Several beads were to be tested as physical support for immobilization. Blocking agents were studied to minimize the nonspecific binding and background signal. Several optical detection methods were used and proved to be appropriated for the system. Moreover, it was expected to prove that the system could be used not only with buffer but also with biological fluids, such as serum. The final goal is to have a system that can be the base to have in the future a microfluidic device to detect miRNA in blood as a CVD biomarker.

2. Materials and Methods

The methodologies, used during this work, are defined in this chapter. First, all reagents and materials are listed. Then the microfabrication process used for the assembly of the optimized microfluidic device used is described step-by-step. The experimental setup is illustrated and protocols used during this work are detailed. Finally, the analysis methodology used for the results acquired is explained.

2.1 Reagents and Materials

2.1.1 Solutions

Phosphate buffered saline (PBS) (Sigma-Aldrich P4417) stock solution of 10mM was prepared by dissolving one tablet in 200 mL of DI water (pH 7.4, 25°C; 137 mM NaCl, 2.7 mM KCl, 10 mM Na_2HPO_4 and 2 mM KH_2PO_4) and is used on the preparation of several solutions and as the main buffer. The PBS working solution was filtered through a 0.2 μm syringe filter purchased from Whatman GmbH. Milli-Q water (18MΩ.cm, Millipore) was also used in the preparation of several solutions. When experiments in a bare channel were performed, silanization of a glass surface was required a working solution of 1% (3-aminopropyl)triethoxysilane (APTES) was prepared using a filtered 99% APTES stock solution (ACROS Organics 430941000) and diluted in Milli-Q water. In chemiluminescence assays, 3-morpholino-2-hydroxypropanesulfonic acid sodium salt (MOPSO) was also tested as a buffer and it was purchased to Sigma-Aldrich M8767.

Several types of blocking agents were tested during this work. Bovine Serum Albumin (BSA) was purchased to Sigma-Aldrich A2153 and was prepared from a stock solution of 1μg/ml that is diluted to a 4% (w/v) BSA solution with filtered PBS. Sodium Polyacrilate (PAA) 45% (w/w) (1200 [416010] or 8000 [416029] average molecular weight) and PAA 35% (15000 [416037] average molecular weight) were all purchased to Sigma-Aldrich and diluted with PBS to 5% (w/w) working solution. Salmon Sperm DNA was obtained from a stock solution of 200μg/ml and diluted to a 100 μg/ml working solution.

Polyethylene glycol (PEG) was used as a suspension solution for the Beads. PEG (8000 Da average molecular weight) was purchased from Sigma-Aldrich P4463 and diluted to a working solution of 33% (w/w).

Streptavidin (Sigma-Aldrich S4762) stock solution was diluted to a 1mg/ml working solution in PBS and stored at -20°C.

For the chemiluminescence experiments Streptavidin, horseradish peroxidase conjugate (Strep.-HRP) was purchased from Invitrogen S-911 and was diluted from the stock solution to 1 mg/ml in PBS and stored at -20°C. Also for the same experiments Luminol SuperSignal® West Femto Chemiluminescent Substrate kit was purchased from Thermo Scientific 34094.

For colorimetric assays 3,3',5,5'-Tetramethylbenzidine (TMB) was used. Pierce™1-step Ultra TMB blotting Solution was purchased to Thermo Scientific 37574.

For hybridization experiments in serum, Fetal Calf Serum (FCS) is used (Thermo Fisher 16250-078) and Human Serum (provided by IMN).

All the experiments were performed at INESC-MN's facilities.

2.1.2 Beads

In this work three types of Beads were studied, namely Controlled Pore Glass (CPG) Beads, Q-Sepharose Fast Flow Beads and DEAE Sepharose Fast Flow Beads. The first was purchased to EMD Millipore (CPG1000B500G) and the last two were purchased to GE Healthcare (17051001 and 17070901, respectively).

CPG beads are used as a solid support for liquid chromatography. These beads present a narrow pore size distribution and a large internal surface. In the present work CPG beads with 100 nm nominal pore diameter and an average mesh of 80 μm were used. The beads were functionalized with APTES, presenting a positive charged surface. The functionalization principle on these beads is the same on a bare channel used in [82]. The APTES reacts with water hydrolyzing ethoxy groups. These groups form a hydrogen bonding with the hydroxyl groups of the glass surface and give rise to siloxane covalent bonds. Due to the positively charged amine groups in the APTES monolayer the channel also becomes positively charged allowing an electrostatically immobilization of the complex streptavidin-single-stranded DNA (ssDNA) Probe.

Q-Sepharose ® Fast Flow Beads are also used in chromatography, in particular the one involving ion exchange. They are composed of 6% crosslinked agarose beads that are functionalized in the surface with quaternary ammonium (Q) strong anion exchange groups, giving to the beads a positively charged surface that allows as well an electrostatically immobilization of the complex streptavidin-ssDNA Probe. DEAE Sepharose ® Fast Flow Beads (DEAE Beads), like the latter, are used in chromatography as ion exchange platform. They are composed of 6% crosslinked agarose beads that are functionalized on the surface

with diethylaminoethyl (DEAE) weak anion exchange groups. This means that the DEAE beads ion exchange capacity will depend on the pH (they are positively charged at a neutral pH) while the Q beads are completely charged between pH 3.0 and 11.0. As the working conditions are similar to physiological conditions (pH around 7.4), this will not have much relevance.

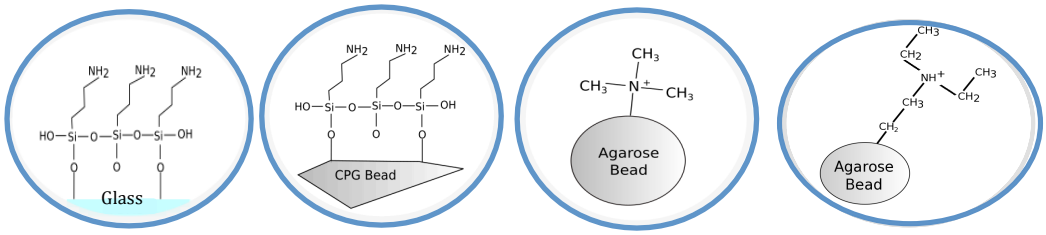

Figure 5 - Schematic of the surface functionalization on the bare channel, CPG, Q-Sepharose ® and DEAE-Sepharose ® Beads, respectively from left to right.

2.1.3 DNA Oligonucleotides

In order to test the beads as a platform for DNA immobilization and hybridization, synthetically modified oligonucleotides sequence were purchased to StabVida Genomics Lab. The oligonucleotides were kept stored at -20°C in aliquots of 100μM. The oligonucleotides working solution was prepared upon utilization and different concentrations tested in this work were achieved by sequential dilution of the stock solution with PBS. The oligonucleotides used are described in Table 2. Probe DNA was modified at the 3'end with a biotin molecule to allow the binding of streptavidin (affinity coupling).

In this work three types of optical detection were tested. For immobilization experiments Probe DNA was labeled with a fluorophore at the 3'-end and two different fluorophores were used, 6-FAM and Atto-430. 6-FAM (6-Carboxyfluorescein) (similar to FITC in both molecular structure and spectral properties) has an excitation peak at 495 nm and an emission peak at 520 nm. Atto-430 has an excitation peak at 433 nm and an emission peak at 545 nm. Fluorescence detection was performed. For hybridization experiments three types of detections were used. They were fluorescence, chemiluminescence and colorimetry detection. For the first, both targets, complementary and non-complementary (negative control), were labeled with a fluorophore at the 3'-end, Atto-430. For chemiluminescence and colorimetric experiments, targets mentioned before were biotinylated to enable first a chemiluminescence detection with Streptavidin-HRP and the luminol solution, and after that a colorimetric detection with TMB.

Table 2 - Name, sequence, modifications (Mod) and application of the oligonucleotides used in this work.

Oligonucleotide	Sequence	5' Mod	3' Mod	Used for
ssDNA Probe Affinity coupling	5'-CAGGTCAAAAGGGTCCTTAGGGA-3'	6-FAM	Biotin	Optimization of the immobilization step
ssDNA Probe Affinity coupling	5'-CAGGTCAAAAGGGTCCTTAGGGA-3'	None	Biotin	Used as probe to capture the target molecule
ssDNA complementary target	5'-TCCCTAAGGACCCTTTTGACCTG -3'	None	Atto-430	Target molecule used in Fluorescence experiments
ssDNA non - complementary target	5'-CGTGTCGTTCACATCTGTCCGT -3'	None	Atto-430	Negative control for Fluorescence
ssDNA complementary target	5'-TCCCTAAGGACCCTTTTGACCTG -3'	None	Biotin	Target molecule used in Chemiluminescence experiments
ssDNA non - complementary target	5'-CGTGTCGTTCACATCTGTCCGT -3'	None	Biotin	Negative control for Chemiluminescence

2.2 Microfabrication

Three different molds were used. One for the bare channels experiments, that consist on a simple linear channel and which was already available. The second and the third molds were similar having a microfluidic system composed by a larger and wider channel followed by a smaller one. The differences between them were only the dimensions of the channels and the number of channels per mold that were optimized. The second mold was also available. The microfabrication process explained here was done for the third mold only.

As the microfluidic channel is composed by a larger and wider channel followed by a smaller one two different hard mask were necessary. For both of them the process is similar

and the fabrication process is done by a standard lithography. First, the design of the masks was done using the AutoCAD 2012 software. After cleaning a glass substrate (Corning glass, 2.5x5 cm), an Aluminium (Al) layer of 100nm was deposited by a Nordiko 7000 magnetron sputtering system. This was done under clean-room conditions (INESC MN, 100/10). Then using an automatic coating track a positive photoresist (PFR 7790G, JSR) layer of 1µm was spincoated on to the Al layer. The design of the mask is transferred to the photoresist by a direct write lithography (DWL), where the photoresist is exposed to a HeCd laser beam (442 nm) that scans the surface of the sample line by line, according to the mask design. The development of the photoresist followed the lithography, leaving selected parts of the Al layer exposed. Those areas were then etched by wet etching using an aluminium etchant (Microchemicals TMAW238WA). (see Figure 6)

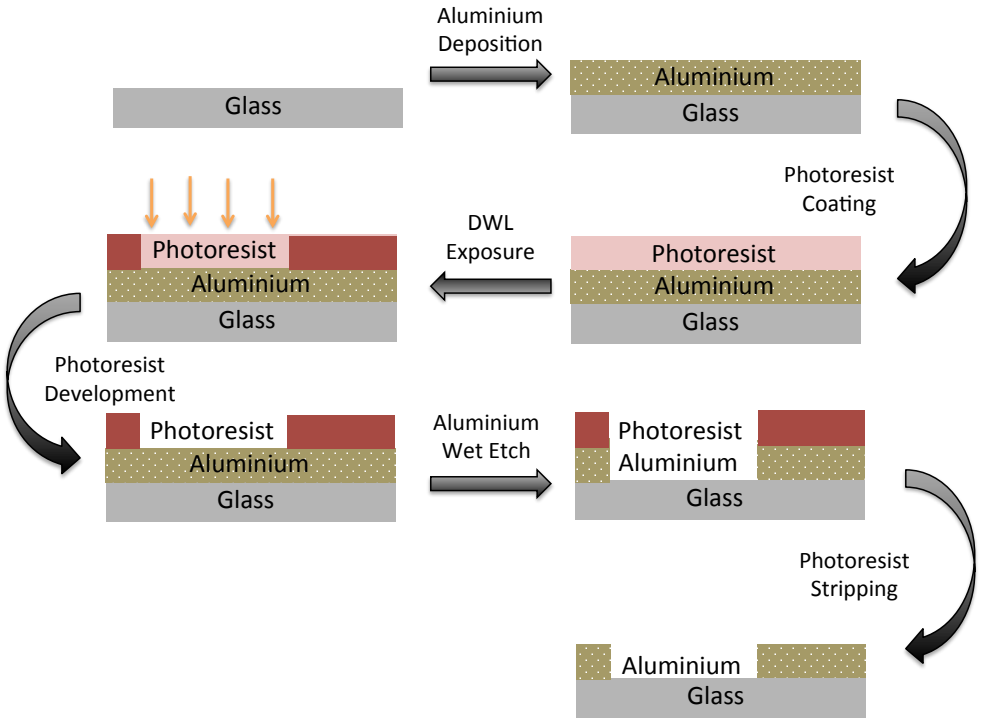

Figure 6 - Schematics of the hard mask fabrication (side view). Dimension of the materials not to scale.

The next step was the fabrication of a SU-8 mold. For this it was necessary to clean a silicon substrate first using acetone and then submerging the silicon substrate in Alcanox for 15min in a 65°C hot water bath. After this an SU-8 (Microchemicals 2015) layer was spincoated onto the cleaned silicon substrate using a Laurel WS-650-23 spincoater. In this step the process for the two masks was different. For the smaller channel a layer of 20 µm was spincoated onto the silicon substrate and for the larger channel a layer of 100µm was necessary. For the 20 µm layer the following spinning steps were used:

1st step: spin at 500 rpm for 10 seconds with an acceleration of 100 rpm/min

2nd step: spin at 1700 rpm for 34 seconds with an acceleration of 300 rpm/min

Afterwards a pre-exposure bake was performed in hotplate for 4 minutes at 95°C. After cooling down for one minute the hard mask with the 20μm channels was placed over the SU-8 with the aluminium surface facing down. The silicon substrate with the hard mask was inserted in the slot further from the UV light the exposed to it for 30 seconds. The development of the non-exposed photoresist was done after a post exposure bake at 95°C during 5 min and 2 minutes of cooling down. In the developing step a propylene glycol monomethyl ether acetate (PGMEA) 99% solution (Sigma-Aldrich 484431) was used to submerge the SU-8 substrate during 2 minutes with manual agitation to dissolve the non-exposed parts. The substrate was then cleaned with IPA and blow-dried. After this the second layer with 100 μm height was created The substrate is again spin coated with an SU-8 layer using the following spinning steps to achieved the desired height:

1st step: spin at 500 rpm for 10 seconds with an acceleration of 100 rpm/min

2nd step: spin at 1000 rpm for 30 seconds with an acceleration of 300 rpm/min

Following a pre-exposure bake in hotplate for 10 minutes at 65°C followed by 30 minutes at 95°C. After cooling down for one minute the hard mask with the 100μm channels was placed over the SU-8 with the aluminium surface facing down. The mask was manually aligned with the previous structure using a low power AMSCOPE microscope. The silicon substrate with the hard mask was inserted in the slot more apart from the UV light the exposed to it for 70 seconds. The development of the non-exposed photoresist was done after a post exposure bake at 65°C during 1 min followed by 10 minutes at 95°C. The development was performed for 10 minutes with manual agitation. The substrate is then cleaned with IPA and blow-dried. A final hard bake of 15 minutes at 150°C was performed. (see Figure 7)

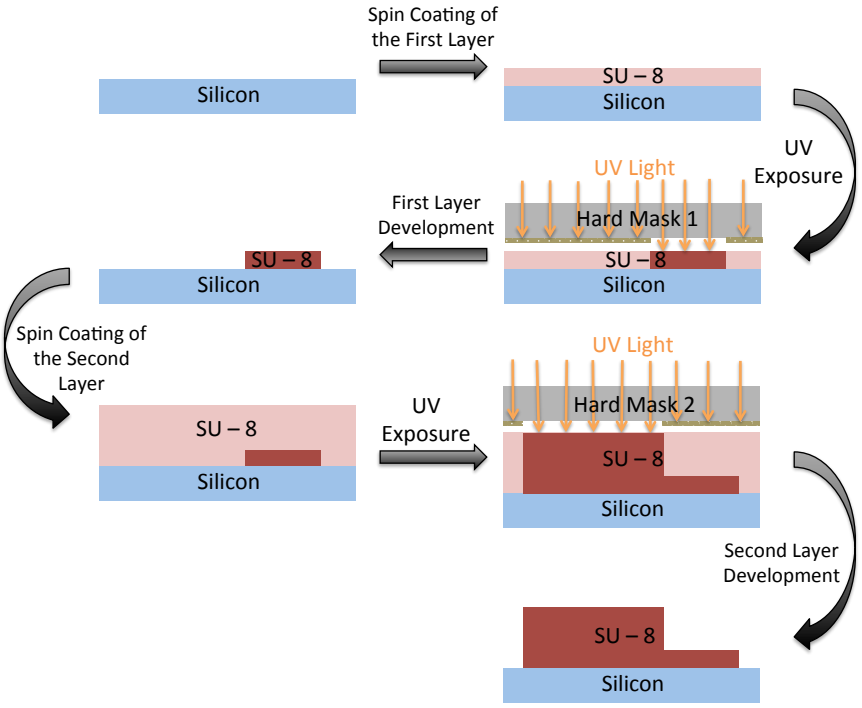

Figure 7 - Schematics of the SU-8 mold fabrication (side view). Dimensions of the materials not to scale.

After this procedure the height of the channels in the SU-8 mold was measured using a Tencor Alpha-Step 200 profilometer. The height of all the larger channels in the mold was around 125-145 µm and for the smaller channels was around 22-23 µm.

The SU-8 mold was then glued with tape to the bottom of a Petri dish (Figure 8).

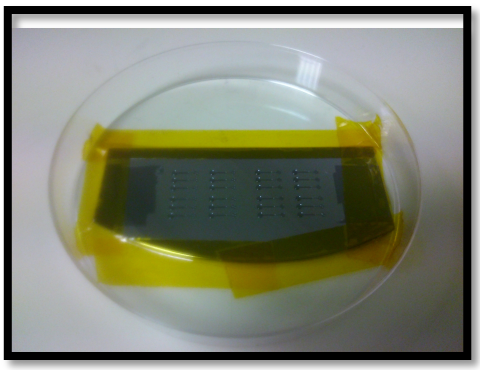

Figure 8 - Final SU-8 mold glued to the bottom of the petri dish with no poured PDMS inside.

The polydimethylsiloxane (PDMS) microfluidic structures were fabricated using a soft lithography technique. To prepare this elastomer it was necessary to mix a 10:1 weight ratio of PDMS and curing agent (Sylgard 184 silicon elastomer kit, Dow Corning) and then the mixture was left to degas in a vacuum for 40 min. The PDMS was poured in the Petri dish with the SU-8 mold covering the bottom part of the Petri dish and filling up with around 1cm height. The Petri dish with the PDMS mixture was left in an oven for at least 90 minutes at

70°C to cure. The cured PDMS was then cut and needles were used to open the inlets and the outlets, 20Ga and 17Ga blunt needles (INSTECH), respectively.

A PDMS membrane was prepared by pouring PDMS over a silicon wafer that was spin coated. The PDMS membrane with 500 µm thickness was achieved by spinning at 250 rpm for 25 seconds with an acceleration of 100 rpm/min. This membrane was also left to reticule in an oven for at least 90 minutes at 70°C. The membrane was then cut into smaller pieces, slightly bigger than the PDMS structures with the channels (Figure 9).

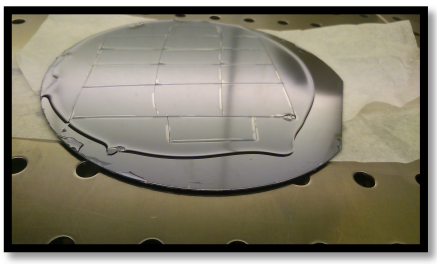

Figure 9 - Cured PDMS membrane divided in small pieces.

To seal the channel, the structure and the membrane were then oxidized using a plasma cleaner (Harrick Plasma) at medium power for 30-60 seconds. The membrane is placed in contact with channel structure right after the plasma treatment and Si-0-Si bonds are formed creating a very strong seal. To enhance the chemical link after the contact and ensure a lasting sealing the structure was then placed over a hotplate for 5minutes as 130°C (Figure 10 and 11).

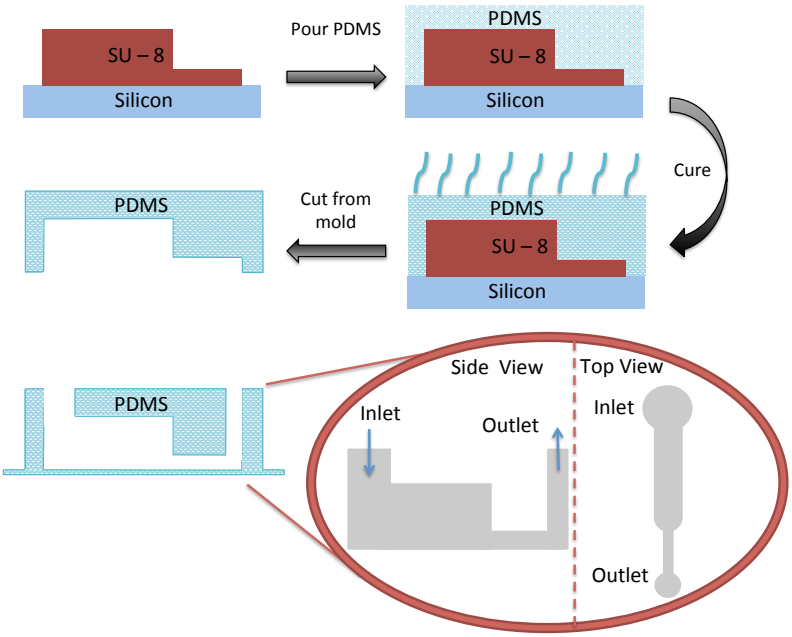

Figure 10 - Schematics of the PDMS fabrication by casting on a SU-8 mold (side view). Dimension of the materials not to scale.

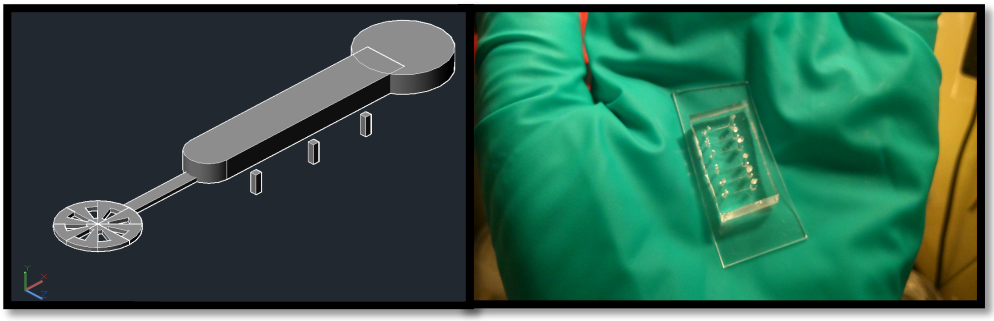

Figure 11 – Right: Schematics of one channel. Left: Final microfluidic device already sealed and with the holes punched.

The fluid manipulation in experimental assays was done with a pumping system (New Era- 4000 microsyringe pump). In particular this micro syringe pump has the ability to both pull (negative pressure created inside the channel) and push (positive pressure created inside the channel) the liquid inside a syringe. Both techniques were tried during this work but in an early stage pull method was defined as the standard method for the assays done. This method proved to be easier and more reliably than the push method, manly because it diminish air bubbles problems and the bead packing was easier and more reproducible in terms of quantity of beads packed. The syringe (1ml insulin luer U-100, Codan) was connected to a luer stub adapter (LS20, INSTECH) and to a tubing (BTPE-90, INSTECH) with a metallic plug (SC20/15, INTECH) in one end. All of this was filled with PBS inside. The metallic plug was inserted in the outlet of the channel, since the fluid in the inlet will be driven to the outlet by negative pressure. It is worth to notice that the metal plug should not be inserted all the way down but at nearly contact distance with the membrane. To dispense the reagents in the inlet pipette tips from eppendorf were used. This complex is then adapted to the pumping system. (Figure 12)

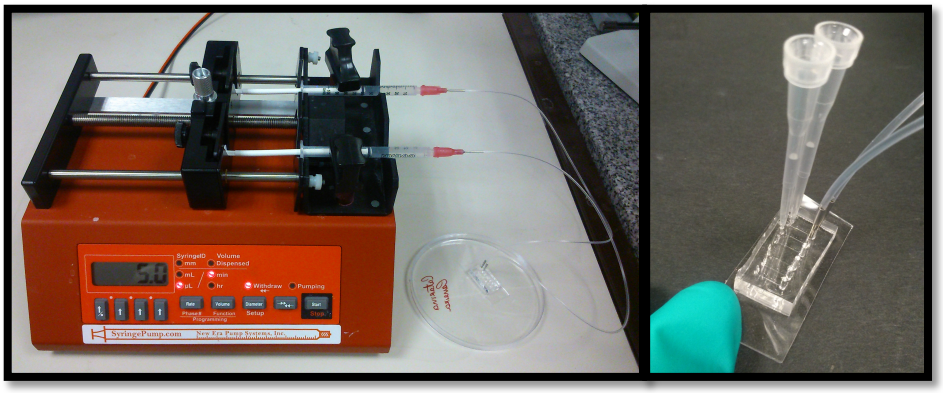

Figure 12 - Experimental setup used to performed all the experiments.

2.3 Fluorescent Measurements

Fluorescence detection method requires the use of a fluorescence microscope (Olympus Microscope CHX41) with a blue light excitation filter that was used throughout the fluorescence assays. The blue light excitation filter used has a band pass illumination path between 450 - 490 nm and a long pass observation path above 500nm. The light source is a 50W mercury lamp. The microscope was coupled to a XC30 camera and the images were acquired using the 10x objective. All the light sensitive reagents were kept isolate from light in eppedorfs cover with paper foil and the experiments were done with minimum light. The measurements were performed at room temperature that was kept constant around 24°C with help of the air conditioning.

An exposure time of 50 miliseconds and gain of 2.5 dB was used for immobilization experiments, unless state otherwise.

For hybridization experiments it was used an exposure time of 5 seconds and a gain of 5dB, unless state otherwise.

2.3.1 Immobilization of Probe DNA

Immobilization of probe DNA assays were carried out into straight PDMS-Glass channel similar to the ones used in [82] with 5 mm length, 200 μm width and 20 μm height. This experiment served as control and to compare with the different beads. Briefly, 1% APTES is passed by the channel at a flow rate of 0,5 μl/min for 10 minutes, to functionalized the surface. A washing step is performed with PBS at 5 μl/min for 1 minute. After that it was flowed a previously mixed solution of streptavidin and biotinylated probe DNA 6-FAM labeled in a ratio of 1:4 and a 10 minutes incubation time at 0,5 μl/min for 10 minutes. The fluorescent measurement was performed during this step measuring first the signal at time zero (without the fluid inside the channel) and then acquiring images from 30 to 30 seconds during the 10 minutes. For this the shutter was open for each individual acquisition, and after that was right away closed to minimized photobleaching. When focusing on the beads a method was done, systematically, to try to have the focus plane on the maximum diameter of the beads in all the images acquired. This methodology was used for the fluorescent measurements, unless state otherwise. Although as mentioned in the introduction the focus plane does not interfere with the results.

To test the immobilization of probe DNA on the beads the second and the third mold were used. For the second mold, the dimensions on the first part of the channel were 1 cm

length, 1mm width and 100 µm height and in the narrow part 3 mm length, 200 µm width and 20 µm height. The immobilization assay was carried out by first pull inside the channel at a high flow rate (105 µl/min) PBS to assure a clean channel, after that a tip with the desired beads to test was inserted in the inlet. This step was not controlled precisely by time. The bead solution consist of 3 µl of 33% PEG solution and 0,3 µl of CPG, DEAE or Q Beads, depending on the beads to be studied. The function of the PEG solution is to suspend the beads and make easier the packing, since is a more viscous solution that the buffer used. The pipette tip inserted on the inlet with 0,3 µl of the last solution is the pulled inside the channel at 5 µl/min. This step was also not controlled precisely by time. After this a washing step must be done to make sure that the PEG is washed away with PBS for 1min at 5 µl/min. then it was flowed a previously mixed solution of streptavidin and biotinylated probe DNA 6-FAM labeled in a ratio of 1:4 and a 10 minutes incubation time at 5 µl/min for 10 minutes and the images were acquired as explained before. In the steps where the time needed to be controlled precisely, it was marked a line with a marker right above the solution that was inside the pipette tip, after this one is inserted into the inlet. The starting flow used in every step was 5 µl/min and only when it was possible to see that liquid in the pipette tip was entering the channel the flow rate was reduced or maintained, depending on the step that was being performed and the timer was immediately started. This control was done for all the experiments here described. When using the third mold the protocol was optimized and the step with the mixed solution of streptavidin and biotinylated probe DNA was performed at 1µl/min for 10 minutes and in this way save 40 µl of reagents when compared with the last protocol. This mold was the one used in the next described experiments.

2.3.2 Blocking Optimization

For the blocking optimization experiments several protocols were used. The first experiment was done to verify if the blocking agents removed DNA probe from the surface of the beads. For that a regular immobilization assay was performed adding an additional step at the end to flow during 10 minutes the blocking agent under study. This allowed the definition of an optimal time for the blocking step. The protocol followed begun with pulling inside the channel PBS at a high flow rate (105 µl/min), after that a tip with the desired beads to test was inserted in the inlet. Then 0,3 µl of the bead solution was pulled inside the channel at 5 µl/min, followed by a washing step with PBS for 1min at 5 µl/min. Then it was flowed a previously mixed solution of streptavidin and biotinylated probe DNA 6-FAM labeled in a ratio of 1:4 and a 10 minutes incubation time at 1 µl/min for 10 minutes followed by another PBS washing step at 5 µl/min for 1 minute. The blocking agent is inserted into the

channel at 5 µl/min during 10 minutes. The acquisition methodology is the same as stated before and done in the last step mentioned.

To assure that selected time was enough to allow a good blocking two experiments were performed, which differed only in the time, used in the blocking step (2 and 10 minutes, respectively). The protocol was similar to the last but in this case the blocking was performed first than the probe DNA immobilization. The protocol followed begun with pulling inside the channel PBS at a high flow rate (105 µl/min), after that a tip with the desired beads to test was inserted in the inlet. Then 0,3 µl of the bead solution was pulled inside the channel at 5 µl/min, followed by a washing step with PBS for 1min at 5 µl/min. Then the blocking agent was flowed inside the channel at 5 µl/min during 2 minutes in one set of experiments and 10 minutes in another. After that another PBS washing step at 5 µl/min for 1 minute was done. Finally, it was flowed a previously mixed solution of streptavidin and biotinylated probe DNA 6-FAM labeled in a ratio of 1:4 and a 10 minutes incubation time at 1 µl/min for 10 minutes. The acquisition methodology is the same as stated before, for both experiments.

2.3.3 Hybridization Experiments

After the experiments for the blocking optimization it was verified first if the hybridization occurred using the blocking agent that was selected using for that a fixed concentration of target DNA (100 nM). Different concentrations of target DNA were also tested. For all the hybridization experiments done in this work, each experiment was performed in two separated channels simultaneously, unless state otherwise, one with the complementary target and another with the non-complimentary target (negative control). Once more the protocol followed begun with pulling inside the channel PBS at a high flow rate (105 µl/min), after that a tip with the desired beads to test was inserted in the inlet. Then 0,3 µl of the bead solution was pulled inside the channel at 5 µl/min, followed by a washing step with PBS for 1min at 5 µl/min. Next, it was flowed a previously mixed solution of streptavidin and biotinylated probe DNA in a ratio of 1:4 and a 10 minutes incubation time at 1 µl/min for 10 minutes followed by a PBS washing step for 1min at 5 µl/min. Then the blocking agent was flowed inside the channel at 5 µl/min during 2 minutes. After that another PBS washing step at 5 µl/min for 1 minute was done. After this as the pump pulls the two syringes at the same time, it was necessary to disconnect the metal plug in the outlet from one channel, maintaining the pipette tip in the inlet with PBS to minimize liquid evaporation inside the channel. This was done because it was only possible to acquired one channel each time due to the dimensions of the channel. Finally, it was first flowed in the channel that

was still connected, ssDNA non-complementary target Atto-430 labeled for 10 minutes at 1 µl/min and images were acquired as stated before. After connecting again the second channel, and disconnected the last channel that was measured, ssDNA complementary target Atto-430 labeled was flowed for 10 minutes at 1 µl/min in the second channel and images were acquired. All the images were saved in .tiff format and analyzed using the image software Image J.

2.4 Chemiluminescence and Colorimetry Measurements

Chemiluminescence was used also as a method of detection for lower concentrations than the ones detected by fluorescence when doing hybridization experiments. The colorimetric method was also tested to prove that was another possible way of detection. For the chemiluminescence and colorimetry a Leica DMLM microscope was used that was coupled to a DFC300FX camera. The images were acquired using the 10x objective. The measurements were performed at ambient temperature that was kept constant around 24°C with help of the air conditioning. Instead of using target molecules labeled with fluorophores, target molecules modified with biotin at the 3'end were used to allow the binding of Strep.-HRP . For the chemiluminescence and colorimetric assays an alteration of protocol was performed. In this case it was necessary to block the surface of the channel, before having beads inside, with 4% BSA to avoid unspecific biding of streptavidin-HRP onto the PDMS.

The protocol followed for the hybridization experiments started with pulling inside the channel PBS at a high flow rate (105 µl/min), after that a tip with the desired beads to test was inserted in the inlet. Then a blocking step with 4% BSA was performed at 1ul/min for 5 minutes, followed by a PBS washing step at 5 µl/min for 1 minute. Then 0,3 µl of the bead solution was pulled inside the channel at 5 µl/min, followed by a washing step with PBS for 1min at 5 µl/min. Next, it was flowed a previously mixed solution of streptavidin and biotinylated probe DNA in a ratio of 1:4 and a 10 minutes incubation time at 1 µl/min for 10 minutes followed by a PBS washing step for 1min at 5 µl/min. Then the blocking agent was flowed inside the channel at 5 µl/min during 2 minutes. After that another PBS washing step at 5 µl/min for 1 minute was done. In the next step it was flowed in one channel ssDNA non-complementary target biotin labeled and in the other ssDNA complementary target biotin labeled, simultaneously, for 10 minutes at 1 µl/min followed by a PBS washing step at 5 µl/min during 1 minutes. Finally it was flowed a 100 µg/ml Strep.HRP solution inside the channel at 1 µl/min for 10 minutes followed by a last PBS washing step 5 µl/min during 4 minutes to make sure that all the unbound Strep.HRP was washed away. After this the acquisition was performed, one channel at a time, following the same steps described for the fluorescence methods. Starting again with the non complementary target channel 1:1 luminol

and hydrogen peroxide solution flowed inside the channel at 20 µl/min.. During the acquisition the microscope was covered with a black cover and all the lights in the room were turned off to minimize noise signals. Also upon preparation of 1:1 luminol and hydrogen peroxide solution, minimum light was used in the room and the eppendorf covered with paper foil. The same procedure was done for the complementary target channel. An exposure time of 10 second was used with a 10x gain and the image was only acquired when no changes were perceptible between two images displayed in the computer monitor, that usually occurred after 20seconds-50seconds after the beginning of the chemical reaction. Because of that an amount of at least 20µl 1:1 luminol and hydrogen peroxide solution was used for each channel, meaning that for the two channel 20 µl were necessary.

After this it was possible to also do a colorimetric detection using the same channels, since HRP reacts with TMB. Using 30 µl of TMB solution that was flowed inside the channels, one at a time, at 10ul/min during 3 minutes images were acquired. In this case an image at time zero was acquired (without TMB inside the channel) and after the TMB entered the channel and the timer had start counting, images at 30 second, 1,2 and 3 minutes were acquired. In this experiment minimum light was used in the room and the light of the microscope was in maximum position. An exposure time of 15 µsecond was used with a 10x gain. All the images were saved in .tiff format and analyzed using the image software Image J.

2.5 Analysis Methodology

2.5.1 Fluorescence Measurements

When analyzing the bare channel images a region of interest with square shape inside the channel was selected and then the background was defined as a region outside the channel. The Image J software allows the image to be splinted in the blue channel, green channel and red channel and the green was the one used to measure the intensities. The output is a mean RGB intensity value in the regions selected. An absolute value was obtained by subtracting the background average intensity with the average intensity from the channel region. If the channel presented homogenous fluorescence intensity, only one measurement inside the channel was performed, with a region of interest being the entire channel. Though, if the channel presented non-homogenous fluorescence intensity, three regions along the channel were selected and a mean of the three was used instead. This region selection method was also used by other [82].

For the channel with beads instead of a square shape, a round one was used to analyze the beads area. For sequence images an effort was made so that the area of the region of the interest was maintained along the same experiment, both for beads region and background regions. In this case the background region was considered to be inside the channel where no beads were present. When comparing complementary target channel with a non-complementary target channel, both background areas and bead areas were kept constant, when possible.

2.5.2 Chemiluminescence Measurements

For the chemiluminescence measurements all the experiments were done with beads and the same method for region selection, used in the fluorescence measurements, was applied. It was also verified that select 3 individual beads and averaged them or select an area with several beads inside and having the average intensity value of that area would not affect greatly the final values.

2.5.3 Colorimetric Measurements

When analyzing colorimetric images the same method for region selection was applied. After analyzing the images the results were processed. The absolute values presented in graphs are the mean values from three experiments, unless state otherwise, with the error bars correspond to the standard deviation from that three experiments. For the blocking study graphs that are normalized to the initial value are also presented. In the hybridization assays the results are main presented as a ratio between the complementary target value and the non-complementary target value. Usually for colorimetric measurements the transmission of light is evaluated by having the values normalized to the initial transmission. Since the initial transmission on the beads region was very regular in the experiments it was considered constant and not used to calculate the ratio between the complementary target value and the non-complementary target value.

3. Results and Discussion

In this chapter, the results obtained using the methods described in the previous chapter are presented. These results were treated using the software Image J (image analysis) and Prism 6 (results presentation).

First, using fluorescence detection different beads were tested as physical support for probe DNA immobilization. After choosing the best physical support, an optimization of the flow rate used for the electrostatic binding of the probe DNA onto the beads was performed. Since the optimal flow rate required considerable reagent consumption, it was also important to optimize the channel dimensions. Using this new channel, hybridization of 100nM target DNA was attempted. To improve the hybridization ratio of c-DNA and nc-DNA blockings studies were performed. Working towards the detection of lower target concentrations and to try to achieve lower signal backgrounds, chemiluminescence and colorimetric detection methods were tested. Finally, the optimized assay was used to test the applicability of the system for Fetal Calf serum and Human serum, as a dilution buffer.

3.1 Physical support choice - Immobilization of Probe DNA on Different Functionalized Beads

The first step to develop a bead-based microfluidic system for DNA/RNA detection the choice was to choose the most adequate functionalized bead and to verify that the use of beads as platform enhances the signal of immobilizing probes when compared with a similar experiment in a bare channel.

Three beads were tested, as stated before, and probe immobilization occurred due to electrostatic interactions between the backbone of the DNA single strand (negatively charged) and the surface groups on the beads (positively charge).

The beads were introduced inside the channel by pressure-driven flow and retained in a dam structure. Figure 13 presents the results obtained and in Figure 14 a diagram of the channel is presented, schematizing the region where the beads are trapped and where the signal is measured (A). Figure 14.B, C and D present fluorescent images from the bare channel, the DEAE Sepharose ® beads and the Q-Speharose® and CPG beads, respectively. These images were captured in the last minute of the immobilization step.

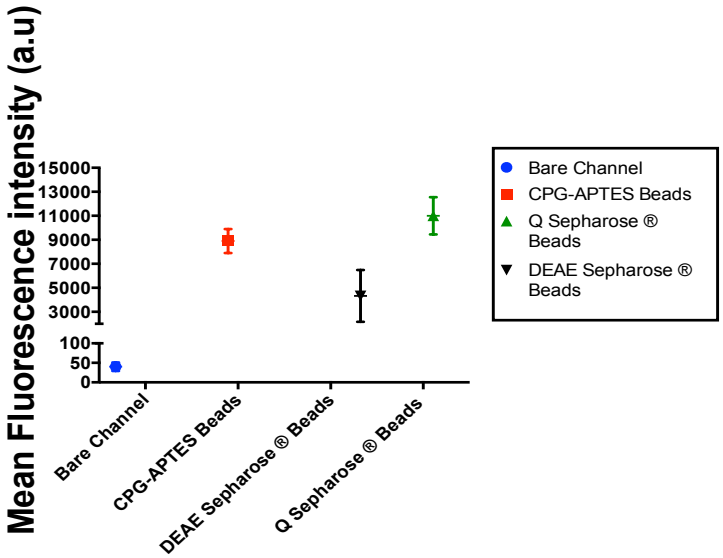

Figure 13 - Immobilization of probe DNA onto several physical platforms. The error bars represent the standard deviation of three repeated measurements. (Olympus Microscope CHX41, exposure time: 50ms, gain: 2.5dB, magnification:10x).

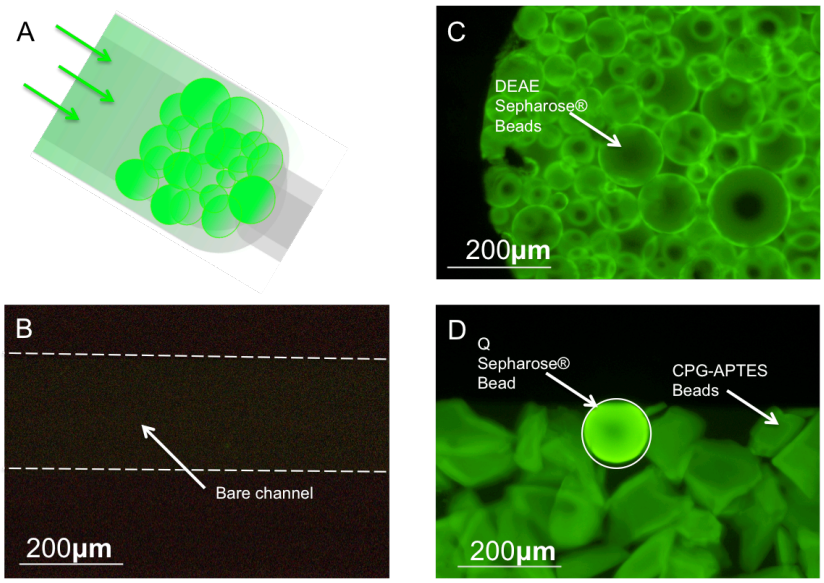

Figure 14 - A. Diagram of the restriction area inside the channel where the beads accumulated and where the images were acquired. The arrows represent the direction of the flow. B. Experimental image from the bare channel for the immobilization of probe DNA. C. Channel with DEAE Sepharose ® beads. D. Channel with CPG and Q-Sepharose ® beads exposed to the same experimental conditions. All the experimental images were acquired in Olympus Microscope CHX41, exposure time: 50ms, gain: 2.5dB, magnification:10x.

By analysis of Figure 13 it is clear that the beads that allow more immobilization of DNA probes onto the surface are the Q-Sepharose ® Beads, assuming that the emitted light (and so the fluorescence intensity) is proportional to the concentration of probe DNAs that were immobilized. Nevertheless, CPG beads are the second best choice for a physical support. Since the values for the Q-Sepharose ® Beads and the CPG beads were very similar, an experiment where the two beads were exposed to the same conditions was performed to be sure which one presented higher levels of immobilization. As it is possible to

see in Figure 14 D. the last two beads mentioned are present in the same channel and it is clearly visible that Q-Sepharose ® Beads have higher fluorescence intensity. The DEAE Sepharose ® beads presented a wide range of variability, calculated as the standard deviation of the means of three individual measurements. Some of this variability in the results could be related with the micro channel characteristics, such as the surface treatment used for the sealing. In this part of the work, surface oxidation using corona discharge treatment was used to perform the bonding between the PDMS structure and the PDMS membrane and it is known from the literature that reliability and repeatability of this technique presents 20% of bonding strength fluctuation [86]. Although it is an irreversible bonding method, robust and that can easily sustain high pressure applications when performing the experiments it was noticed the occurrence of some leakage problems usually with origin in one local in the interface of bonding that started to lift, hence creating a leakage. To avoid this problem, later during this work, bonding was performed using oxygen-plasma treatment ending with leakage problems. In fact if during one experiment the channel clogged, the bonding remained intact and it was possible to see instead the PDMS channel swelling with liquid. Also using high flow rates, and having high pressure inside the channel did not affected the boding either. It was possible to conclude that oxygen plasma treatment proved to be better than sealing the structures with corona discharged, presenting a more robust sealing, capable of withstanding both higher positive and negative pressures.

The variability in the DEAE Sepharose ® beads experiments can also be explained due to the surface groups. Although the DNA binds tightly to the beads, when comparing the charged group of Q-Sepharose ® and DEAE-Sepharose ® it is possible to hypothesized another reason for the values present in Figure 13. Q-Sepharose ® beads have a quarternary amine which carries a non-titratable positive charge and the DEAE-Sepharose ® beads, contains a diethylaminoethyl group, with a tertiary amine, protonated (and positively charged). It is positively charged at neutral pH and at an alkaline pH values the positive charge of the DEAE group is titrated. From the literature it is known that DEAE group start to lose its charge above a pH of 9. The buffer used had a theoretical pH around 7.4 that was not checked in every experiment and could present little fluctuations. Although those fluctuation are small and not enough to prevent an electrostatic binding of the DNA probe, it could account for some variability on the DEAE-Sepharose ® beads experiments.

A bead-bound quarternary amine extends the range of anion exchange to pH 12, such is the case of the Q-Sepharose ® beads, and it is called a strong anion exchanger. When looking at the chemical structure of the surface groups in both DEAE-Sepharose ® and Q-Sepharose ® in Figure 15 we can hypothesize that due to steric hindrance the

electrostatic binding of the probe is affected. The tertiary amine on the DEAE-Sepharose ® beads has ethyl groups that are larger than the methyl groups in the quarternary amine on the Q-Sepharose ® beads. Steric hindrance is greater at the nitrogen atom in the surface groups on the DEAE-Sepharose ® than that in the nitrogen atom in the surface groups on the Q-Sepharose ®. Another reason can be the ionic capacity of the Q-Sepharose ® beads that is higher than the ionic capacity of DEAE-Sepharose ® beads, meaning that the Q-Sepharose ® beads has an ability to load more ions to the resin.

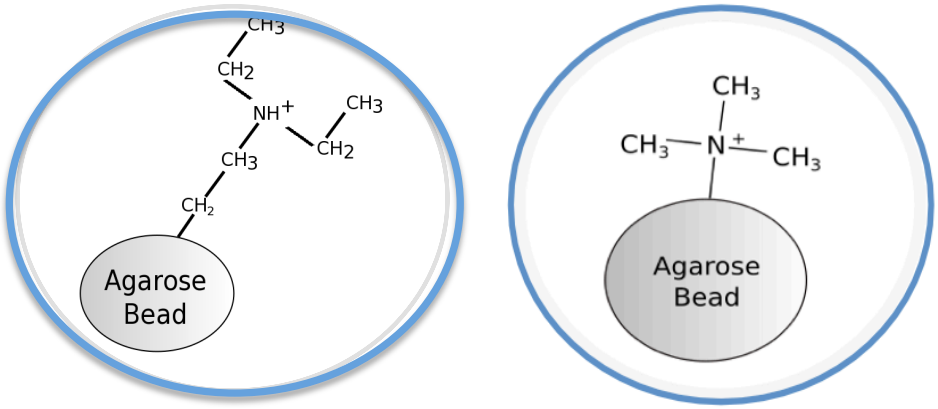

Figure 15 - Diagram of the functional groups on the surface of DEAE Sepharose ® beads (right) and Q-Sepaharose ® beads (left).

Regarding the DNA binding onto a silica surface it is known that ssDNA has stronger binding than double-stranded DNA (dsDNA) to silica [87]. This has been explained by increased opportunity for hydrophobic interactions between the unpaired bases of single-stranded DNA and the silica surface. Also ssDNA is more flexible, and therefore able to maximize the number of complementary DNA-silica interactions. The number of each type of interaction – phosphates-silanol, hydrophobic, and sugar hydroxyl – was lower for dsDNA compared to ssDNA. Also the linear charge density of dsDNA is twice the ssDNA charge. When using a silica surface that was silanized with APTES the surface becomes positively charged as shown in other works [88]. Silanization begins with the hydrolysis of ethoxy groups in APTES, a process catalyzed by water, leading to the formation of silanols. APTES silanols then condense with surface silanols forming a monolayer of APTES via a lateral siloxane network in which amino groups are oriented away from the underlying silicon surface. This process is similar for the CPG APTES functionalized beads. The structure and thickness of this monolayer are known to be affected by preparation conditions and choice of reaction solutions. In this work an aqueous solution was used to perform the silanization and in this case the APTES films grew by electrostatic or hydrogen bonding according to the literature [89].

When comparing the values of immobilization on a bare channel with the values of porous beads it was clear that there was an increase in the surface to volume-ratio provided by the beads, thus allowing more hybridization sites for the target DNA. This lead to an enhancement in the sensitivity and the LoD, in particular, a 200 fold higher signal intensity was obtained when using Q-Sepharose ® Beads, in comparison with a bare channel.

In all the experiments preformed a continuous pressure-driven flow was used. From the literature it is know that an active flow through the microfluidic channels provide one of the most efficient capture environment since the flow guarantees a continuous supply of analytes to the capture molecules, compensating greatly any sample depletion due to surface binding.

Pressure-driven flow has a parabolic velocity flow profile, which causes sample plug dispersion and peak broadening. Moreover, channel dimensions cannot be too small, as high pressure is required to counter the fluidic resistance in such channels. Another factor that is usually considered in these experiments is flow rate. As flow in microchannels is laminar, mass transfer is diffusion limited and it is important to have a continuous flow of reagents in order to ensure the presence of analyte at the boundary layer. As stated before, for pressure-driven systems, it is often advantageous to use large channels to avoid back-pressure. However, such systems are less attractive because they present increased reagent and sample consumption. A balance must be reached between the size of the microfluidic device and flow rates to obtain optimal assay performance [90]. The use of micro beads in the channel promotes both laminar and turbulent mixing and an effective mixing increases the velocity of diffusion-controlled reactions [91].

When performing the last assays, a 5µl/min flow rate was used in the immobilization step during 10 minutes and a minimum volume of 50µl was used. The bare channel assay used a 0,5µl/min flow rate during the 10 minutes and fewer reagents are used. Since decrease of waste is a concern in microfluidics, an assay to optimize the flow rate was performed.

For the analysis of the results the method used was the one described in section 2.5. This method was chosen since it was verified that analyzing individual beads or a larger area with several beads did not affect the final result (See Appendix 6.1).

3.2 Immobilization of Probe DNA onto Q-Sepharose ® Beads – Flow Rate Optimization

It was compared an immobilization step performed at 5µl/min and at 0,5µl/min, both during 10 minutes. The results are presented in Figure 16.

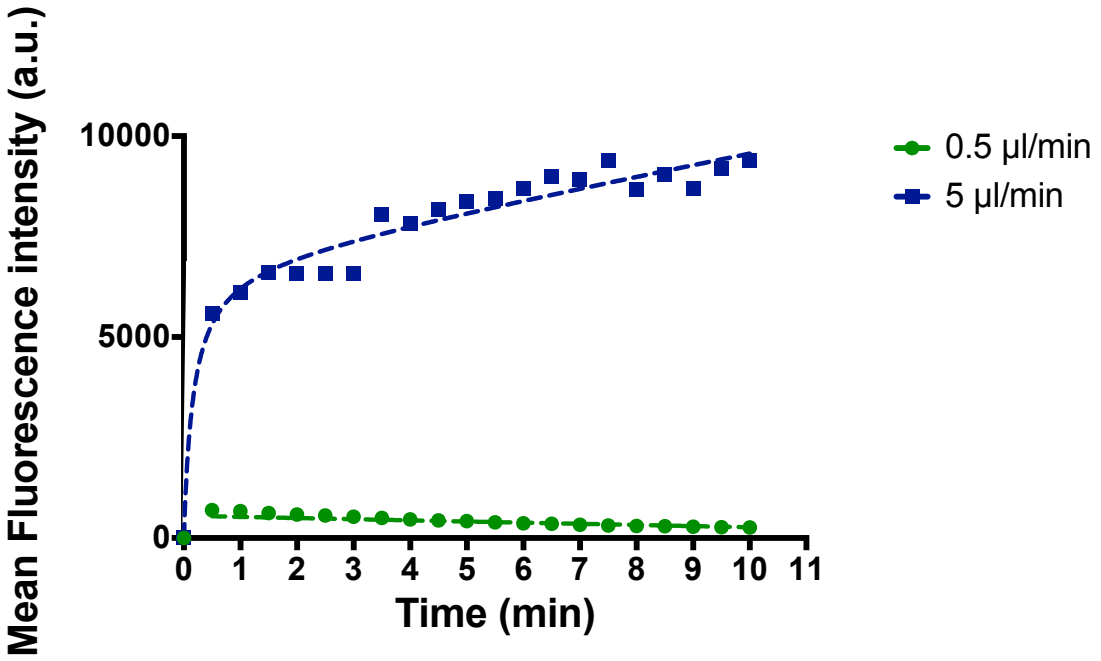

Figure 16 - Fluorescence intensity of immobilization assays. Two flow rates were tested 5 µl/min (blue) and 0.5 µl/min (green). The dash lines fitting the data are a guide to the eye. (Olympus Microscope CHX41, exposure time: 50ms, gain: 2.5dB, magnification:10x).

From the Figure 16 it is possible to verify that when using a flow rate of 0,5 µl/min the immobilization onto the beads is not effective contrasting with the 5µl/min flow rate, in which it is possible to see a hyperbolic behavior similar to other binding kinetics curves.

Depending on the flow rate two regimes can exist: a transport-limited regime and a reaction-limited regime. In the reaction limited regime total analyte capture is limited by the rate of capture or the inherent association constant K_{on}. In this case no depletion layer exists outside the bead.

In the transport-limited regime total analyte capture is limited by the flow, or transport, of analytes to the beads.

In Figure 17 it is possible to visualize the different fluorescence intensities on different parts of the channel. (A) and (C) are located near the restriction zone were all images are acquired. (B) and (D) are near the inlet and it is possible to see that the intensity of the fluorescence signal is similar in that zone. That indicates that for the 0.5 µl/min flow rate there is a transport-limited regime in the restriction zone. The DNA is being capture by the first beads and there isn't sufficient concentration of probe DNA reaching the beads in the restriction zone.

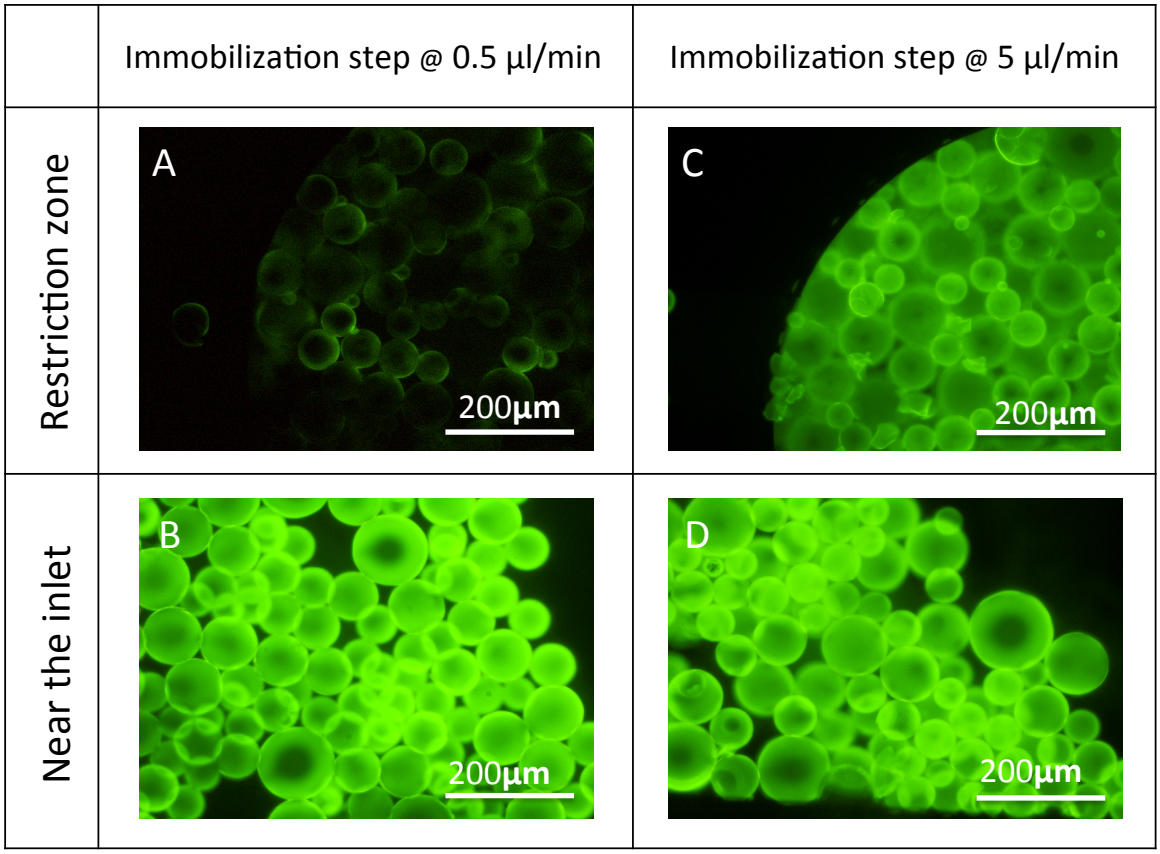

Figure 17 - Experimental images from the data present in Figure 17. A. Fluorescence intensity in the restriction zone using a 0,5 µl/min flow rate. B. Beads near the inlet zone using a 0,5 µl/min flow rate (A and B are from the same channel and same assay). C. Fluorescence intensity from the beads in the restriction zone for the experiment at 5 µl/min. D. Beads near the inlet zone using 5 µl/min flow (C and D are from the same channel and same assay). (Olympus Microscope CHX41, exposure time: 50ms, gain: 2.5dB, magnification:10x).

In the literature it is stated that at low flow rate, when the bead surface becomes saturated, while there are plenty of remaining unbound sites inside the bead, the rate of reaction is limited due to the need for the analyte to be transported to the internal binding sites via convection and diffusion. Because the bead interior is more transport-limited, most of the fluorescent signal quickly develops at the outer rim of the bead. In this case, this is visible in Figure 17 B. and A. where the bigger beads are more intense at the rim since they are transport limited and a clearly fluorescence gradient is observed

Photobleaching is characterized by a reduction in signal and can be caused by an excessively long excitation step. Typically this is not a problem due to the low power and short excitation exposure times associated with today's fluorometers. Another conclusion is that the decrease in intensity for the immobilization step using 0,5µl/min flow rate is due to photobleaching phenomena since it has a linear dependence.

One can also conclude that when the outer surface of the bead saturates with bound

probe DNA, unbound probe DNAs, which cannot bind to any unbound sites near the rim of the bead, can be transported further into the bead before capture. This porous medium enables an extended signal development, in which the final signal is an aggregation of the total fluorescence on multiple focal planes across the semi-transparent, agarose bead. This was already verified by mathematical models [92].

Porous microbeads offer the advantage for delivery of analytes into the interior core, as the labeled analyte complex is much smaller than the pore size of the fibrous network. In this work were used Q-Sepharose ® Beads (6% cross-linked agarose) with average particle size of 90µm and pore sizes 4,000kDa (50nm), according to literature [93]. Streptavidin has a size of 60-kDa (5nm in diameter) and it is shown in literature that upon binding of the biotin to streptavidin the thickness of the complex increases 0.05 nm and ssDNA with 22 nucleotides long (using 0.43nm for base pair) should have around 9.5nm [94][95]. The complex Streptavidin-Probe DNA should be small enough to diffuse inside the porous. Under high rates of delivery, fluorescent signal should develop further inside the bead. In Figure 18 B and D it is possible to differentiate beads where the center is less bright and beads that have already homogenously fluorescence intensity, which is correlate with the size of the beads. As expected, the probe DNA will take more time to diffuse to the center of larger beads.

Accordingly to the literature the amount of penetration into the bead is non-linear with respect to the rate of sample delivery. This is due to reaction kinetics and to the slower transport of DNA probe inside the bead [92]. It is also possible to conclude that the binding is reaction-limited at the rim of the bead under high flow rates of delivery and inside the beads it is transport-limited. These results are in agreement with previous studies.

In this work the immobilization step time was fixed for 10 minutes. Nevertheless, having the sample flowing inside the channel during more time would allow an increase in DNA probe capture. This increase in time is preferable to an increase in sample volume where more reagents are used.

3.3 Channel Dimensions Optimization

When performing the last assays a 5µl/min flow rate was applied in the immobilization step during 10 minutes and a minimum volume of 50µl was used. When comparing with the protocol performed in [82] for the bare channel where a 0,5µl/min was applied, 45µl of reagents are used in excess. To reduce the reagents volume an optimization of the channel dimensions was performed. This was also helpful to avoid smaller beads trapped in the narrow part of the channel thus leading to clog problems. In a simplistic way, and since the

heights were maintained, the principal dimension to be considered in this case was the width of the larger channel where the beads were trapped. The width in the larger channel (zone 1 in Figure 18) was changed from 1mm to 200µm, which represents a decrease of a 5 fold. Assuming that the flow rate is proportional, with this change in dimension, the equivalent flow rate of 5µl/min becomes now 1µl/min in this new channel.

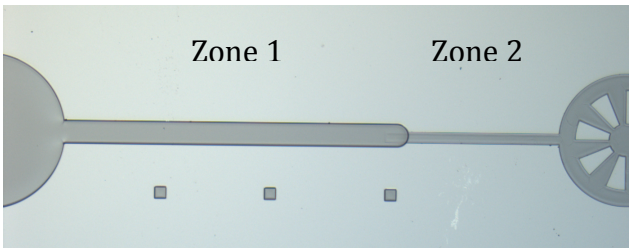

Figure 18 - New channel structure. Zone 1 represents the larger channel and the zone two represents the smaller one.

To test this hypothesis an immobilization assay was performed in the new channel using for the immobilization step 1µl/min. The results are presented in Figure 19.

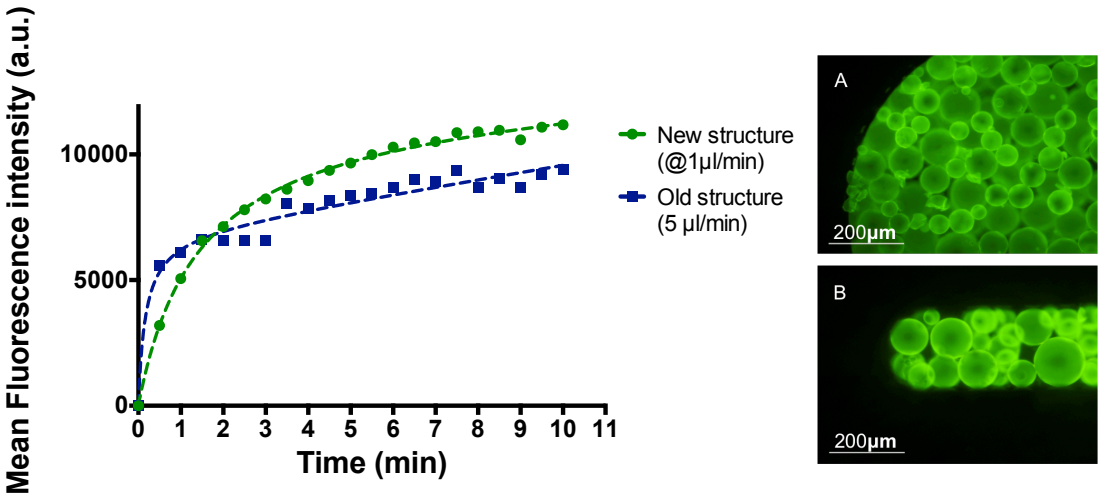

Figure 19 - Left. Results comparing the use of 5 µl/min flow rate in the new channel with the old results. Right. A. Experimental image from the older structure. B. Experimental image from the new channel. The images are from the experiments represented in the graphic. The dash lines fitting the data are a guide to the eye. (Olympus Microscope CHX41, exposure time: 50ms, gain: 2.5dB, magnification:10x).

It was verified that indeed 1µl/min presented a similar result to the 5µl/min in the old structure and that the trend was maintained. In this way, it was possible to perform the immobilization step during the 10 minutes using a minimal volume of 10 µl. This represents a saving of 80% of reagent sample when compared with volume used for the 5µl/min flow rate in the old structure, maintaining the amount of immobilization of DNA probe onto the beads surface. Also it was possible to conclude from the results in Figure 19 that the amount of fluorescent signal increased considerably in the first minute, reaching half of the final

fluorescence intensity. This can be explained by the close packing of the beads thus decreasing the diffusive transport time from the bulk to the probe surface. It stabilized after 9 minutes, reaching 95% of the final value. It is important to state that the final value may not be at a saturation state and that experiments were not performed to evaluate saturation of probe DNA immobilization.

The immobilization experiments were performed using FITC as a fluorophore molecule. Since for the hybridization assays the only available target DNAs were labeled with Atto-430, immobilization using DNA probe-Atto 430 labeled was also done using the new flow rate. Although the immobilization results are not directly compared with the hybridization values since there is some variability between fluorophores. Nevertheless, is reasonable to expect to have lower signal intensities for hybridization assays.

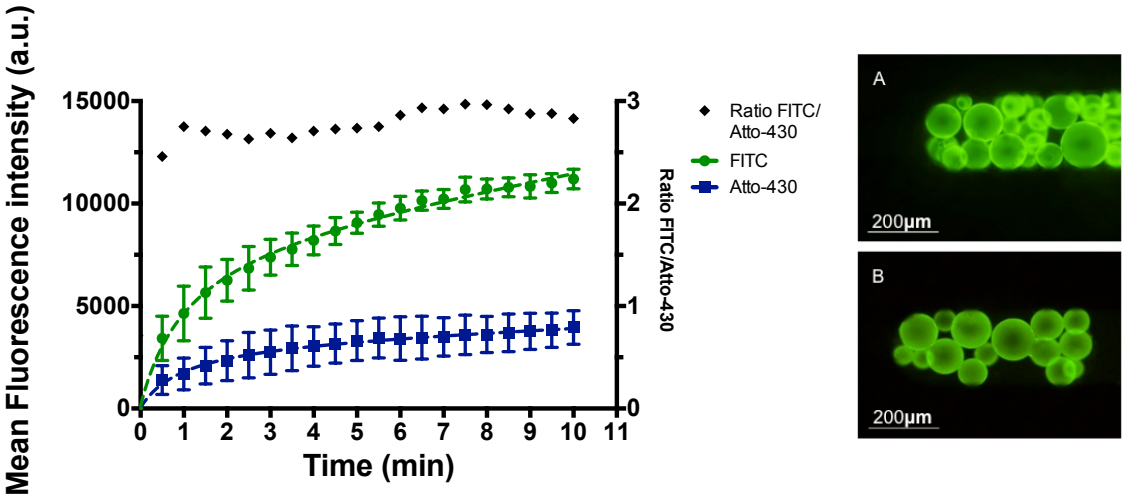

Figure 20 - Immobilization assays using two different labels, FITC (green) and Atto-430 (Blue). The ratio is calculated by dividing the absolute mean fluorescence intensity from the FITC experiments by the values from the Atto-430 experiments. Fluorescence intensity after 10 minutes of an immobilization assay using FITC. B. Fluorescence intensity after 10 minutes of an immobilization assay using Atto-430. The error bars are the standard deviation of three repeated measurements. The dash lines fitting the data are a guide to the eye. (Olympus Microscope CHX41, exposure time: 50ms, gain: 2.5dB, magnification:10x).

In Figure 20 we can see that trend line is maintained as expected and that the immobilization using probe DNA-Atto430 presents lower fluorescence intensity. Nevertheless the ratio between FITC and Atto-430 is maintained during the experiment, which can indicate that the difference in intensity is due to different fluorophores intensities (FITC appears to have 3 fold high intensity over Atto-430) and not because of different rate of probe DNA immobilization. Another way to verify this could have been to have measured a drop of FITC and Atto-430 under the same conditions and evaluate fluorescence intensity. It is also worth mentioned that the molecules used in all experiments were already in the laboratory, and some of them were already one year old which could also have contributed for such

differences and that is why some experiments were performed only one time, since the reagents were limited.

It was also verified that having a washing step of 1 minute after the immobilization did not decreased greatly the signal of immobilized probes onto the surface beads. For instance, using images from the experiments in Figure 21 it is possible to see that signal intensities were similar. For the FITC experiment after a washing step of 1 minute the signal decreased 2% and for the Atto-430 the signal decreased 8%. This means that the majority of probe DNA inside and surrounding the beads are successfully bound to the surface beads.

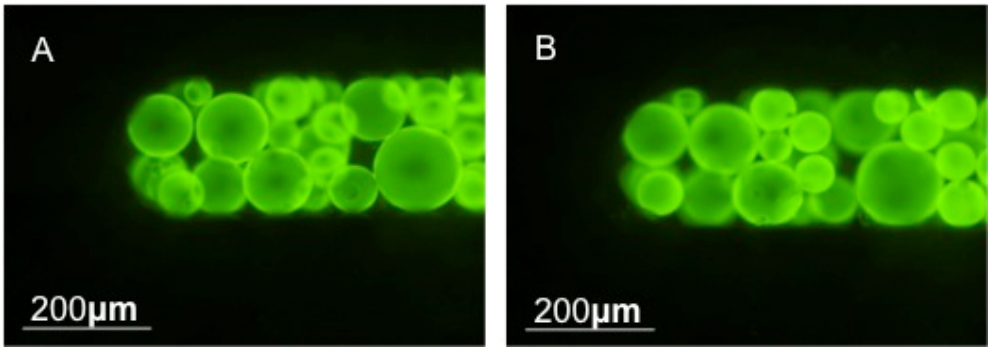

Figure 21 - A. Imaged acquired after 10 minutes of an immobilization experiment. B is the same channel presented in A and the image was acquired after one minute of washing with PBS. (Olympus Microscope CHX41, exposure time: 50ms, gain: 2.5dB, magnification:10x).

3.4 Understanding the effect of the Complex Streptavidin + DNA Probe in Immobilization and Hybridization

As stated in the introduction, in this work it was used the affinity of streptavidin to biotin to create a complex streptavidin-biotinylated DNA probe to perform immobilization onto the beads. It was used a ratio of 4:1 M DNA-biotin to streptavidin with a prior incubation step before solution insertion into the channel. This ratio was used following the work done in [82] but that protocol was optimized for assays in a bare channel. To study the influence of the complex streptavidin-biotinylated DNA probes several studies were performed. One of the experiments consisted in just flow DNA probe into the channel during the immobilization step and another experiment was just to flow streptavidin FITC labeled, to compare with the immobilization protocol used. The results are presented in Figure 22.

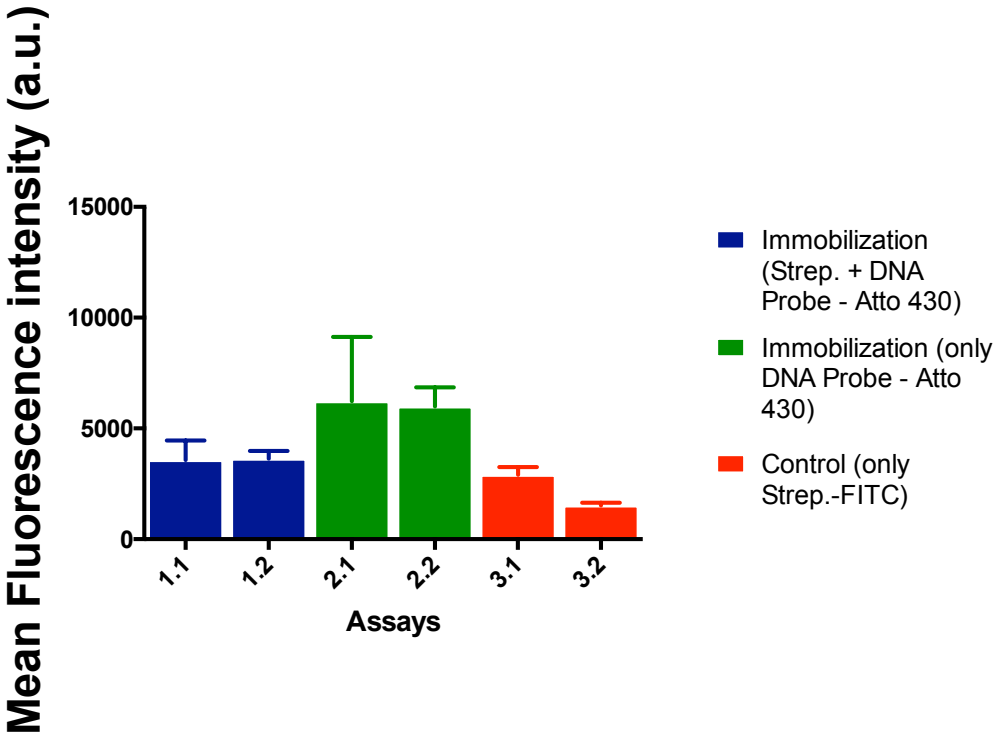

Figure 22 - Results from experiments to understand the effect of the complex Streptavidin-biotinylated DNA probe. 1.1, 2.1 and 3.1 bars represent the fluorescence intensity after 10 minutes of immobilization time. 1.2, 2.2 and 3.2 represent the values for fluorescence intensity after one minute washing step. The error bars are the standard deviation of three repeated measurements. (Olympus Microscope CHX41, exposure time: 50ms, gain: 2.5dB, magnification:10x).

From the results shown in the Figure 22 it was possible to conclude that the immobilization only with DNA probe Atto-430 was more efficient than the other represented in blue having an increase of immobilization of 42%. However, it was more prone to variability. One explanation for the higher intensity signal when using only DNA probe could be the size. As stated before ssDNA has around 9.5nm and the complex streptavidin-biotinylated DNA probe is bigger. Being smaller it should be easier for the ssDNA probe to reach near the beads and diffuse inside them. Once more, it was visible that a one-minute washing step did not decreased the signal intensity that much. The control using only streptavidin FITC labeled cannot be compared with the other experiments since it was used a different fluorophore. Nevertheless it was possible to conclude that, although it appeared to exist some immobilization of the streptavidin onto the bead surface, after the one-minute washing step, 47% of the streptavidin was washed away. One can hypothesized that when using the complex streptavidin-biotinylated DNA probe in the immobilization step it was indeed the DNA probe that was bound electrostatically to the beads surface. Nevertheless,

and as mentioned before, having this complex could work as an amplification step and it could also help to have the DNA probes in such a position that could enable an easier target hybridization, instead of having probe DNAs completely bound to the beads in all the strand length. To test this, two hybridization experiments were performed using 100nM target concentration. In one the immobilization was performed using the complex streptavidin-biotinylated DNA probe and in the other it was just used DNA probe. The results are presented in Figure 23 as form of cDNA/ncDNA ratio.

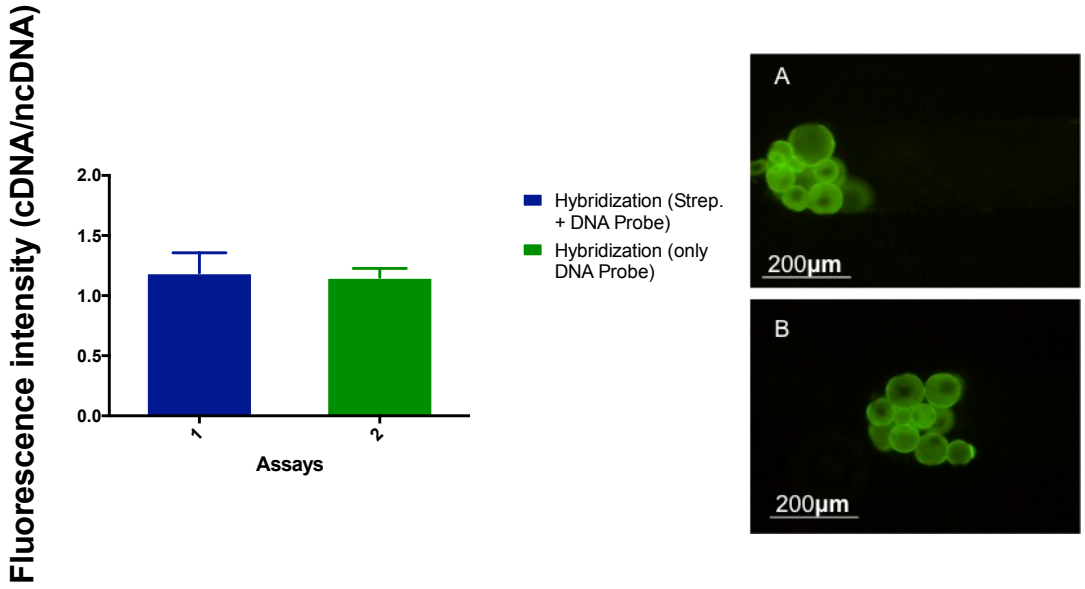

Figure 23 - Hybridization assays. In blue the immobilization was done using the complex streptavidin biotinylated DNA probe. In green the immobilization was done only with DNA probe. A. Experimental image of 100nM cDNA acquired at the end o the hybridization step that used the complex. B Experimental image of 100nM cDNA acquired at the end o the hybridization step that used only DNA probe. The error bars are the standard deviation of three repeated measurements. (Olympus Microscope CHX41, exposure time: 5s, gain: 5dB, magnification:10x).

From Figure 23 it was possible to conclude that although the immobilization of probe DNA appeared to be lower when using the complex streptavidin-biotinylated DNA probe, for the hybridization this was not visible. In fact, the ratio between cDNA/ncDNA was slightly higher when the complex was used. This could be due to the hypothesis mentioned above. Also the amount of target concentration that was being used was not enough to saturate all the DNA probes immobilized onto the beads. The use of a higher target concentration, could allow for the difference to be accentuated. Since the aim was not having saturated beads but instead higher sensitivity towards lowers concentrations, a decision was made to maintain the immobilization protocol using the complex streptavidin-biotinylated DNA probe. Maintaining this immobilization protocol also contributed to have a similar protocol for immobilization in a bare channel and thus having less variability if comparison between the bead assay and the bare channel assay was needed, as stated in the introduction. With this

experiment it was possible to conclude that the ratio between cDNA/ncDNA was very low. To try to improve this ratio an experiment with a BSA (4%) blocking step was performed.

3.5 Detection of 100 nM Target DNA

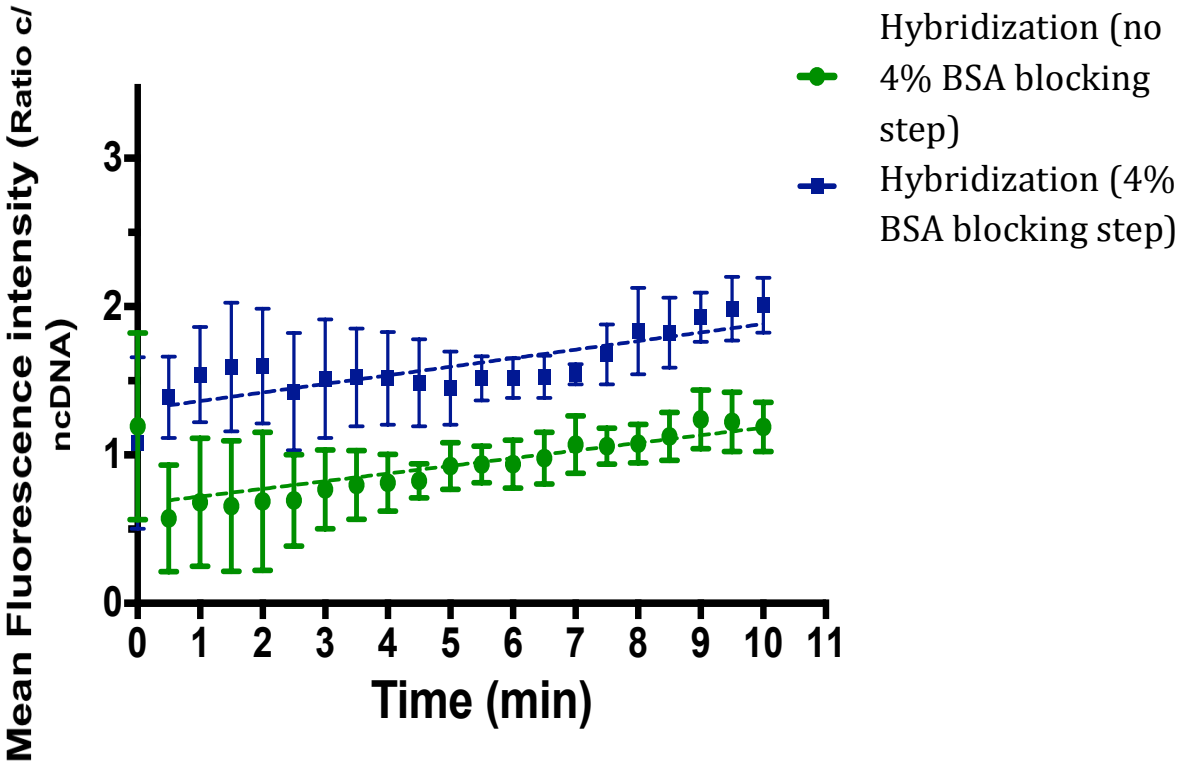

Figure 24 - hybridization experiments. In blue a blocking step with BSA was performed. In green no blocking step was done. The error bars are the standard deviation of three repeated measurements. The dash lines fitting the data are a guide to the eye. (Olympus Microscope CHX41, exposure time: 5s, gain: 5dB, magnification:10x).

Figure 24 shows the results from experiments with a BSA (4%) blocking step, prior to the step where cDNA or ncDNA was inserted into the channel. This was done to try to prevent unspecific binding of target DNA onto the beads.

Analyzing the results, it appeared that the hybridization ratio increased linearly during the assay. This was especially clear in the hybridization without a blocking step. For the hybridization with BSA blocking step this was not so clear. The ratio increased first and the decreased, which could mean that some of the BSA blocking the surface was removed allowing for nonspecific binding. Also it is not certain that the blocking of the beads was homogenous, explaining this behavior.

Nevertheless, the results show that the ratio was improved in average 0.6 when compared with the hybridization assay without blocking. Without a blocking step the

cDNA/ncDNA ratio was higher than 1 almost at the end of the assay. This proved that a blocking step was needed to reduce the nonspecific binding of ncDNA to the beads surface, although the use of BSA (4%) could not be the best. Several blocking studies optimizations were performed to obtain the best blocking protocol for the Q-Sepharose ® beads.

3.6 Blocking Optimization

Working towards the detection of lower target concentrations, the surface-blocking step was optimized by testing different blocking agents. The blocking agents included several PAAs, BSA and, as control, PBS. PAA is an anionic polyelectrolyte that presents carboxylic groups in the main chain negatively charged. Being negatively charged it can bind electrostatic to the beads. Several molecular weights were studied namely 8000, 1200 and 15000 (g/mol). It was expected that the best PAA agent presented a similar molecular weight to the ssDNA target (ncDNA: 7301g/mol and cDNA: 7974g/mol). Since the polyacrylate chain length is function of the molar mass, it is expected the best PAA agent to be the PAA 8000. PAA chains that are longer than the ssDNA, could bind to the beads surface and still be long enough to interfere with hybridization by exerting repulsion forces, since it is negatively charged as the DNA. A small PAA chain could not be sufficient to perform an efficient block. Also several weight percent were tested to choose the optimal viscosity of the PAA solution. Salmon sperm (10µg/ml) was also tested as a blocking agent.

The blocking optimization was first tested by performing immobilization assays.

3.6.1 Optimization Through Immobilization Assays

To start the blocking studies a blocking of the beads surface was performed during 10 minutes with each blocking agent. The results are presented in Figure 25.

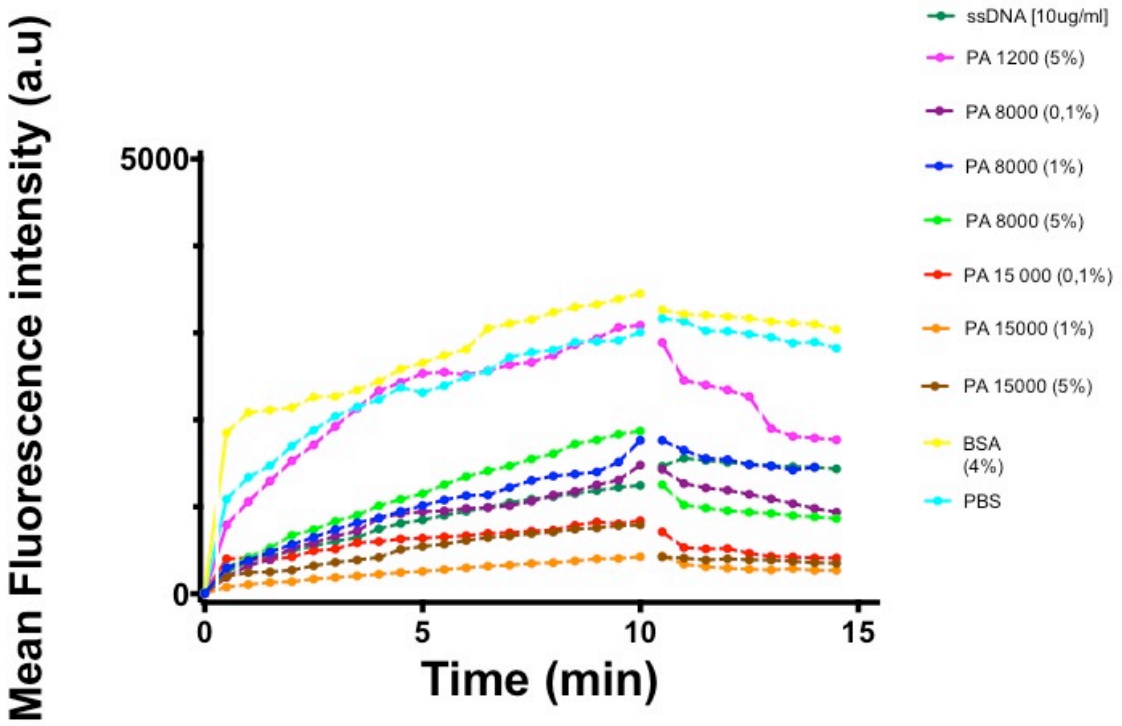

Figure 25 - Blocking studies. Several blocking agents were tested. After 10 minutes of the blocking assay a washing step of four minutes was performed. The dash lines fitting the data are a guide to the eye. (Olympus Microscope CHX41, exposure time: 50ms, gain: 2.5dB, magnification:10x).

By observing Figure 25 it was possible to verify that BSA (4%) and PAA 1200 (5%) were the worst blocking agents, having similar fluorescence intensity signal to the experiment performed with PBS. At this point, PAA 1200 (5%) was discarded as blocking agent. The blocking agents that appeared to block more effectively were the three PAA 15000. The three PAA 8000 and the salmon sperm DNA were in the middle with a very similar fluorescence signal. Nevertheless, it was important to understand if during the blocking step, after having DNA probe already immobilized on the surface of beads, was there a substitution of probe DNA by the blocking agent. If this occurs, the blocking agent is not adequate. The right blocking agent should block the surface but be weak enough so that there is minimal removal of immobilized probe DNA from the beads surface. To evaluate this point another experiment was performed starting with a high fluorescence signal from the probe DNAs already immobilized onto the beads surface. The decrease in the signal was observed during a 10 minutes step where the blocking agents were flow inside the channel. The results are presented in Figure 26.

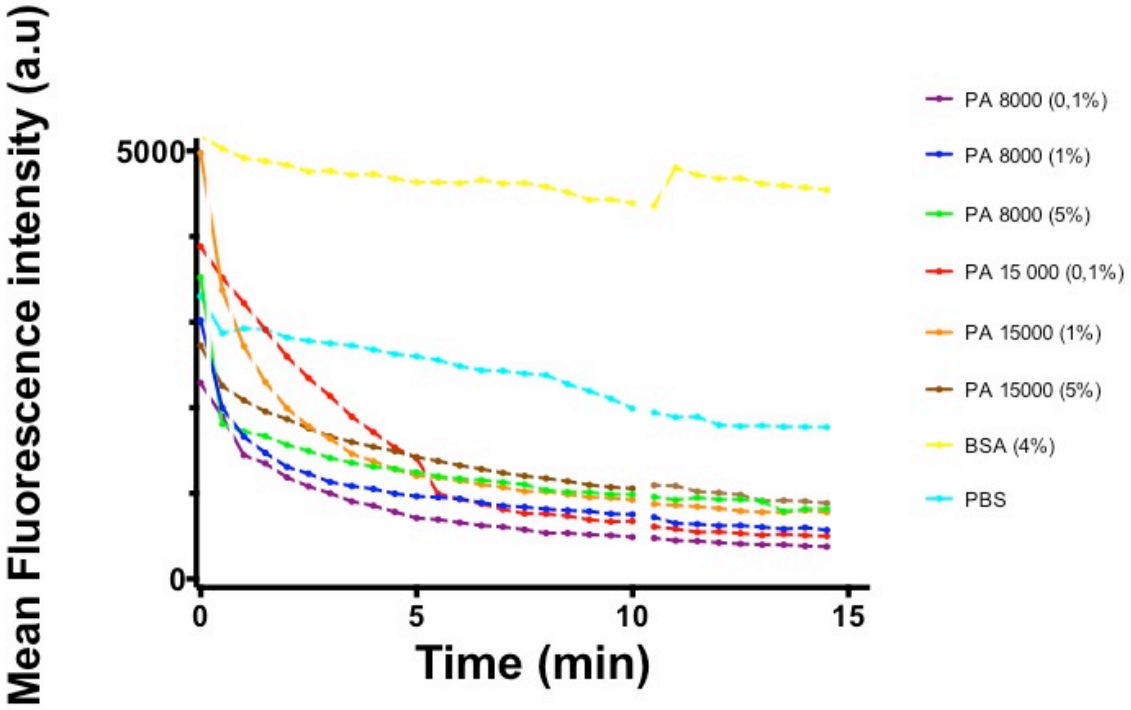

Figure 26 - Blocking studies optimization. In this experiment, after having the DNA probe immobilized on the surface blocking agents were passed through the channel and a decrease in fluorescence intensity was observed. The dash lines fitting the data are a guide to the eye. (Olympus Microscope CHX41, exposure time: 50ms, gain: 2.5dB, magnification:10x).

From the Figure 26 it was possible to conclude that for all the PAA's the signal decreased quickly in the first five minutes. Using BSA (4%) and PBS did not contribute greatly to the removal of immobilized probe DNA.

To better understand these results a graphic is presented in Figure 27 where the values were normalized to fluorescence intensity in t=0.

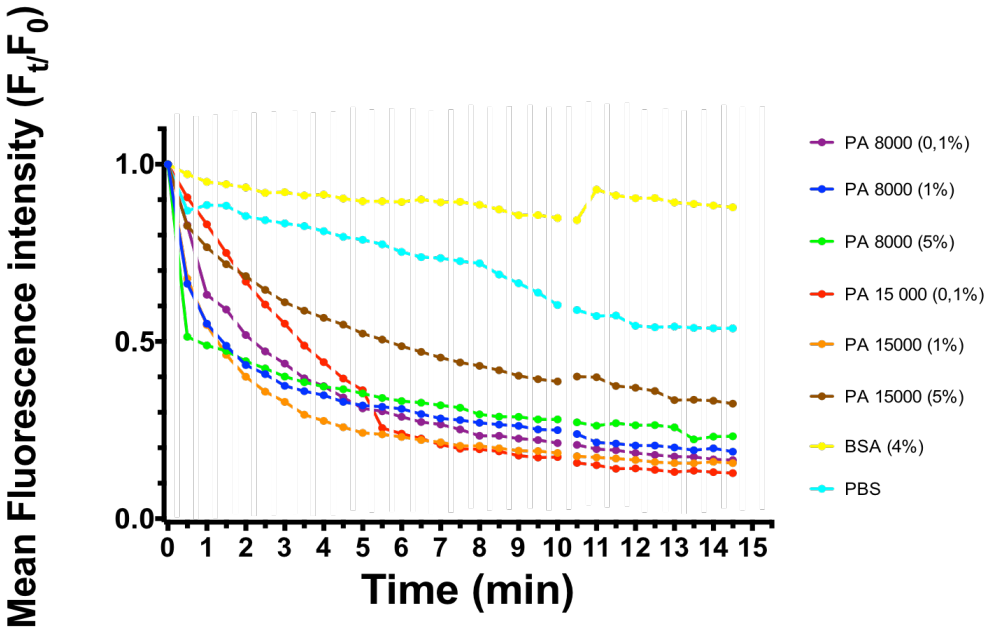

Figure 27 - Blocking studies. Same data presented in the Figure 25 but here expressed as a ratio normalized to the initial fluorescence value of each experiment. The dash lines fitting the data are a guide to the eye. (Olympus Microscope CHX41, exposure time: 50ms, gain: 2.5dB, magnification:10x).

From Figure 27 one can conclude that the PAA that removes less DNA probes from the beads surface was PAA 15000 (5%), removing around 50% of initial DNA probes. Looking now to the complete duration of the experiment, the next blocking agent that removed less DNA probes was the PAA 8000 (5%) but in this case 70% of initial DNA probes were removed. One way to avoid this large removal of DNA probes is to reduce the blocking step duration. From the graphic we can see that after 2 minutes, every blocking agent still allowed to have bound to the beads surface, at least 50% of the initial DNA probes. Another experiment was performed where after two minutes of blocking the beads surface an immobilization step followed. This experiment allowed to clarify if a two minutes blocking step was enough. The results are presented in Figure 28.

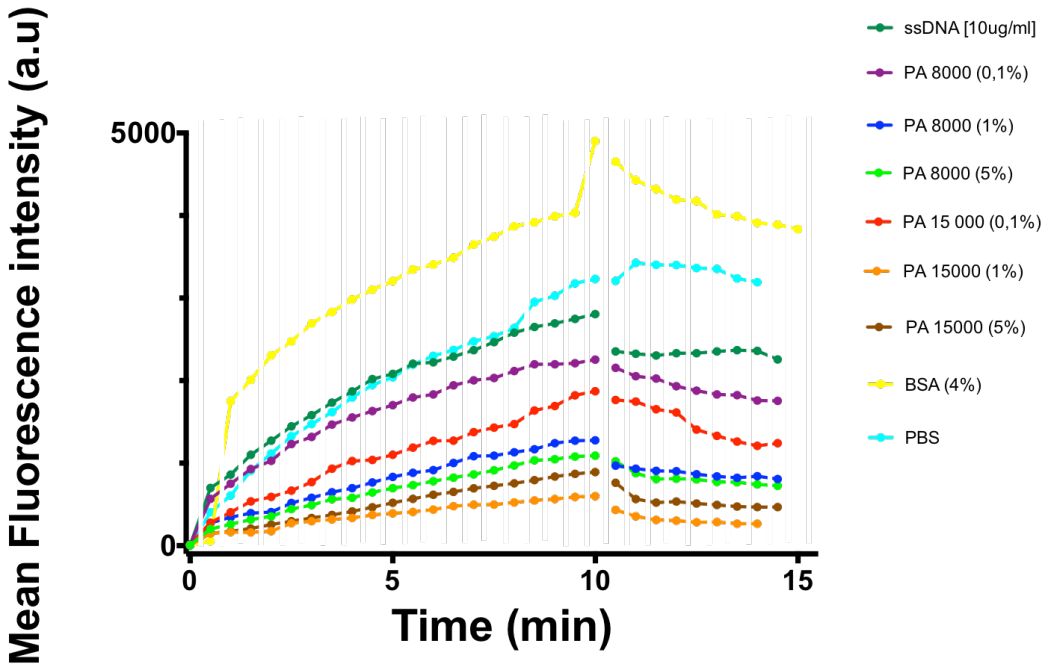

Figure 28 - Blocking studies: Study of a 2 minutes washing step. The dash lines fitting the data are a guide to the eye. (Olympus Microscope CHX41, exposure time: 50ms, gain: 2.5dB, magnification:10x).

From the Figure 28 it was possible to conclude that for a blocking step of 2 minutes the salmon sperm DNA was not that effective, having a similar behavior to the one where PBS was used. The best blocking agents were the PAA 15000 (1%), PAA 15000 (5%) and PAA 8000 (5%) blocking 84%, 75% and 68% of the probe DNA using as final value the one from the PBS experiment, where just buffer was used for the blocking step. Although the PAA 15000 (1% and 5%) presented a better blocking agent when performing immobilization it is important to remember that the blocking is intended for hybridization experiments. Due to that, it is important to test at least one PAA 15000 as a blocking agent in a hybridization

assay since it was hypothesized that the PAA with longer chains (PAA 15000) would affect the reaction hybridization. The results from such experiments are presented in Figure 29.

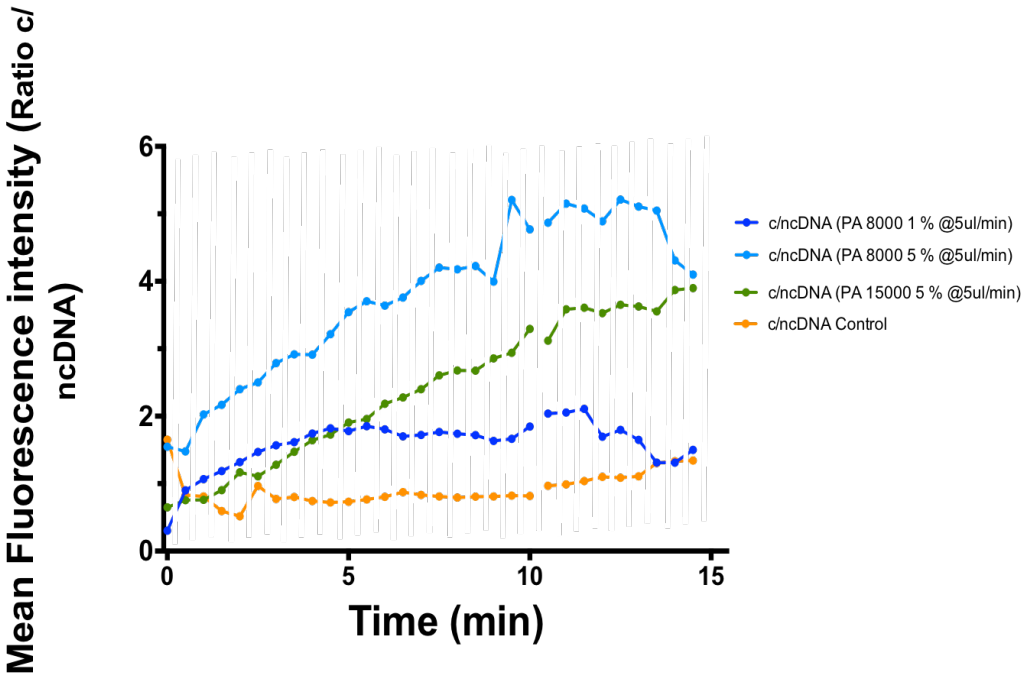

Figure 29 - Hybridization assay using three different blocking agents, PA 8000 1% (dark blue), PA 8000 5%(light blue) and PA 15000 5% (green). The dash lines fitting the data are a guide to the eye. (Olympus Microscope CHX41, exposure time: 5s, gain: 5dB, magnification:10x).

PAA 15000 (5%) and two PAA 8000 (5 and 1%) were chosen to perform the hybridization experiments with a blocking step. The control was simply a hybridization experiment with no blocking step. It was possible to conclude that for the three experiments with a blocking step, the hybridization ratio was improved from the control. This could mean that some nonspecific binding was prevented due to the blocking. When comparing the three blocking agents it was verified that the considered hypothesis about the molecular weights should be right since PAA 8000 (5%) presented a higher c/ncDNA ratio when compared with the PAA 15000 (5%). The PAA 8000 (1%) presented lower values than the last two. This could be explained by the dilution factor since there are less PAA molecules in the sample solution thus leading to a less effective blocking of the beads surface. The PAA 8000 (5%) was the blocking agent selected to perform the following experiments. In order to verify that the 2 minutes blocking time was indeed better that the 10 minutes, a hybridization assay was performed with blocking steps of 2 and 10 minutes using now PAA 8000 (5%) to block the beads surface. The results are presented in Figure 30.

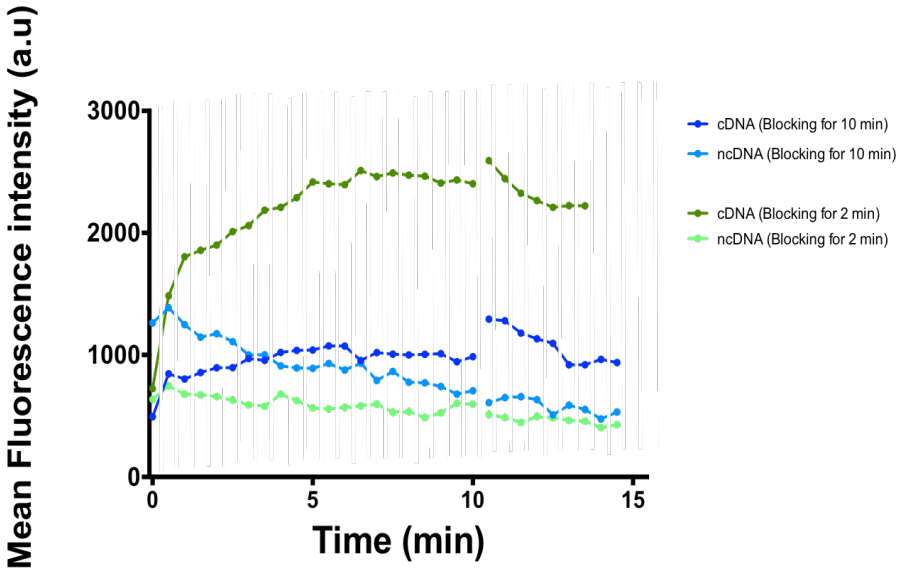

Figure 30 - Hybridization assays using two different blockings with PA 8000 5%. The dash lines fitting the data are a guide to the eye. (Olympus Microscope CHX41, exposure time: 5s, gain: 5dB, magnification:10x).

With these experiments it was possible to confirm that indeed performing a blocking step for 2 minutes using as blocking agent PAA 8000 (5%) was the optimal protocol tested during this work. Also it was possible to conclude that the cDNA data for the blocking during two minutes followed a hyperbolic response curve as expected, based on the Langmuir adsorption theory. The Langmuir adsorption theory assumes that there are two competing processes driving hybridization: adsorption (binding of target molecules to immobilized probes to form duplexes) and desorption (the reverse process of duplexes dissociating into separate probe and target molecules) [93].

In the Figure 31 is represented the c/ncDNA ratio from the experiments related to Figure 30. The c/nc ratio is now 3.5 in the end of the hybridization step, which means a 3-fold increase when compared with the ratio for the hybridization assays without a blocking step.

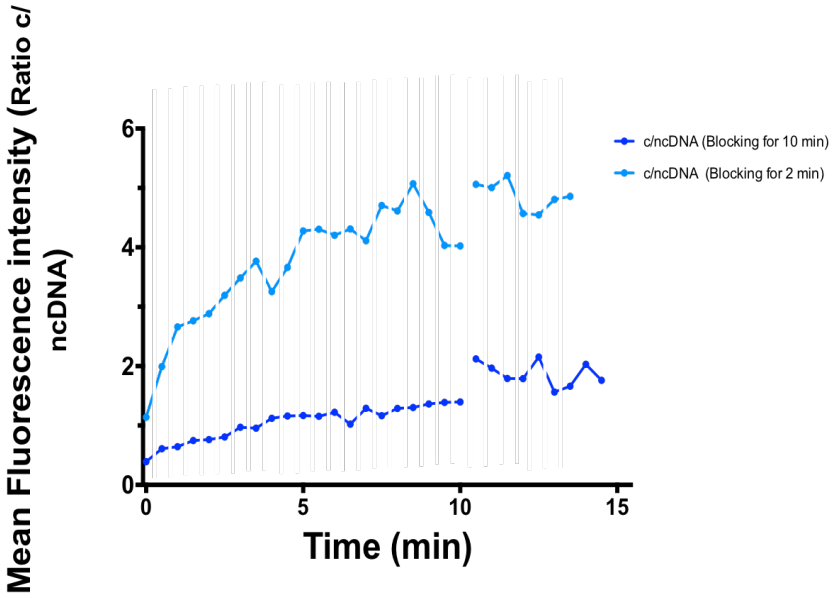

Figure 31 - Hybridization ratio from the data presented before. The c/nc ratio is calculated by dividing the absolute fluorescence intensity of the complementary signal (c) by the background reference (nc). The dash lines fitting the data are a guide to the eye. (Olympus Microscope CHX41, exposure time: 5s, gain: 5dB, magnification:10x).

3.6.2 Towards Lower Concentrations

After having the protocol optimized, experiments with lower target concentration were performed to determine the sensitivity of the system. Four target concentrations were tested (100, 10, 5 and 1 nM). The results are presented in the Figure 32.

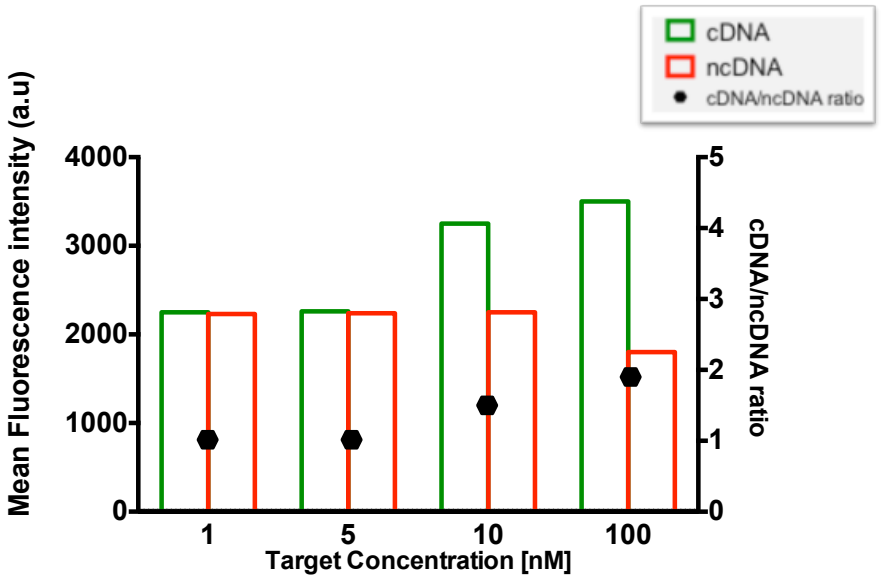

Figure 32 - Hybridization assay using fluorescence as detection method 1,5,10 and 100nM of target concentration. (Olympus Microscope CHX41, exposure time: 5s, gain: 5dB, magnification:10x).

Working with lower concentrations a new problem arose. From Figure 32, it was conclude that it was possible to distinguish target concentrations of 100 and 10 nM, between cDNA and ncDNA, but for 5 and 1 nM the signal was similar. The problem in this case was that the Q-Sepharose ® beads presented a basal fluorescence signal, probably due to the agarose components on the beads, since it was already verified that in agarose gels the agarose autofluorescence severely limits detection sensitivity. In order to evaluate if it was possible to photobleach the beads, they were left under the fluorescence light with the shutter completely open during 10 minutes. The result is presented in Figure 33.

After 10 minutes the signal had an intensity of 87% when compared with initial signal intensity. Nevertheless, to reach a similar state is enough to have the beads exposed for 3 minutes. It was possible to conclude that although the beads suffer some photobleaching, performing an initial step like this, in the beginning of the experiments, to decrease the autofluorescence of the agarose would not have a high impact.

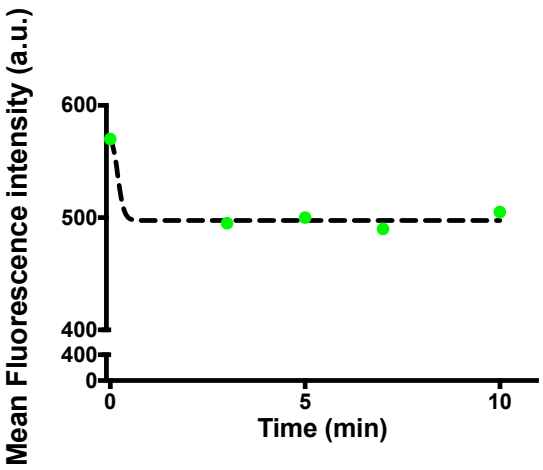

Figure 33 - Photobleaching effect on the beads. The dash line fitting the data is a guide to the eye.

To avoid the autofluorescence problem different methods of detection were tested, namely chemiluminescence and colorimetry.

3.7 Chemiluminescence assays

Luminescence is described as the emission of light from a substance as it returns from an electronically excited state to ground state. Chemiluminescence is light produced by a chemical reaction. It is believed that luminescence is the most sensitive detection method currently in use due to the ability of signal multiplication and amplification. For the chemiluminescence assays, an HRP-functionalized streptavidin molecule is used to detect the biotinylated target DNA strands that are captured on the surface by the immobilized complementary strand. The use of HRP as a colorimetric marker is widely practiced, since HRP presents high stability and high turnover rate. This technique allows detection without the use of a fluorescence lamp.

First, a chemiluminescence hybridization assay was performed using the optimized protocol from the fluorescence detection method. However, it was noticed the presence of a high background signal due to an adsorption of streptavidin-HRP onto the PDMS channel. To overcome this problem, an additional blocking step was used to block the PDMS surface of the channel. Since the blocking was destined to the channel, the blocking step was performed before the insertion of the beads into the channel. The blocking agent used was BSA (4%) since it was concluded in other works that it was an adequate blocking agent to avoid Streptavidin HRP adsorption onto the surface. [82] In Figure 34 it is presented the values for the experiments using a 1-1000pM target concentration range.

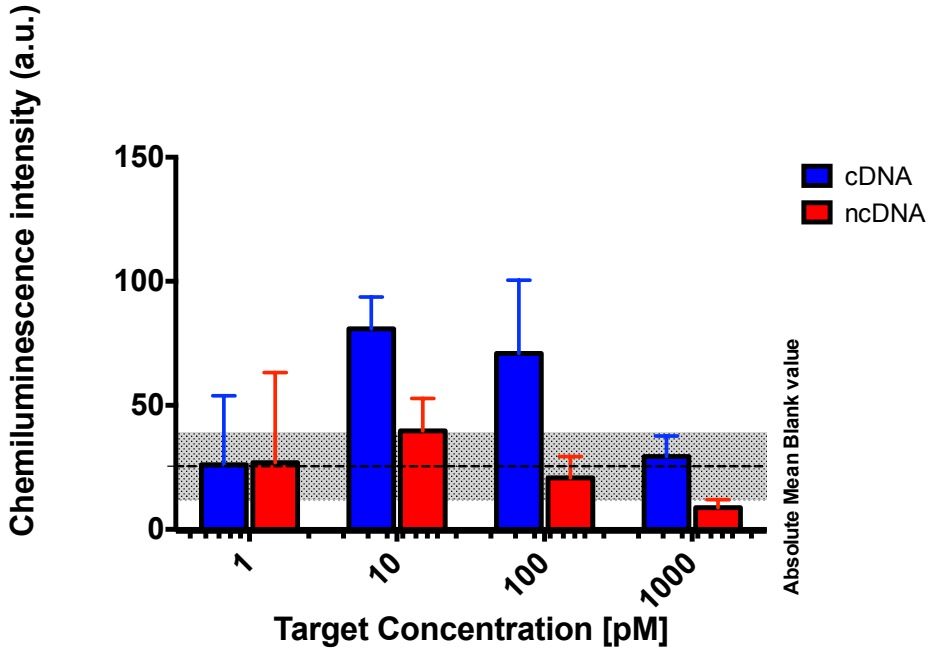

Figure 34 - Hybridization assay using chemiluminescence as detection method testing several target concentrations. The error bars are the standard deviation of three repeated measurements. (Leica microscope DMLM, exposure time: 10s; gain: 10x, objective: 2.5x).

The absolute mean blank value represents the range of signal obtained when using a zero concentration blank solution (only PBS buffer). It was possible to observe from Figure 34 that for the blank experiments the signal was higher than in experiments with a given concentration of target DNA.

MOPSO was used as buffer until the step of hybridization, where then PBS was used. This was done to decrease this blank value since it was thought that the reason behind this were the consecutives washing steps with PBS, that through salt effects were removing the blocking agents. This allowed a nonspecific adsorption of streptavidin-HRP, giving a high signal. The results are not shown in this work because it was concluded that although it allowed a smaller blank value, the use of MOPSO as a buffered did not allowed hybridization

and it wasn't detected any signal. MOPSO was chosen to perform the experiment since it is usually used to buffer at pH 6.2-7.6 and since it presents minimal salt effects, not interacting or affecting ions involved in the reaction. With this experiment it was possible to understood that minimal salt effects interactions are necessary not only for the hybridization to occur but also for immobilization of probes and effective blocking steps, even thought some removal of both immobilized probes and blocking agents could occur.

From Figure 34 it was possible to conclude that it was possible to clearly distinguish the cDNA signal from the ncDNA signal until 10pM of target concentration. In Figure 35 it is presented the cDNA/ncDNA ratios of the last experiments and the LoD, calculated using Equation 5. The LoB is 1.194 and the LoD is 2.14, corresponding to a LoD of 10^{-11} M of target sample based on the sample volume of 20μL.

Compared with the work done in [82] using the bare channel it was achieved a 100 fold increase in sensitivity.

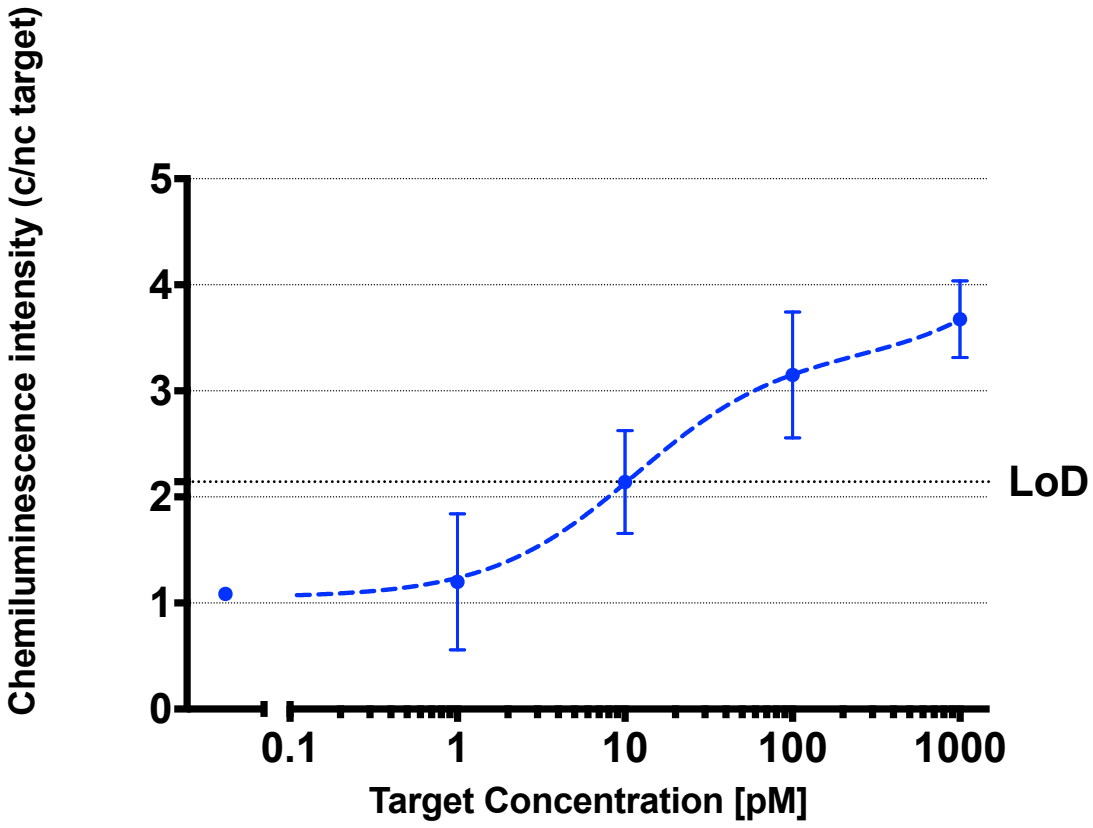

Figure 35 - Hybridization assay using chemiluminescence as detection method. The results are expressed as a function of the c/nc ratio. The c/nc ratio is calculated by dividing the absolute fluorescence intensity of the complementary signal (c) by the background reference (nc). The error bars are the standard deviation of three repeated measurements. The dash line fitting the data is a guide to the eye. (Leica microscope DMLM, exposure time: 10s; gain: 10x, objective: 2.5x).

3.8 Colorimetric assays

Colorimetric detection method was also tested and it was verified that this method is also suitable for hybridization detection of target DNA although the sensitivity appeared to be worse that in the chemiluminescence detection method. The results are presented in Figure 36.

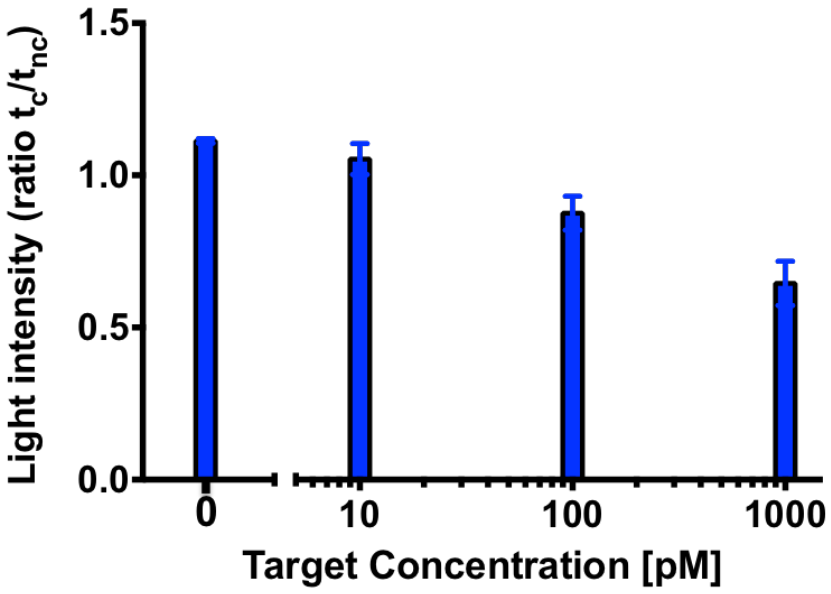

Figure 36 - Hybridization assay using a colorimetric detection method. The error bars are the standard deviation of three repeated measurements. (Leica microscope DMLM, visible light exposure time: 15μs; gain: 10x, objective: 2.5x).

In this case it was not possible to detect 10 pM but instead 100pM. This represents a 10-fold decrease in the sensitivity to detect target DNA when compared with the last method. It is worth mention that for this particular detection method the protocol used was the same for the chemiluminescence assay. After chemiluminescence detection TMB solution was inserted inside the channel at 10μL/min flow rate and images were acquired. A high target DNA concentration hybridized results in a higher amount of precipitated on the surface, reducing the intensity of light that passed through the channel.

3.9 Serum Experiments

To evaluate the applicability of the system to biological samples, the target molecules were diluted in FCS and human serum. The target concentration used was 100nM and it was also performed a comparison experiment using serum as dilution buffer on a bare channel. The results are presented in the Figure 37.

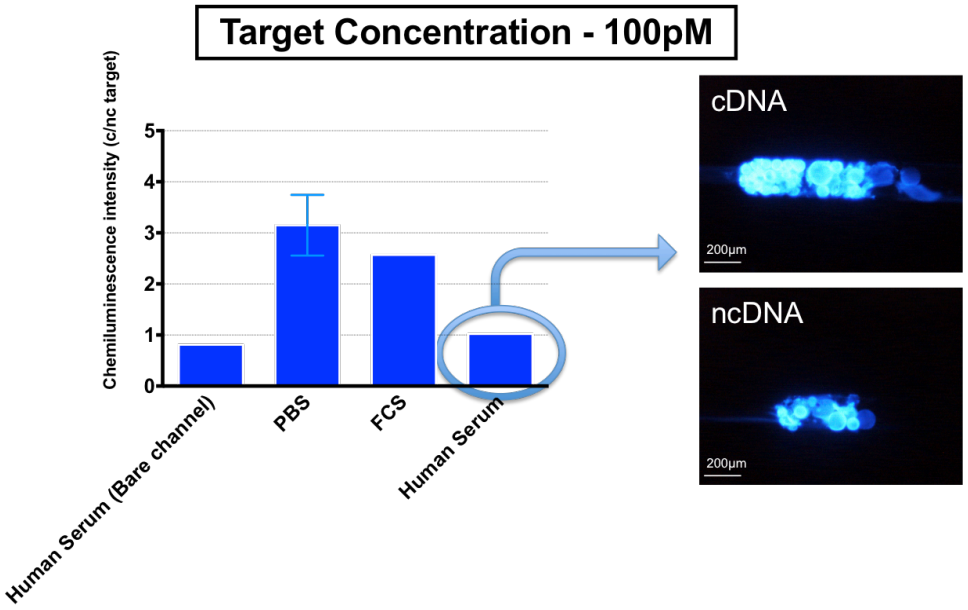

Figure 37 – Hybridization assays in PBS, FCS and Human serum (HS) using as detection method. The error bar in the PBS experiment represents the standard deviation of three repeated measurements. The error bars are the standard deviation of three repeated measurements. (Leica microscope DMLM, exposure time: 10s; gain: 10x, objective: 2.5x).

Using FCS the c/ncDNA ratio was in an expected range with a similar result to the one with PBS. Nevertheless, using Human serum the ratio decreased to one, meaning that it was not possible to distinguish between cDNA and ncDNA. Moreover, it was possible to verify, by analysis of the images in Figure 38 that the intensity of the signal was very high. The results for the channels using Human serum were the ones with the lowest c/ncDNa ratio. Figure 38 shows pictures from the bare channel and the channels with beads using PBS and Human serum. Analyzing the images it is possible to conclude that the low ratio in the bare channel was due to small resolution of the system since the signal was to small to distinguish cDNA from ncDNA. Also it appeared to have some debris accumulation inside the channel that gave a high signal but it didn't represent the presence of target DNA hybridized in the channel. A higher concentration should be used to test if with human serum this approach can be used. When comparing the intensity of the signal between the channels with beads, where PBS was used, and the channel with beads, where human serum was used, it was clear that the signal was more intense in this last one. It was not known if the human serum used was from a patient with a cardiac disease, which could have present some miRNAs over expressed that are free to hybridize with the DNA probe, but since this miRNAs were not biotin ended there should not be a reason for the streptavidin–HRP bind to the miRNAs, giving a higher signal. One can hypothesized that the human serum has present molecules that can enhance the chemical reaction between the streptavidin-HRP and the Luminol, giving a high and saturated signal. This could explain why the signals between cDNA and ncDNA were similar. Serum is plasma after coagulation factors have

been removed. Plasma is composed of 90 percent water with antibodies, coagulation factors, and other substances such as electrolytes, lipids, and proteins required for maintaining the body, such as albumin. A complete listing of the identity and quantity of endogenous metabolites that can be detected in human serum is available in the Serum Metabolome Database [96].

According to the literature, substitute phenols, naphtols, aromatic amines and boronates are some of the molecules that enhance the chemiluminescence chemical reaction [97].

Also it is worth mention that these experiments should be repeated to confirm the results. Nevertheless, this is proof that the system can be used to detect DNA diluted in Human serum, although some adjustments to the protocol must be done. More studies are in need to optimize this detection in this biological matrix.

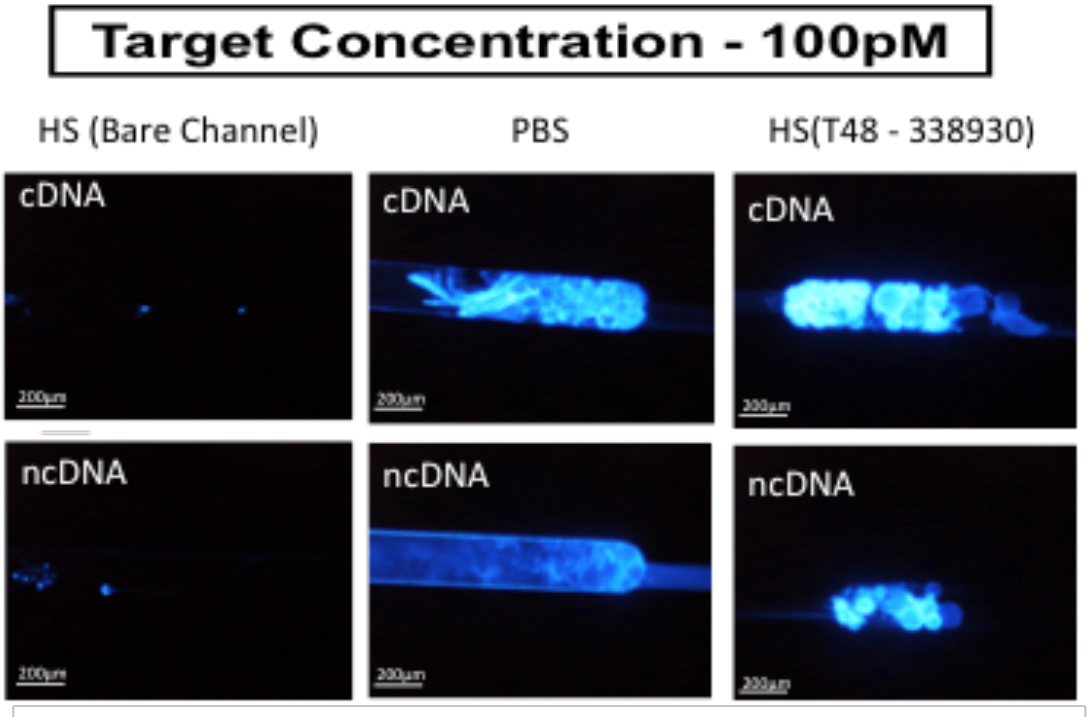

Figure 38 - Experimental images obtained from the experiments with FCS and Human Serum. The images were acquired in the end of the hybridization step (Leica microscope DMLM, exposure time: 10s; gain: 10x, objective: 2.5x).

4. Conclusion and Future Outlooks

Microfluidics diagnostic devices have been developing at a high rate over the past years and DNA hybridization is one of the most powerful techniques applied in diagnostics assays. More recent work is focusing on the creation of PoC devices with high selectivity and sensitivity. One way to improve the sensitivity of the assay is by using a porous bead ensemble.

In this work a microfluidic bead-based system to detect DNA and RNA was successfully developed and optimized. Q-Sepharose ® fast flow beads proved to be the best bead system for immobilization of DNA probes. Immobilization, blocking and hybridization protocols were optimized to decrease nonspecific binding and background signal. The immobilization of DNA probe onto the beads surface is due to an electrostatic interaction between the positively charged surface of the bead and the negatively charged DNA backbone. Fluorescence, chemiluminescence and colorimetry detection methods were performed and showed to be adequate to detect DNA hybridization.

By measuring the immobilization step by step, it was possible to better understand binding kinetics of these three dimensional systems and corroborate other results from other works.

The effect of using the complex streptavidin-biotinylated DNA probe was elucidated and proved to work in this system too, although the reasons for using the complex are different from the bare channel assay done in previous works.

An optimization of the flow rate and channel dimensions was performed resulting in a protocol where fewer reagents were used, maintaining or even enhancing the intensity of the signal for immobilization and hybridization experiments. It was found that a good blocking agent for Q-Sepharose ® fast flow beads are the PAA molecules, being the PAA 8000 (5%) the best blocking agent.

Using a fluorescence detection method a DNA target concentration of 10 nM was detected and with ability to differentiate between cDNA and ncDNA. Using a chemiluminescence method a high sensitivity was reached and the system was able to detect as low as 10pM with a LoD of 2.14 (10^{-11} M of target sample) and a the LoB is 1.19. This represented a 100-fold improvement in sensitivity when compared with protocols using a bare channel. Colorimetric detection also allowed the distinction of cDNA from ncDNA but with a 100pM sensitivity, which makes the chemiluminescense method the preferred method of detection in this work.

Finally, serum experiments of bovine and human origin were performed showing that the system can be used to detect DNA in biologic matrixes, where miRNA can be present. For

the FCS the result was not that different from the one when using PBS and a clear distinction between cDNA and ncDNA was made. However, when using the Human serum it was not possible to make a distinction between cDNA and ncDNA. This could be due to the presentence of some molecules in human serum that could affect the chemiluminescence reaction. Further studies are in demand to better understand these factors.

Some of the challenges that this technology has to overcome is the sensitivity of the system, since the concentration of circulating miRNAs detected in human plasma is rather low (<10pM). Although this system is reaching the biological relevant concentrations [98] there is still a need to improve the sensitivity and the reproducibility of the system. One way to overcome this challenge is to associate a pre–concentration step using for instance sensitive DNA isothermal amplification method that could allow to reach fM sensitivity's. Low temperature isothermal amplification methods have no need for thermal cycling thus requiring simplified microfluidic device features, which is an advantage when comparing with other pre-concentrations methods such as PCR. Also there are reports on a similar system using agarose beads functionalized at the surface with streptavidin molecules allowing a the immobilization of biotinylated DNA probes due to the strong streptavidin-biotin affinity, that reported a LoD of 10^{-10} M. It would be interesting to test these beads on this particular system with a similar protocol used in this work to see if a better result would be achieved. The use of high affinity nucleic acid analogues as DNA probes, such as peptide nucleic acids (PNA) and locked nucleic acids (LNA) could also improve the sensitivity and specificity of the system. In particular PNAs appear to be a promising solution since they have an uncharged pseodopeptide backbone (instead of the negatively charge phosphate-sugar DNA backbone) and because of this they show greater affinity in binding to complementary DNA. To bridge the gap between experimental status and the clinical biomedical applications, a detection technique using non-labeled target should be used. Mass sensitive techniques like surface plasmon resonance (SPR) sensors (sensitive to "optical mass") are also extremely attractive as platforms for the biosensing nucleic acids since they're label free. The creation of a microfluidic multiplexing system, for parallel detection, could also have a lot of impact since for diagnostic application in CVDs a range of miRNAs is deregulated. To have a range of biomarkers tested allows for a more precise diagnostic. The association of the system with a smartphone-based optical detection is a potentially easy-to-use, handheld, true point-of-care diagnostic too.

5. References

[1] Patrinos, G.P. and Ansorge, W.J, *Molecular Diagnostics* (2nd edition), Academic Press – Elsiever, 2010.

[2] Jayamohan, H. *et al., Applications of microfluidics for molecular diagnostics*, Methods Molecular Biology,vol.949, pp.305-334, 2013.

[3] Yager P, *et al., Point- of-care diagnostics for global health*. Annual Revision Biomedical Engineering, vol.10, pp.07–144 , 2008.

[4] "World Health Organization." [Online]. Available: http://www.who.int/ [Accessed: 14-Oct-2015].

[5] "European Society of Cardiology" [Online]. Available: http://www.escardio.org [Accessed: 14-Oct- 2015].

[6] Qureshi, A. *et al.*, *Biosensors for cardiac biomarkers detection: a review*, Sensors and Actuators B: Chemical, vol. 171-172, pp. 62–76, 2012.

[7] Yager P, *et al.*, *Microfluidic diagnostic technologies for global public health*, Nat. Insight, vol. 442, pp.412–18, 2006,

[8] Nahavandi, S. *et al., Microfluidic platforms for biomarker analysis*, Lab Chip, vol.14, pp.1496-1514, 2014.

[9] Wong, N.D., *Epidemiological studies of CHD and the evolution of preventive cardiology*, Nature reviews. Cardiology, vol.11, n.5, pp.276–89, 2014

[10] Kumar, A. and Cannon, C.P., *Acute Coronary Syndromes: Diagnosis and Management*, *Part I. Mayo Clinic Proceedings*, vol.*84,* n.10, pp.917–938, 2009.

[11] Yousef, M. *et al.*, *A Review on Diagnostic Procedures for the Cardiovascular System*, IJSR, vol.2, n.2, pp.2319-7064, 2013,

[12] McDonnell, B*. et al., Cardiac Biomarkers and the case for point-of-care testing*, Clin. Biochem, vol.42, p. 549-561, 2009.

[13] Vasan, R.M., *Biomarkers of Cardiovascular Disease: Molecular Basis and Practical* Considerations, Circulation *vol*.113, pp.2335-2362, 2006.

[14] McLean, A. and Huang, S.J., *Cardiac Biomarkers in the Intensive Care Unit*, Annals of Int. Care, vol.2, n.8, 2012,

[15] Hill, H.R. *et al.*, *The flow cytometric analysis of cytokines using multanalyte fluorescence microarray technology*, Methods, vol.38, pp.312-316, 2006.

[16] Jung, J.W., *et al*., *Label-free and quantitative analysis of C-reactive protein in human serum by tagged-internal standard assay on antibody arrays*, Biosensors and Bioelectronics vol.24, pp.1469-1473, 2009.

[17] Song, S. Y., *et al*., *A flouro-microbead guiding chip for single and quantifiable immunoassay of cardiac troponin I (cTnI),* Biosensors and Bioelectronics, vol. 26, pp. 3818-3824, 2011.

[18] Wu, W.Y., *et al., PDMS-gold nanoparticle composite film based silver enhanced colorimetric detection of cardiac troponin I*, Sensors and Actuators B: Chemical, vol.147, pp. 289-303, 2010.

[19] Christodoulides, N., *et al*, *A microchip-based multianalyte assay system for the assessment of cardiac risk*, Analytical Chemistry, vol.74, pp. 3030-3036, 2002

[20] Darain, F., *et al*., *On-Chip detection of myoglobin based on fluorescence*, Biosensors and Bioelectronics, vol.24, pp. 1744-1750, 2009,

[21] Cho, I.H., *et al., Chemiluminometric enzyme-linked immunosorbent assays (ELISA) –on-a-chip biosensorbased on cross flow chromatography*, Analyrica Chimica Acta, vol. 632, pp. 247-255, 2009.

[22] Meyer, M.H., *et al*., *SPR-based immunosensor for the CPR detection- a new method to detect a well known protein*, Biosensors and Bioelectronics, vol. 21, pp. 1987-1990, 2006.

[23] Liu, J.T., *et al*., *Surafce plasmon resonance biosensor with high anti-fouling ability for the detection of cardiac marker troponin T*, Analytica Chimica Acta, vol. 703, pp. 80-86, 2011.

[24] Woolley, C.F., and Hayes, M.A., *Sensitive detection of cardiac biomarkers using a microbead immunoassay*, Anal. Methods, vol.7, pp.8632-8639, 2015.

[25] Romaine, S.P.R., *et al., MicroRNAs in cardiovascular disease: an introduction for clinicians*, Heart vol. 101, pp. 921-928, 2015.

[26] Rooij, E., *The art of miRNA research*, Circulation Research, vol.108, pp.219-234, 2010.

[27] Bartel, D.P., *MicroRNAs: Genomics, Biogenesis, Mechanism, and Function*, Cell ,vol. 116, pp.281-297, 2004.

[28] Ambros, V., *et al., The C.elegans heterochromic gene lin-4 encodes small RNAs with antisense complimentary to lin-14*, *Cell,* vol 75, pp. 843-854, 1993.

[29] Ruvkun, G.,*et al., Posttranscriptional regulation of the heterochronic gene lin-14 by lin-4 mediates temporal pattern formation in C. elegans*, *Cell, vol.* 75, pp. 855-862, 1993.

[30] Kondkar, A.A. and Abu-Amero, K.K, *Utility of circulating MicroRNAs as Clinical Biomarkers for Cardiovascular Diseases*, Biomed Research International, vol 2015, pp.1-10, 2014.

[31] He, L. and Hannon, G.J., *MicroRNAs: Small RNAs with a big role in gene regulation*, Nature Reviews Genetics, vol. 5, pp. 522- 531, 2004.

[32] Chendrimada, t., *et al, TRBP recruits the Dicer complex to Ago2 for microRNA processing and gene silencing*, *Nature*, vol. 436, pp. 740- 744, 2005.

[33] Mendell, J.T. and Chang T.C, *MiRNAs in vertebrates physiology and human disease*, Annu. Rev. Genomics Hum. Genet., vol 8, pp.215-239, 2007,

[34] Creemers EE, Tijsen AJ, Pinto YM, *Circulating MicroRNAs: Novel Biomarkers and Extracellular Communicators in Cardiovascular Disease?,* Circ Res., vol.119, pp-483-495, 2012.

[35] Chen X., *et al*., *Characterization of microRNAs in serum: a novel class of biomarkers for diagnosis of cancer and other diseases*, *Cell Res*., vol18, pp.997–1006, 2008.

[36] El-Hefnawy, T., *et al., Characterization of amplifiable, circulating RNA in plasma and its potential as a tool for cancer diagnostics*, *Clin Chem*., vol 50, pp. 564 –573, 2004.

[37] Kosaka N, *et al., Secretory mechanisms and intercellular transfer of microRNAs in living cells. J Biol Chem*., vol 285, p.17442–17452, 2010.

[38] Kinet V., *et al*., *Cardiovascular extracellular miRNAs: emerging diagnostics markers and mechanisms of cell to cell RNA communication*, Frontiers in Genetic, vol.4, nº214, pp.1-7, 2013.

[39] Arroyo J.D., *et al., Argonaute2 complexes carry a population of circulating microRNAs independent of vesicles in human plasma*, Proc Natl Acad Sci U S A, vol. 108, pp.5003–

5008, 2011.

[40] Vickers, K.C., *et al., MicroRNAs are transported in plasma and delivered to recipient cells by high-density lipoproteins*, Nature Cell Biology, vol. 13, nº4, pp.423-433, 2011.

[41] Guire, DeV., *et al*, *Circulating miRNAs as sensitive and specific biomarkers for the diagnosis and monitoring of human diseases: Promises and challenges*, Clinical Biochemistry, vol. 46, n.10-11, pp- 846–860, 2013.

[42] Alpert, J.S., *et al*., *The Universal definition of myocardial infarction: a consensus document :Ischaemic heart disease*, Heart, vol.94, pp.1335-1341, 2008.

[43] van Empel V.P., De Windt L.J. and da Costa Martins P.A., *"Circulating miRNAs: Reflecting or Affecting Cardiovascular Disease?"*, Curr Hypertens Rep., vol.14, n.6, pp.498-509, 2012.

[44] Wang, GK, *et al*., *Circulating microRNA: a novel potential biomarker for a erly diagnosis of acute myocardial infarction in humans,* Eur Heart J, vol.31, pp. 659- 666, 2010.

[45] Corsen MF, *et al*., *Circulating microRNA-208b and microRNA-499 reflect myocardial damage in cardiovascular disease*, Circ Cardiovasc Genet, vol.3, pp-499-506, 2010.

[45] Windera C, *et al*., *Diagnostics and prognostics impact of six circulating microRNAs in acute coronary syndrome*, Journal of Molecular and Cellular Cardiology, vol.51, n.5, pp. 872-875, 2011.

[46] Hoekstra M, *et al*., *The perpheralblood mononuclear cell microRNA signature of coronary arterydisease*, Biochem Biophys Res Commun, vol.394, pp. 792-797, 2010.

[47] Plannell-Saguer M. and Rodicio M.C., *Anlytical Aspects of microRNA in diagnostics: A review*, Analytica Chimica Acta, vol. 699, pp-134-152, 2011.

[48] Kim S.W., *et al*., *A sensitive non-radioactive northern blot method to detect small RNAs*, Nucleic Acids Res., vol.38, n.98, 2010.

[49] Wu W., *et al*., *Simple nonradioactive detection of microRNAs using digoxigenin (DIG)-labeled probes with high sensitivity*, RNA, vol. 20, n.4, pp. 580–584, 2014.

[50] Castoldi, M, *et al., A sensitive array for microRNA expression profiling (miChip) based on locked nucleic acids (LNA*), RNA, vol.12, pp.913–920, 2006.

[51] Chen Y, *et al*., *Reproducibility of quantitative RT-PCR array in miRNA expression*

profiling and comparison with microarray analysis, BMC Genomics, vol. 10 :407, 2009.

[52] Koshiol J, *et al., Strengths and limitations of laboratory procedures for microRNA detection*, Cancer Epidemiol Biomarkers Prev, vol.19, n.4, pp.907–911, 2010.

[53] Tijen A.J., *et al*., *MiR423-5p as a circulating biomarker for heart failure*, Circ Res., vol. 106, pp.1035-1039, 2010.

[54] Pritchard, C.C., Cheng, H.H. and Tewari, M., *MicroRNA profiling: approaches and considerations*, Nature Reviews Genetics, vol.13, pp.358–369, 2012.

[55] Benes V. and Castoldi M., *Expression profiling of microRNA using real-time quantitative PCR, how to use it and what is available*, Methods, vol. 50, n.4, pp.244-9, 2010.

[56] Friedlander, M.R, *et al., Discovering microRNAs from deep sequencing data using miRDeep*, Nature Biotechnology, vol.26, pp. 407–415, 2008.

[57] Wyman, *et al., Repertoire of microRNAs in epithelial ovarian cancer as determined by next generation sequencing of small RNA cDNA libraries*, PLoS ONE 4, 2009.

[58] Jensen E, *Technical Review: In Situ Hybridization*, The Anatomical Record, vol 297, n.8, pp.1349–1353, 2014.

[59] Fan H.Z, et al., *Dynamic DNA hybridization on a Chip Using Paramagnetic Beads*, Anal Chem., vol 71, pp-4851-4859, 1999.

[60] Chan AS, *et al*., *A simple microfluidic chip design for fundamental bioseparation*, Journal of Anal Methods in Chemistry, pp.1-6, 2014.

[61] Weng X., Jiang H and Li D., *Microfluidic DNA hybridization assays*, Microfluidic Nanofluidic, vol.11, pp.367-383, 2011.

[62] Dutse SW and Yusof NA, *Microfluidics-based Lab-on-chip Systems in DNA-Based Biosensing: An overview*, Sensors, vol.11, pp.5754-5768, 2011.

[63] Tabeling, P., *Introduction to Microfluidics*, New York: Oxford University Press, 2003.

[64] Kim P, *et al*., *Soft lithography for microfluidics: A Review*, Biochio Journal, vol.2, n.1, pp. 1-11, 2008.

[65] Eddings M.A., Johnson MA and Gale BK, *Determining the optimal PDMS-PDMS bonding techniques for microfluidic device*, J. Micromech. Microeng. , vol 18 , pp.1-4, 2008.

[66] Fan Z.H., *et al., Dynamic DNA hybridization on a chip using paramagnetic beads, Anal of Chamistry*, vol.71, pp.4851-4659

[67] Sun Y and Kwok YC, *Polymeric microfluidic system for DNA analysis*, Anal Chim, Acta vol. 556, n.1, pp. 80-96, 2006.

[68] Ferguson BS, *et al*., Integrated microfluidic electrochemical DNA sensor, Anal Chem, vol.81, pp. 65903- 6508, 2009.

[69] Lange SA, *et al*., *Microcontact priting of DNA molecules*, Anal Chem, vol.76, pp. 1641-1647, 2004.

[70] Kim J, Heo J and Crooks RM, *Hybridization of DNA to bead immobilized probes confined within a microfluidic channel*, Langmuir, vol.22, pp. 10130-10134, 2006.

[71] Chung Y, *et al*., *Microfluidic Chip for fast nucleic acid hybridization*, Lab Chip, vol. 3, pp. 228-233, 2003.

[72] Lingam S., Dendukuri D. and Krishnakumar S., *Focus on microfluidics and nanotechnology approaches for the ultra sensitive detection of microRNA*, *MicroRN, vol. 3, pp.* 18-28, 2014.

[73] Thompson J.A. and Bau H.H., *Microfluidic, bead-Based assay: theory and experiments*, Journal of Chromatography B, vol.878, pp.228-236, 2010.

[74] Kohara Y, *et al., DNA probes on beads arrayed in a capillary, 'Bead-array', exhibited high hybridization performance*, Nucleic Acid Research, vol.30, n.16, 2002.

[75] Li H. and He Z., *Magnetic bead based DNA hybridization Assay with chemiluminescence and chemiluminescent imaging detection*, Analyst, vol.134, pp.800-804, 2009

[76] Berti F, *et al*., *Microfluidic-based electrochemical geno-sensor coupled with magnetic beads for hybridization detection*, Talanta, vol. 77, pp. 971-978, 2009.

[77] Senapati S., *et al*., *Rapid on-chip genetic detection microfluidic platform for real world applicatio*n, Biomicrofluidics, vol.3, n.022407, 2009.

[78] Lim CT and Zhang Y, *Bead-based microfluidic immunoassays: The next generation*, Biosensors and Biolelectronics, vol.22, pp.1197-1204, 2007.

[79] Chan A.S., *et al, A simple microfluidic chip design for fundamental bioseparation*, Journal of Analytical Methods in Chemistry, vol. 2014, pp. 1-6, 2014.

[80] Chou J, *et al*., *Pourous Bead-based iagnostics platforms:Bridiging the gaps in Healthcare*, Sensors, vol.12, pp.15467-15499, 2012.

[81] Rodiger S, *et al., Nucleic acid detection based on the use of microbeads: a review*, Microchim Acta, 2014.

[82] Müller – Landau H, *Integrated Microfluidic Detection of Prostate Cancer MicroRNAs using Amorphous Silicon p-i-n Photodiodes*, Barchelor Thesis, Hochschule Kaiserslautern-Universty of Applied Sciences, Kaiserslautern (Germany), 2015.

[83] Neish C., et al., *Direct visualization of ligand-protein interaction using atomic force microscopy*, *Br. J. Pharmacol,* vol. 135, pp. 1943-1950, 2002.

[84] Pires N.M.M., *et al., Recent Developments in Optical Detection Technologies in Lab-on-a-Chip Devices for Biosensing Applications*, *Sensors*, vol.*14*, n.8, pp.15458-15479, 2014.

[85] Ambruster D.A. and Pry T., *Limit of Blank, Limit of Detection and Limit of quantification*, Clin Biochem Rev, vol. 29,(Suppl 1), pp. S49–S52, 2008.

[86] Duffy, D.C., *et al., Rapid prototyping of microfluidic systems in poly(demethylsiloxane*), Anal. Chem., vol. 70, pp.4974–4984, 1998.

[87] Shi B., *et al., DNA Binding to the Silica Surface*., J Phys Chem B, vol.119, n.34, pp.11030-40, 2015.

[88] Pinto, R.M.R., *Electrokinetic and Optical Detection of Nucleic Acids for Biomedical Diagnosis in Microfluidics*, Master thesis, Technical University of Lisbon (Portugal), 2014.

[89] Kim J., *Investigation of the Formation and Structure of APTES Films on Silicon Substrates*, *Pike technologies*, 2010.

[90] Ng A.H.C., Uddayasankar U. and Wheeler AR, *Immunoassays in microfluidic systems*, Anal Bioanal Chem, vol. 397, pp.991-1007, 2010.

[91] Seong GH and Crooks R, *Efficient mixing and reactions within Microfluidic Channels Using Microbead-Supported catalysts*, J. AM. Chem Soc., vol.124, pp.13360-13361, 2002.

[92] Chou J, *et al*., Effects of sample delivery on Analyte capture in Porous Bead sensors, Lab Chip, vol.12, pp. 1-16, 2012.

[93] Burden C.J., Pittelkow Y. and Wilson S.R., *Adsorption models of hybridization and post-hybridization behaviour on oligonucleotide microarrays*, J.Phys.: Condens. Matter, vol.18, pp.5545–5565, 2006.

[94] Biotin - Streptavidin Interactions: Measuring Conformational Change and Differentiating between Specific and Non-Specific Binding - Application Note [Online]. Available: http://www.farfield-group.com/pdfs/014.pdf [Accessed: 25-Oct- 2015].

[95] Bongini L., Lombardi V., and Bianco P., *The transition mechanism of DNA overstretching: a microscopic view using molecular dynamics*, J R Soc Interface., vol.11, n.97, 2014.

[96] Plasma and Serum -Boundless Biology. Boundless, [Online]. Available: https://www.boundless.com/biology/textbooks/boundless-biology-textbook/the-circulatory-system-40/components-of-the-blood-225/plasma-and-serum-850-12095/, [Accessed: 29-Oct-2015].

[97] Khan P., *et al.*, *Luminol-Based Chemiluminescent Signals: Clinical and Non-clinical Application and Future Uses*, Appl Biochem Biotechnol., vol.173, n.2, pp. 333–355, 2014,

[98] Stefanie Dimmeler and Andreas M. Zeiher, *Circulating microRNAs: novel biomarkers for cardiovascular diseases?* , European Heart Journal, vol.31, pp.2705–2707, 2010.

6. Appendix

6.1 Fluorescence analysis methods

The analysis of fluorescence images required the establishment of a method to be used during this work. Two different approaches were studied. In the first approach three beads inside the channel were chosen and the mean intensity fluorescence was measured (Red circles in Figure 6.1). An average of the three was calculated. The final result was obtained by subtracting the background value (yellow circle in Figure 6.1) to the average value of the three selected beads. As an example, in the Table 6.1 it is presented the values for the mean intensity fluorescence and the final result obtained by using this method.

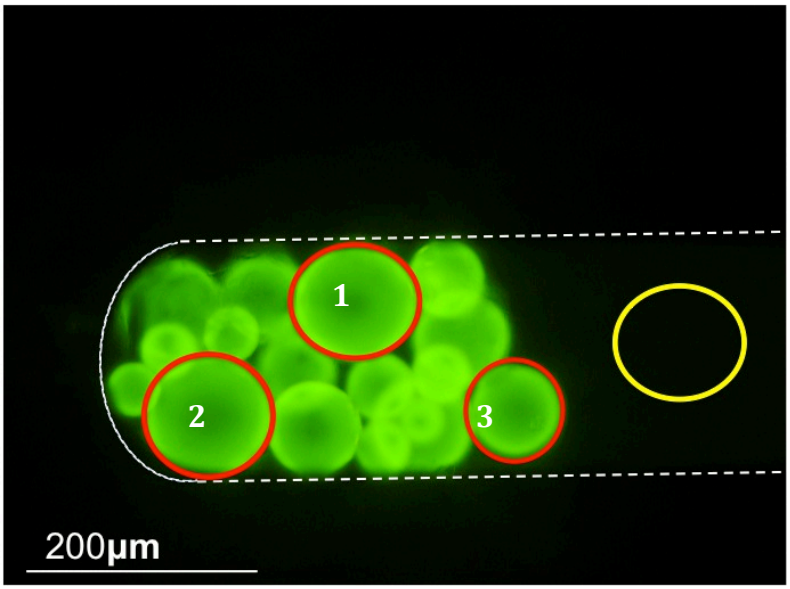

Figure 6. 1 - Fluorescence image of an immobilization assay.

Table 6. 1 - Mean intensity fluorescence values from Figure 6.1.

	Mean intensity	Average	Final result
Red circle 1	12823.443	12888.905	11843.368
Red circle 2	12278.857		
Red circle 3	13564.416		
Yellow circle	1045.537	1045.537	

In the second approach only one area with several beads inside was measured (red circle in Figure 6.2). The final result was obtained by subtracting the background value (yellow circle in the Figure 6.1) to the mean intensity value of the red circle. The Table 6.2 presents the values for the mean intensity fluorescence and the final result obtained by using this method.

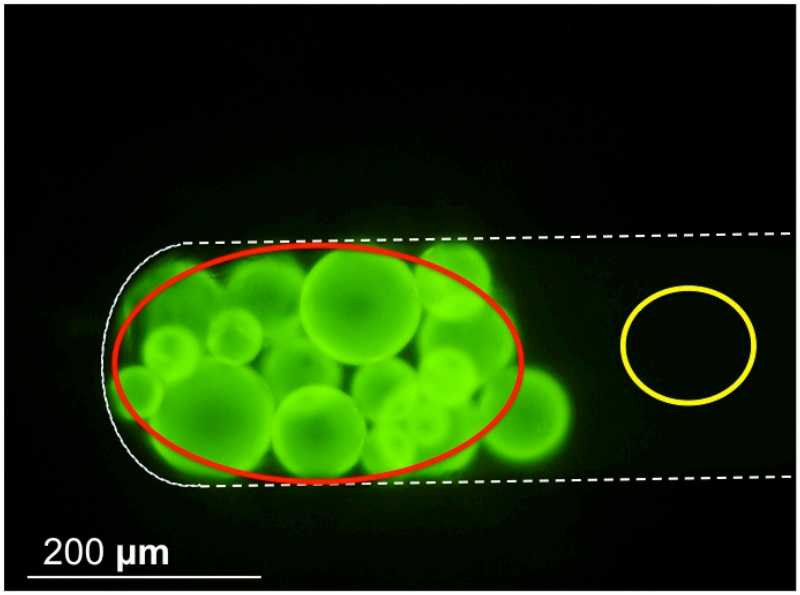

Figure 6. 2 – Fluorescence images of an immobilization assay.

Table 6. 2 – Mean intensity fluorescence values from Figure 6.2

	Mean intensity	Final result
Red circle	12813.794	11771.587
Yellow circle	1042.207	

Comparing the final results from both methodologies it was observed that the difference between each other was less than 1%. It was concluded that both of the methods could be used when analyzing the channels with beads, since the difference between final values was very small. Nevertheless, to have some coherence, only one method was chosen to perform the analysis during this work. The first method was chosen, since this method allowed for selecting only the beads and thus avoiding having the contribution of other debris that sometimes were inside the channel and presented fluorescence signal.

For the chemiluminescence analysis the same study was performed and the conclusion was the same. The method used when analyzing the images was the same chosen for the fluorescence assays.